

UNIVERSITÉ DU QUÉBEC À TROIS-RIVIÈRES

DÉVELOPPEMENT DE COMPOSITES À BASE DE POLYPYRROLE ET TOCN APPLIQUÉ SUR  
DIVERS SUPPORTS

THÈSE PRÉSENTÉE COMME EXIGENCE PARTIELLE DU  
DOCTORAT EN SCIENCES ET GÉNIE DES MATÉRIAUX LIGNOCELLULOSIQUES

PAR  
AAKASH MALIK

DÉCEMBRE 2025

Université du Québec à Trois-Rivières

Service de la bibliothèque

Avertissement

L'auteur de ce mémoire, de cette thèse ou de cet essai a autorisé l'Université du Québec à Trois-Rivières à diffuser, à des fins non lucratives, une copie de son mémoire, de sa thèse ou de son essai.

Cette diffusion n'entraîne pas une renonciation de la part de l'auteur à ses droits de propriété intellectuelle, incluant le droit d'auteur, sur ce mémoire, cette thèse ou cet essai. Notamment, la reproduction ou la publication de la totalité ou d'une partie importante de ce mémoire, de cette thèse et de son essai requiert son autorisation.

## UNIVERSITÉ DU QUÉBEC À TROIS-RIVIÈRES

## DOCTORAT EN SCIENCES ET GÉNIE DES

## MATÉRIAUX LIGNOCELLULOSIQUES (PH.D.)

**Direction de recherche :**

---

Prof. Éric Loranger, Ph.D., ing.	Directeur de recherche
----------------------------------	------------------------

---

Prof. Simon Barnabé, Ph.D.	Codirecteur de recherche
----------------------------	--------------------------

**Jury d'évaluation**

---

Prof. Cyril Muehlethaler, Ph.D. (UQTR)	Président du jury
--	-------------------

---

Prof. Thomas Auvray, Ph.D. (UQTR)	Évaluateur interne
-----------------------------------	--------------------

---

Prof. Benoît Barbeau, Ph.D. (UQÀM)	Évaluateur externe
------------------------------------	--------------------

---

Prof. Éric Loranger, Ph.D., ing. (UQTR)	Directeur de recherche
---	------------------------

---

Prof. Simon Barnabé, Ph.D. (UQTR)	Codirecteur de recherche
-----------------------------------	--------------------------

Thèse soutenue le 21/10/2025

## Remerciements

Tout d'abord, je tiens à remercier sincèrement Dieu Tout-Puissant, Jésus-Christ, pour son aide, sa protection et sa grâce constantes qui m'ont permis de mener à bien cette thèse.

Je tiens à exprimer ma profonde gratitude à toutes les personnes et institutions qui ont contribué à la réalisation de cette thèse doctorale.

Tout d'abord, je remercie sincèrement le professeur Éric Loranger, directeur de recherche, pour sa confiance, son encadrement scientifique rigoureux, et son soutien constant tout au long de ce projet. Je remercie également le professeur Simon Barnabé, codirecteur, pour ses conseils éclairés, sa disponibilité, et ses encouragements tout au long de mon parcours.

Je souhaite également remercier chaleureusement les membres du jury pour avoir accepté de participer à l'évaluation de cette thèse. Je remercie le professeur Cyril Muehlethaler, président du jury, pour sa disponibilité et son engagement dans ce processus. Je remercie également le professeur Thomas Auvray, évaluateur interne, pour l'intérêt porté à mon travail, ainsi que le professeur Benoît Barbeau (UQÀM), évaluateur externe, pour avoir accepté d'apporter son regard expert à cette recherche. Leur implication est précieuse et contribue grandement à la qualité scientifique de ce projet doctoral.

Je tiens également à exprimer ma profonde gratitude au professeur François Brouillette, au professeur Bruno Chabot, à France, à Isabelle, à Kézia, à Ha, à Tung, à Oulame et à Daniel pour leur soutien constant, leurs conseils et leurs encouragements tout au long de mon travail de thèse. Je tiens également à exprimer ma gratitude aux stagiaires que j'ai eu le plaisir d'encadrer pendant mon doctorat : Noa, Alexis, Axel et Hugo.

Je souhaite aussi remercier chaleureusement l'Institut d'Innovations en Écomatériaux, Écoproduits et Écoénergies (I2E3) de l'Université du Québec à Trois-Rivières (UQTR) pour avoir offert un environnement de recherche stimulant et des infrastructures de grande qualité. Je suis également reconnaissant envers le Conseil de recherches en sciences naturelles et en génie du Canada (CRSNG/NSERC) pour le soutien financier accordé à ce projet.

Mes remerciements s'adressent aussi à l'équipe du laboratoire LGP2 – Grenoble INP – CNRS – Université Grenoble Alpes, et tout particulièrement au professeur Julien Bras, pour m'avoir accueilli durant ma mobilité internationale. Cette collaboration a grandement enrichi la portée scientifique et environnementale de mes travaux. Je tiens également à remercier le programme PEPR B-BEST de l'ANR France pour avoir soutenu ce séjour de recherche.

Je tiens à remercier sincèrement mes parents d'avoir été là pour moi émotionnellement même si je suis très loin d'eux.

Enfin, je remercie mes collègues, amis et proches pour leur présence, leur patience et leur soutien moral tout au long de cette aventure doctorale.

## Résumé

Dans un contexte mondial de transition vers une économie circulaire et de réduction de la dépendance aux ressources fossiles, cette thèse porte sur le développement de matériaux biosourcés multifonctionnels à faible empreinte environnementale. Les revêtements à base de polymères dérivés du pétrole posent des défis environnementaux majeurs, notamment leur non-biodégradabilité, l'émission de composés organiques volatils (COV) et la pollution par les microplastiques. L'objectif général de cette thèse est de développer une peinture biosourcée multifonctionnelle, applicable sur substrats rigides, à base de nanofibres de cellulose oxydées TEMPO (TOCN) et de polypyrrole (PPy), modifiés par de l'alcool polyvinylique (PVA) et du glycérol. Cette formulation vise à répondre simultanément à des critères de performances techniques (barrière et propriétés mécaniques) et de durabilité environnementale.

Une revue de la littérature approfondie a justifié le choix des matériaux. Les TOCN présentent une structure fibrillaire dense, une bonne capacité filmogène et une biodégradabilité naturelle. Cependant, leur caractère hydrophile et leur fragilité mécanique nécessitent une modification. Le polypyrrole, un polymère conducteur intrinsèquement noir, est présenté pour ses propriétés électriques et pigmentaires. L'ajout de PVA et de glycérol améliore respectivement l'adhérence aux substrats rigides et la flexibilité du film. La démarche expérimentale de cette thèse repose sur la conception d'un système de peinture aqueuse associant TOCN et polypyrrole. Les nanofibres de cellulose oxydée ont été obtenues par oxydation TEMPO suivie d'une désintégration mécanique, aboutissant à un gel nanofibrillaire riche en groupes carboxylates favorisant l'interaction avec les polymères conducteurs. Le polypyrrole a été synthétisé par polymérisation oxydative in situ en présence de chlorure ferrique ( $\text{FeCl}_3$ ), assurant une dispersion homogène du polymère conducteur dans le réseau de TOCN. Les formulations finales ont été préparées en intégrant du PVA comme liant pour améliorer l'adhésion aux substrats et du glycérol (1–5 ml) comme plastifiant afin de moduler la flexibilité et de réduire la fragilité des films. Le processus de formulation a inclus la préparation de suspensions aqueuses, leur homogénéisation mécanique, la réalisation de couches de

peinture par étalement contrôlé sur substrats bois et papier UPM, puis un séchage à température ambiante pour obtenir des films homogènes.

La caractérisation des matériaux s'est appuyée sur un ensemble de techniques complémentaires. Les propriétés rhéologiques des formulations ont été étudiées afin d'évaluer leur aptitude à l'application et leur comportement pseudoplastique. La morphologie des films a été observée par microscopie électronique à balayage (MEB), tandis que la spectroscopie Raman a permis de confirmer les interactions entre TOCN et PPy et d'identifier les bandes caractéristiques du polymère conducteur. Les propriétés thermiques ont été évaluées par analyse thermogravimétrique (ATG) et calorimétrie différentielle à balayage (DSC) pour déterminer la stabilité thermique et les transitions des matériaux. L'angle de contact a été mesuré sur bois peint pour évaluer l'hydrophilie des surfaces, et des tests qualitatifs de conductivité ont été effectués pour vérifier la continuité du réseau PPy. Pour la partie environnementale, des tests de lixiviation (pH, ICP-OES, HPLC-MS/MS) et de biodégradabilité en sol ont été réalisés, complétés par une étude de réutilisation par solubilisation hydrothermale. Enfin, pour les propriétés d'usage, les taux de transmission d'oxygène (OTR) et de vapeur d'eau (WVTR) ont été mesurés, et la rugosité des surfaces a été analysée par profilométrie 3D Alicona.

Trois articles scientifiques structurent la démonstration expérimentale de cette thèse.

Dans le premier article, la synthèse de composites TOCN-PPy a été réalisée par polymérisation in situ, suivie d'une formulation contrôlée avec du PVA (comme liant), du glycérol (comme plastifiant) et de l'eau (comme solvant) pour obtenir des peintures applicables sur bois. Une caractérisation approfondie a été réalisée : rhéologie, microscopie électronique à balayage (MEB), spectroscopie Raman, angle de contact, analyse thermique (ATG/DSC) et conductivité qualitative. Les formulations enrichies en glycérol ont démontré une bonne dispersion, une conductivité modérée, une flexibilité améliorée et une structure homogène, notamment.

Le deuxième article s'est concentré sur le comportement environnemental de ces revêtements. Des tests de lixiviation (pH, ICP-OES, HPLC-MS/MS) ont été réalisés pour quantifier la libération de fer, de pyrrole et de glycérol dans l'eau. De plus, la

biodégradabilité dans le sol a été testée, ainsi que la réutilisabilité par solubilisation hydrothermale. Les résultats montrent une faible lixiviation des composés toxiques, une désintégration partielle dans le sol (jusqu'à 45 % de perte de masse) et une récupération de matière en milieu aqueux chaud, suggérant un degré de circularité.

Le troisième article explore l'application des revêtements au papier d'emballage (papier UPM). Les propriétés barrières ont été analysées à l'aide du taux de transmission de l'oxygène (OTR) et du taux de transmission de la vapeur d'eau (WVTR), complétées par des essais mécaniques (traction) pour les films de TOCN-PPy-PVA-Gly, et une analyse de surface (Alicona, MEB) du papier UPM couché. Les résultats révèlent une excellente performance de barrière à l'oxygène ( $OTR < 1 \text{ cc/m}^2/\text{jour}$ ) et une dégradation progressive des propriétés de vapeur avec l'augmentation de la teneur en glycérol. Le comportement mécanique est modulable et les images de surface confirment une bonne couverture, la rugosité augmentant avec la teneur en glycérol. Une analyse préliminaire du cycle de vie (ACV) a également été réalisée, indiquant que le TOCN, le polypyrrole et le PVA sont les principaux contributeurs à l'impact carbone, mais qu'il existe des alternatives biosourcées au PVA. Cependant, notre contribution globale reste inférieure à celle du revêtement en poudre de l'entreprise.

En conclusion, cette thèse propose une approche innovante et intégrée pour le développement de peintures biosourcées multifonctionnelles, alliant performance technique et durabilité environnementale. Le système TOCN-PPy-PVA-Gly présente un fort potentiel pour des applications dans les domaines de l'emballage, des surfaces fonctionnelles et des peintures conductrices. Les perspectives d'avenir incluent le remplacement du PVA par des alternatives biosourcées, l'intégration d'agents antibactériens naturels et l'optimisation des procédés pilotes pour un déploiement industriel.

**Mots Clés**

Nanofibres de cellulose oxydées (TOCN) ; Polypyrrole (PPy) ; Peinture biobasée ; Polyalcool vinylique (PVA) ; Glycérol ; Revêtements multifonctionnels ; Propriétés barrières ; Conductivité électrique ; Biodégradabilité ; Analyse du cycle de vie (ACV) ; Revêtements durables ; Économie circulaire ; Emballage biosourcé ; Revêtements intelligents ; Nanocomposites

## Table of Contents

Remerciements .....	iii
Résumé.....	v
Mots Clés .....	viii
Table of Contents .....	ix
List of Figures.....	xvi
List of Tables .....	xviii
List of Abbreviations.....	xix
Chapter 1 - Introduction.....	1
1.1    Circular Economy and Bioeconomy Concepts .....	1
1.2    Biomass-Based Coatings as Sustainable Alternatives .....	2
1.3    Nanocellulose and Conducting Polymers for Coatings .....	3
1.4    Research Objectives .....	3
1.5    Thesis Structure.....	4
Chapter 2 - Literature review.....	7
2.1    Overview of Lignocellulosic Biomass.....	7
2.1.1    Cellulose (40–50% of biomass).....	8
2.1.2    Hemicellulose (25–35% of biomass) .....	9
2.1.3    Lignin (15–20% of biomass) .....	9
2.2    Importance for cellulose-based coatings.....	10
2.3    Nanocellulose: Properties and applications .....	11
2.3.1    Cellulose Nanocrystals (CNCs).....	11
2.3.2    Cellulose Nanofibers (CNFs) .....	11
2.3.3    Bacterial Nanocellulose (BNC) .....	11
2.3.4    Cellulose microfibrils (CMF) .....	12
2.3.5    Applications of Nanocellulose.....	12
2.4    Surface Modification Techniques for Nanocellulose.....	13

2.5	2,2,6,6,tetramethylpiperidine-1-oxyl (TEMPO).....	15
2.5.1	4-acetamido-TEMPO .....	16
2.6	Polypyrrole (PPy) and Conductive Polymers .....	17
2.6.1	Alternative Conductive Polymers.....	17
2.6.1.1	Polyaniline (PANI).....	17
2.6.1.2	Polythiophene .....	18
2.7	Current Status of Coating Technologies .....	18
2.7.1	Conventional Petroleum-Based Coatings .....	19
2.7.2	Emerging Trends Toward Bio-Based Coatings.....	19
2.7.2.1	Focus on biobased approach .....	19
2.7.2.2	Why biobased approach important? .....	19
2.7.2.3	Challenges with biobased approach .....	19
2.7.3	Solution via hybrid approach.....	20
2.7.4	Nanocellulose in Coating Applications.....	20
2.7.4.1	Why nanocellulose component of interest? .....	20
2.7.4.2	Challenge with only nanocellulose in coating? .....	20
2.7.4.3	Strategic approach to solve this issue .....	20
2.7.4.4	Conductive Bio-Based Coatings: Opportunities and Challenges .....	20
2.7.5	Application of TOCN-PPy in Coatings.....	21
2.7.6	Coating application via TOCN-PPy .....	21
2.7.6.1	Conductivity nature.....	21
2.7.6.2	Barrier rigid support nature .....	22
2.7.6.3	Antibacterial nature.....	22
2.7.6.4	Challenges.....	22
2.7.6.5	Summary .....	23
2.8	Potential Application Areas .....	23
2.8.1	Food Packaging Coatings .....	23
2.8.2	Functional Surface Coatings for Wood and Rigid Materials.....	24
2.8.3	Sustainable Paints and Pigmented Coatings .....	24
2.9	Environmental and Toxicological Considerations .....	24
2.10	Perspectives from External Research Groups and Innovation Positioning .....	25

2.10.1	Metal-nanoparticles based coating .....	25
2.10.2	Chitosan based coating.....	25
2.10.3	Lignin based coating .....	26
2.10.4	Multifunctional hybrid coating.....	27
2.10.5	The current work's position in relation to the state of the art .....	27
Chapter 3 - Research project development and methodology .....		29
3.1	Project Overview and Research Framework .....	29
3.2	Fabrication of TOCN Nanocellulose .....	30
3.2.1	Oxidation Protocol .....	32
3.2.2	pH Regulation.....	32
3.2.3	Oxidation cessation .....	32
3.2.4	Conductometric Titration of Carboxylic Acids .....	32
3.3	Synthesis of TOCN-PPy .....	34
3.3.1	Polymerization Protocol.....	35
3.3.2	Key Observations During Synthesis .....	36
3.4	Coating development .....	36
3.4.1	Surface Adhesion Challenges .....	36
3.4.2	Introduction of Copolymer Additives .....	37
3.4.3	Expected Impacts of Copolymer Addition .....	37
3.4.4	Surface Coating Trials and Observations.....	38
3.4.4.1	Coating Behavior on Plywood Surfaces .....	39
3.4.4.2	Summary of Observations .....	40
3.5	Characterization Techniques Employed .....	40
3.6	Key Problems Identified .....	47
3.6.1	Poor Adhesion to Rigid Surfaces .....	47
3.6.2	Brittleness and Cracking .....	47
3.6.3	Surface Defects and Drying Instabilities .....	47
3.7	Proposed Strategies for Problem Solving .....	48
3.7.1	Fine-Tuning Copolymer and Plasticizer Content .....	48
3.7.2	Multi-Recipe Development Approach .....	48
3.7.3	Process Optimization.....	49
3.7.4	Long-Term Environmental Testing.....	49

Chapter 4 - Scientific Article 1: Synthesis, formulation and characterization of	
paints based on TOCN–PPy–PVA–Gly.....	50
4.1 Preface.....	50
4.2 Résumé.....	51
4.3 ABSTRACT .....	52
4.4 INTRODUCTION.....	53
4.5 MATERIALS AND METHODOLOGY .....	56
4.5.1 Materials.....	56
4.5.2 Synthesis of TOCN-Polypyrrole (TOCN-PPy) .....	56
4.5.3 Preparation of Paint Formulations Incorporating TOCN- PPy, PVA, and Glycerol .....	57
4.5.3.1 Preparation of the PVA Base Formulation .....	57
4.5.3.2 Incorporation of Glycerol .....	57
4.5.3.3 Thermal Processing.....	57
4.5.3.4 Experimental design for paints development .....	58
4.5.3.5 Making of Paint Films .....	58
4.5.4 Substrate coating.....	59
4.6 Characterisations .....	59
4.6.1 Rheometer .....	59
4.6.2 Scanning electron microscopy (SEM) .....	59
4.6.3 Raman Spectroscopy .....	60
4.6.4 Contact angle .....	60
4.6.5 Thermogravimetric analysis .....	60
4.6.6 Differential scanning calorimetry .....	61
4.6.7 Qualitative Conductivity Analysis .....	61
4.7 RESULTS AND DISCUSSION .....	61
4.7.1 Rheological measurements (Suspensions).....	62
4.7.2 Scanning electron microscopy (Films).....	65
4.7.3 Raman Spectroscopy (Films).....	66
4.7.4 Contact angle (Wood painted surfaces) .....	69
4.7.5 Thermogravimetric Analysis (Films).....	70
4.7.6 Differential scanning calorimetry (Films) .....	72
4.7.7 Qualitative Conductivity Analysis (Films) .....	74

4.7.8	Proposed structure of TOCN-PPY, TOCN-PPy-PVA and TOCN-PPy-PVA-Gly.....	76
4.8	CONCLUSION .....	78
4.9	CRedit (CONTRIBUTOR ROLES TAXONOMY).....	79
4.10	Declaration of generative AI and AI-assisted technologies in the writing process .....	79
4.11	ACKNOWLEDGEMENTS.....	80
4.12	REFERENCES .....	80
Chapter 5 - Scientific Article 2 : Environmental fate of TOCN-PPy-PVA-Gly paint coatings.....		
		84
5.1	Preface.....	84
5.2	Résumé.....	85
5.3	ABSTRACT .....	86
5.4	INTRODUCTION.....	87
5.5	MATERIALS AND METHODOLOGY.....	89
5.5.1	Materials.....	89
5.5.2	Experimental Strategy .....	90
5.5.3	Leaching characterisations.....	91
5.5.3.1	pH measurement via Thermo Scientific ORION Star A215 pH meter .....	91
5.5.3.2	Inductively Coupled Plasma Optical Emission Spectroscopy (ICP-OES) .....	91
5.5.3.3	High-Performance Liquid Chromatography coupled with tandem Mass Spectrometry (HPLC-MS/MS) .....	92
5.5.4	Soil Biodegradation Testing .....	94
5.5.5	Hydrothermal Reusability Assessment .....	94
5.6	RESULTS AND DISCUSSION .....	94
5.6.1	pH testing (for washing impact of TOCN-PPy) .....	94
5.6.2	Iron release and regulatory context via ICP-OES .....	96
5.6.3	HPLC-MS/MS analysis of pyrrole and glycerol leaching .....	98
5.6.3.1	Pyrrole Detection Results (ESI+) .....	98
5.6.3.2	Glycerol Detection Results (ESI-).....	99
5.6.4	Soil biodegradation testing .....	101

5.6.5	Hydrothermal Reusability Assessment .....	102
5.7	CONCLUSION .....	104
5.8	CRedit (CONTRIBUTOR ROLES TAXONOMY) .....	105
5.9	Declaration of generative AI and AI-assisted technologies in the writing process .....	105
5.10	ACKNOWLEDGEMENTS.....	105
5.11	REFERENCES .....	106

## Chapter 6 - Scientific article 3 : Barrier and mechanical properties of TOCN–

	PPy–PVA–Gly films with LCA of paint on UPM paper .....	109
6.1	Preface.....	109
6.2	Résumé.....	111
6.3	ABSTRACT .....	111
6.4	INTRODUCTION.....	112
6.5	MATERIALS AND METHODOLOGY .....	114
6.5.1	Materials, synthesis, formulation, and casting of paint films ....	114
6.5.2	Mechanical Characterization .....	115
6.5.3	Barrier Properties Measurements .....	115
6.5.3.1	Oxygen Transmission Rate (OTR).....	115
6.5.3.2	Moisture Vapor Transmission Rate (MVTR).....	116
6.5.4	Coating and Drying Process .....	116
6.5.5	Surface morphology .....	117
6.5.6	SEM spectroscopy .....	117
6.5.7	Integration of Life Cycle Assessment (LCA) .....	118
6.6	RESULTS AND DISCUSSION .....	120
6.6.1	Mechanical Performance of films .....	120
6.6.2	Barrier Properties of films .....	123
6.6.2.1	OTR.....	123
6.6.2.2	WVTR.....	124
6.6.3	Surface morphology of coated paper surfaces .....	125
6.6.4	SEM spectroscopy .....	127
6.6.4.1	Paper uncoated and coated surface .....	127
6.6.4.2	Paper uncoated and coated cross-section surface.....	129

6.6.5	Life Cycle Analysis .....	131
6.7	CONCLUSION .....	135
6.8	CRedit (CONTRIBUTOR ROLES TAXONOMY) .....	136
6.9	Declaration of generative AI and AI-assisted technologies in the writing process .....	137
6.10	ACKNOWLEDGEMENTS .....	137
6.11	REFERENCES .....	137
Chapter 7 - Supplementary Experimental Analyses and Methodological		
	Constraints .....	141
7.1	Formulation Behavior and Initial Optimization .....	142
7.1.1	Design of an Initial Formulation Model .....	142
7.1.2	Influence of PVA Concentration on Viscosity and Film Integrity .....	143
7.1.3	The Function and Enhancement of Glycerol as a Plasticizer ....	143
7.1.4	Extra Validation and Optimization Data Acquired During Internship Work .....	144
7.2	Early-Stage Antibacterial Observations .....	146
7.3	Constraints of Characterization .....	147
7.4	Antibacterial Testing Initiatives .....	149
7.4.1	Justification for Antibacterial Assessment .....	150
7.4.2	Formulation of Antibacterial Testing Protocols .....	150
7.4.3	Bacterial Strains and Their Preparation .....	151
7.4.4	Comprehensive Examination of Antibacterial Testing Methodologies and Outcomes .....	151
Chapter 8 - Conclusion .....		
	References .....	157

## List of Figures

Figure 1.1 Biomass usage in concept of circular bioeconomy [3] .....	2
Figure 1.2 Series of chapters .....	6
Figure 2.1 Lignocellulosic biomass composition [23].....	8
Figure 2.2 Cellulose structure [27].....	9
Figure 2.3 Hemicellulose [29] .....	9
Figure 2.4 Lignin macromolecule structure [32].....	10
Figure 2.5 Nanocellulose application [48].....	13
Figure 2.6 Ionic group addition processes [47] .....	14
Figure 2.7 Structure of TEMPO [58] .....	16
Figure 2.8 Structure of 4-acetamido-TEMPO [60] .....	16
Figure 2.9 Polypyrrole structure [62].....	17
Figure 3.1 TEMPO Oxidation [53] .....	31
Figure 3.2 Pictures taken during TEMPO oxidation process .....	31
Figure 3.3 IKA Process [102].....	34
Figure 3.4 IKA and TOCN formation.....	34
Figure 3.5 Formation of TOCN-PPy.....	35
Figure 3.6 TOCN-PPy on plywood.....	39
Figure 4.1 Formation of TOCN-PPy-PVA-Glycerol based paints .....	58
Figure 4.2 Rheological behaviour of TOCN-PPy-PVA-Glycerol based paints .....	63
Figure 4.3 Scanning electron microscopy for the TOCN-PPy, TOCN-PPy-PVA and TOCN-PPy-PVA-Gly2 .....	66
Figure 4.4 Raman spectroscopy of TOCN-PPy-PVA-Glycerol based paints .....	68
Figure 4.5 Thermogravimetric analysis of TOCN-PPy-PVA-Glycerol based paints .....	71
Figure 4.6 Differential scanning calorimetry analysis of TOCN-PPy-PVA- Glycerol based paints .....	73
Figure 4.7 (a) Circuit with aluminum disk, (b) open circuit, (c) with TOCN- PPy-PVA, (d) with TOCN-PPy-PVA-Gly2, (e) with TOCN- PPy-PVA-Gly2, (f) with TOCN-PPy-PVA-Gly5 .....	75
Figure 4.8 (a) Pyrrole, (b) Polyvinyl alcohol, (c) Glycerol, (d) TOCN, (e) Proposed TOCN-PPy structure .....	76
Figure 4.9 PVA-Glycerol interaction.....	77

Figure 5.1 Experimental workflow for evaluating the environmental behavior of TOCN-PPy-PVA-Glycerol coatings. ....	91
Figure 5.2 Calibration standards (Concentration (PPM) vs CPS) for ICP-OES analysis of Fe at two emission lines (Fe 238.204 and Fe 259.939) .....	92
Figure 5.3 pH values of water collected after each washing cycle (W0-W4) for TOCN-PPy films. Measurements were taken in triplicate .....	95
Figure 5.4 Iron concentrations (mg/L) in washing solutions from various TOCN-PPy-based formulations measured by ICP-OES .....	97
Figure 5.5 Percent weight loss of TOCN-PPy-based coatings after 60 days of soil burial. Weight loss increased with glycerol content .....	101
Figure 5.6 Schematic of the hydrothermal recovery process used to evaluate recyclability of TOCN-PPy-PVA-Gly coatings .....	103
Figure 6.1 System boundaries of the life cycle assessment (LCA) for TOCN-PPy-based paints, covering raw material acquisition, synthesis, coating deposition, washing, and projected end-of-life. ....	118
Figure 6.2 Tensile Stress vs Deformation for TOCN-PPy-PVA-Glycerol base paint films .....	123
Figure 6.3 Water Vapor Transmission Rate (WVTR) of TOCN-PPy-PVA-Glycerol Films at 50% and 70% Relative Humidity .....	125
Figure 6.4 2D Alicona surface images showing morphological changes in coated and uncoated UPM paper .....	127
Figure 6.5 SEM surface morphology of uncoated and TOCN-PPy-PVA-Gly-coated UPM paper at 100× magnification .....	129
Figure 6.6 Cross-sectional SEM images of uncoated and TOCN-PPy-PVA-Glycerol-coated UPM paper samples at 2000× magnification .....	130
Figure 6.7 LCA each component impact for TOCN-PPy-PVA .....	134
Figure 6.8 Comparative life cycle impact of TOCN-PPy-based coatings formulated with varying glycerol content (Gly0, Gly1, Gly2, Gly5), indicating the influence of formulation on overall sustainability performance (According to IPCC 2021 GWP100 V1.03) .....	135
Figure 7.1 <i>Listeria monocytogenes</i> impact on TOCN, TOCN-PPy, TOCN-PPy-Synthetic glue .....	147
Figure 7.2 EDS of TOCN-PPy, TOCN-PPy-PVA and TOCN-PPy-PVA-Gly2 .....	149

## List of Tables

Table 4.1 Viscosity of TOCN-PPy-PVA-Glycerol based paints .....	65
Table 4.2 Contact angle measurement of TOCN-PPy-PVA-Glycerol based paints .....	69
Table 5.1 Experimental Design: Formulations of TOCN-PPy-PVA-Glycerol Coatings with Varying Glycerol Content .....	90
Table 5.2 Pyrrole detection in water extracts after 24 h immersion via HPLC- MS/MS. All samples showed non-detectable levels .....	99
Table 5.3 Glycerol detection in water extracts using HPLC-MS/MS. Detection was observed only in Gly2 and Gly5 samples, increasing with glycerol loading .....	100
Table 6.1 Composition of TOCN-PPy-based paint per A4 UPM paper sheet (0.062 m <sup>2</sup> ), showing quantities of each raw material for scaling in LCA .....	119
Table 6.2 Tensile properties of TOCN-PPy-PVA-based films.....	122
Table 6.3 OTR data for the TOCN-PPy-PVA-Gly coating .....	124
Table 6.4 Quantitative Surface Topography Parameters of TOCN-PPy-PVA- Glycerol Coated and Uncoated UPM paper Analyzed by Alicona Profilometry.....	126
Table 6.5 Input materials, energy flows, and emission factors used in the LCA model with corresponding data sources .....	133

## List of Abbreviations

<b>Abbreviation</b>	<b>Full Term</b>
CNF	Cellulose Nanofibers
DSC	Differential Scanning Calorimetry
Gly	Glycerol
HPLC-MS/MS	High Performance Liquid Chromatography – Tandem Mass Spectrometry
ICP-OES	Inductively Coupled Plasma – Optical Emission Spectroscopy
LCA	Life Cycle Assessment
MEB	Scanning Electron Microscope (French: Microscopie Électronique à Balayage)
OTR	Oxygen Transmission Rate
PPy	Polypyrrole
PVA	Polyvinyl Alcohol
SEM	Scanning Electron Microscopy
TEMPO	2,2,6,6-Tetramethylpiperidine-1-oxyl
TGA	Thermogravimetric analysis
TOCN	TEMPO-Oxidized Cellulose Nanofibers

# Chapter 1 - Introduction

The continuous pursuit of sustainable development has propelled the integration of circular economy and bioeconomy principles into modern industrial practices. Among the key pillars supporting this transition, the valorization of lignocellulosic biomass and the development of bio-based functional materials have gained significant attention. This chapter introduces the background and context motivating the research, identifies the problems associated with traditional coatings, presents the research objectives and scope, and outlines the structure of the thesis.

## 1.1 Circular Economy and Bioeconomy Concepts

The increasing global emphasis on environmental sustainability has led to the emergence of two key paradigms: the circular economy and the bioeconomy, which are described as per [1]. The circular economy promotes minimizing resource consumption, maximizing product life cycles, and designing materials that can be reused, recycled, or safely degraded. The bioeconomy focuses on the sustainable production and conversion of biomass into value-added products, such as materials, chemicals, and energy.

Together, these frameworks aim to transition industries away from the traditional "take-make-dispose" linear model toward regenerative systems as per [2], for assisting in diminishing dependence on fossil fuels, decreasing greenhouse gas emissions, and advocating for the utilization of renewable and biodegradable materials. The Figure 1.1 illustrates the circular bioeconomy cycle using biomass as a feedstock.

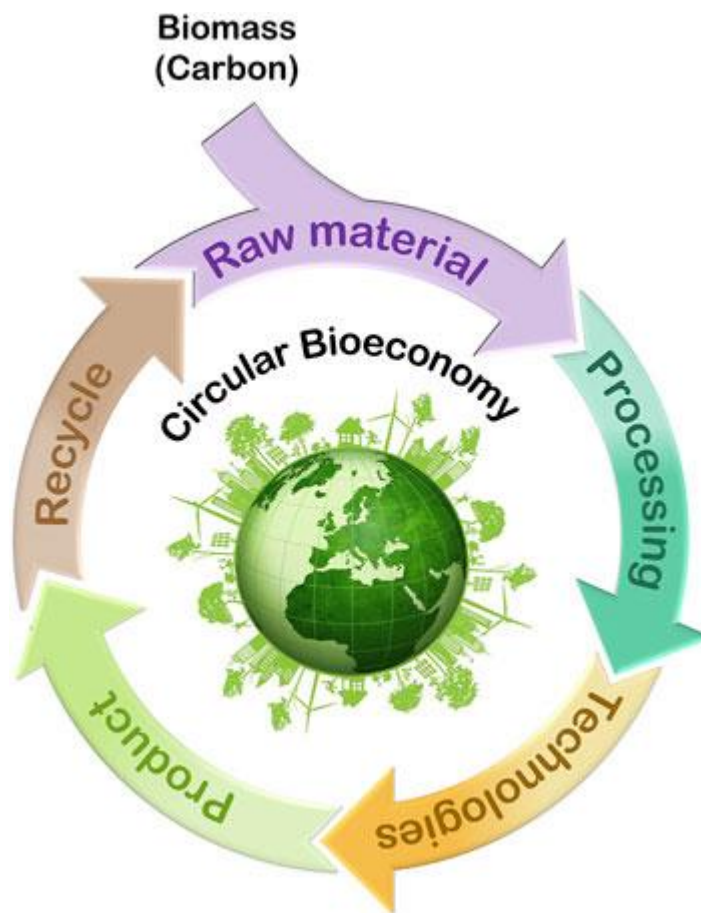


**Figure 1.1** Biomass usage in concept of circular bioeconomy [3]

In the context of material science, the development of bio-based coatings aligns with these principles by offering renewable, environmentally responsible alternatives to conventional synthetic coatings [4].

## 1.2 Biomass-Based Coatings as Sustainable Alternatives

Conventional petroleum-based coatings, although providing superior durability and performance, have considerable environmental issues, including a substantial carbon footprint during production and the release of volatile organic compounds (VOCs). Non-biodegradability and microplastic pollution [5-7].

Biomass-derived coatings from renewable feedstocks, including lignocellulosic materials, offer viable alternatives by minimizing environmental impacts, promoting resource circularity, and providing biodegradability at the end of their life cycle stages [8-9].

However, challenges such as moisture sensitivity, mechanical brittleness, and limited functional properties often restrict the direct application of bio-based coatings. Thus, functional enhancement strategies, such as chemical modification and composite formulation, are required to broaden their applicability [10-11].

### **1.3 Nanocellulose and Conducting Polymers for Coatings**

Nanocellulose, particularly TEMPO-oxidized cellulose nanofibers (TOCNs), has gained attention as a high-performance material for different applications as per [12-15] due to its high tensile strength (when incorporated with other copolymer), surface modifiability, low density, and biodegradability. However, pure nanocellulose coatings typically suffer from: Brittleness; Hydrophilicity; Lack of electrical conductivity. To mitigate these constraints, conductive polymers like polypyrrole (PPy) present a supplementary option by delivering electrical conductivity, serving as a natural black pigment, and improving barrier characteristics via their dense conjugated networks [16-17]. Thus, combining TOCN with polypyrrole, and further modifying the composite with additives like polyvinyl alcohol (PVA) and glycerol, creates a multifunctional platform for developing flexible, adhesive, conductive, and partially biodegradable coatings.

### **1.4 Research Objectives**

The main objective of this research is to develop and characterize sustainable TOCN-PPy-based coatings modified with copolymers to optimize their functional performance and environmental behavior.

The specific objectives include the synthesis of TOCN-PPy composites through in-situ oxidative polymerization, the improvement of coating adhesion and flexibility by integrating PVA and glycerol, the characterization of surface properties, mechanical strength, and barrier performance, and the assessment of application potential in packaging, surface treatments, and functional coatings. This study conducts comprehensive Fe-leaching experiments, addressing a critical safety concern for food-contact applications, unlike other research not focused on iron leaching. Due to the utilization of iron salts as oxidizing agents in PPy polymerization, there exists a previously

potential for residual Fe to migrate from the coating under specific conditions. Consequently, evaluating Fe leaching is a crucial factor in ascertaining the environmental and food-safety compatibility of the formulated coatings.

## 1.5 Thesis Structure

This thesis is structured into seven main chapters, each addressing a specific aspect of the research work and contributing to a coherent progression from the scientific context to the practical application and environmental evaluation of the developed TOCN–PPy–PVA–Gly coatings. Figure 1.2 presents a schematic overview of this structure, which is described in detail below:

**Chapter 1 – Introduction** presents the background of the research, rooted in the principles of circular economy and bioeconomy. It introduces the challenges posed by petroleum-based coatings and positions nanocellulose and conductive polymers as promising alternatives. The research objectives, scope, and thesis organization are also defined.

**Chapter 2 – Literature Review** section provides a comprehensive analysis of the current state of knowledge concerning lignocellulosic biomass, nanocellulose (especially TOCN), and conductive polymers such as polypyrrole. It critically reviews existing coating technologies, identifies their limitations, and highlights the potential for bio-based, conductive coatings in packaging and functional surfaces.

**Chapter 3 – Research Project Development and Problem Analysis** outlines the preliminary methodology and experimental development conducted outside of the published articles. It details the synthesis of TOCN, the polymerization of polypyrrole, the formulation of paints using PVA and glycerol, and the observed problems related to adhesion and brittleness. It also introduces the rationale behind using plasticizers and binders to improve coating performance.

**Chapter 4 – Article 1** is the peer-reviewed article focuses on the synthesis and physicochemical characterization of TOCN–PPy–PVA–Gly paints. It discusses

formulation strategies and presents results from rheology, SEM, Raman spectroscopy, thermal analysis (TGA/DSC), contact angle measurements, and qualitative conductivity tests.

**Chapter 5 – Article 2** article investigates the environmental behavior of the developed coatings. It includes leaching studies (pH, ICP-OES, HPLC-MS/MS), soil biodegradability tests, and an evaluation of reusability via hydrothermal solubilization. The article addresses concerns about polypyrrole's environmental impact and supports the material's suitability for sustainable applications.

**Chapter 6 – Article 3** article focuses on the performance of the coatings when applied to UPM paper substrates. It assesses mechanical strength, oxygen and water vapor transmission rates (OTR/WVTR), surface morphology via Alicona and SEM, and integrates a preliminary life cycle assessment (LCA) to evaluate environmental impacts associated with formulation changes.:

Important additional research that supports the design and development of the TOCN-PPy coating system but was left out of the thesis's article-based parts is included in **Chapter 7**. The purpose of these extra experiments is to transparently describe the practical behavior, processing limitations, and methodological restrictions that were encountered during the material creation process. In order to place the results within larger research trends and show how this work complements or adds to current knowledge, the results are interpreted in conjunction with external papers. The choice of feasible compositions was influenced by the sensitivity in viscosity, film integrity, and surface morphology that were discovered during early formulation trials that concentrated on the interactions between TOCN-PPy dispersions, structural polymers, and plasticizers. There is also discussion of instrumental limits, such as the challenges of identifying components at low concentrations. Overall, this chapter places the coating system in a broader scientific framework by fusing ideas from external studies with internal experimental judgments.

The thesis is concluded in **Chapter 8** with a summary of the main findings, a list of the scientific and technological contributions, and suggestions for further research. The study's key findings are summarized in this chapter, which highlights the importance of

TOCN-PPy hybrid coatings in developing sustainable functional coating technologies. It goes on to discuss the work's practical ramifications, such as possible industrial uses, scaling issues, and unresolved issues that need more research. The chapter concludes by offering suggestions for further study, such as improved performance testing to facilitate practical implementation, material optimization, and integration with other bio-based polymers.

Furthermore, the initially planned antibacterial testing was omitted from this study due to its considerable time demands, necessity for specialist facilities, and the comprehensive experimental optimization required, which exceeds the timetable of the current project. Although antibacterial efficacy is crucial for specific coating applications, its accurate evaluation necessitates an extensive research endeavor – encompassing strain selection, culture preparation, standardized contact-time protocols, and long-term efficacy assessments – more appropriate for a specialized, full PhD-level study.

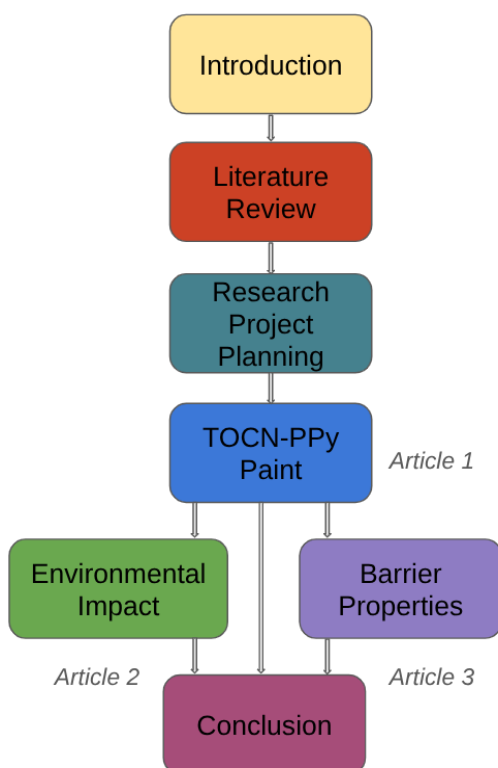


**Figure 1.2** Series of chapters

## Chapter 2 - Literature review

A comprehensive understanding of the fundamental materials, modification techniques, and prior research is essential to frame the development of advanced bio-based coatings. This chapter systematically reviews the relevant literature concerning lignocellulosic biomass components, nanocellulose fabrication and functionalization, conductive polymers like polypyrrole, and current trends in sustainable coating technologies. Identified research gaps, potential applications, and environmental considerations are also discussed to justify and guide the present research work.

### 2.1 Overview of Lignocellulosic Biomass

Lignocellulosic biomass is one of the most abundant renewable resources available globally, composed mainly of three biopolymers: cellulose, hemicellulose, and lignin [18]. These structural components are organized within the plant cell wall in a highly hierarchical manner, providing mechanical strength, flexibility, and resistance to environmental stresses [19].

In a sustainable bioeconomy paradigm, lignocellulosic biomass is crucial due to its vast geographic spread, abundant availability and renewability, affordability, and potential for conversion into high-value chemicals and minerals [20].

In recent years, lignocellulosic biomass has gained significant attention as a feedstock for bio-based materials, including nanocellulose, bioplastics, bio-based composites, and advanced coatings [21]. The Figure 2.1 shows Lignocellulosic biomass comprises three essential components—cellulose, hemicellulose, and lignin, in which the P-coumaryl, coniferyl, and sinapyl alcohol are the fundamental compounds, known as monolignols, that polymerize via radical reactions to constitute lignin. Upon incorporation into the lignin structure, they form the p-hydroxyphenyl (H), guaiacyl (G), and syringyl (S) units, respectively [22].

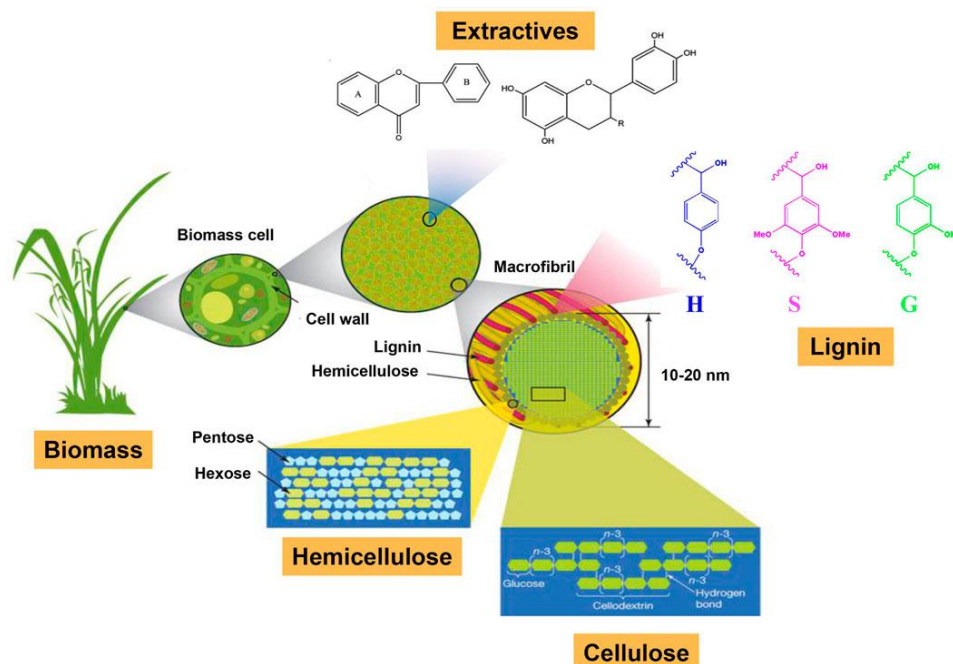


**Figure 2.1** Lignocellulosic biomass composition [23]

The structure of lignocellulosic biomass comprises multiple essential components, each imparting unique chemical and functional characteristics. Their compositions are detailed below [24].

### 2.1.1 Cellulose (40–50% of biomass)

A linear polysaccharide made of  $\beta$ -1,4-linked D-glucose units, forming crystalline microfibrils responsible for the mechanical strength of the cell wall [25]. The most prevalent organic polymer on planet is cellulose. There are several hydroxyl groups along the cellulose backbone as a result of the polysaccharide structure of cellulose. These hydroxyl groups can create dense crystalline structures by forming well-organized hydrogen bonding networks. The amorphous area of cellulose is created by the uneven arrangement of incomplete cellulose chains [26]. Figure 2.2 illustrates the structure of cellulose.

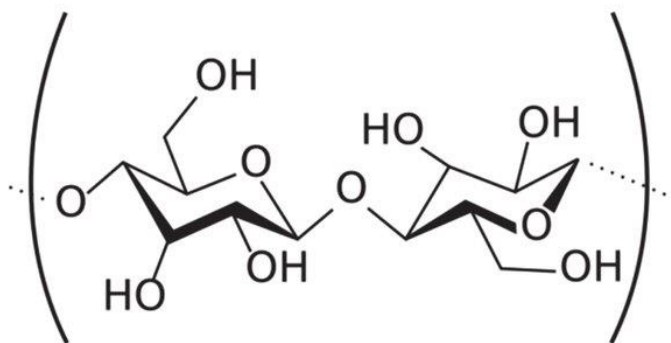


**Figure 2.2** Cellulose structure [27]

### 2.1.2 Hemicellulose (25–35% of biomass)

A heterogeneous group of polysaccharides (e.g., xylans, mannans) that are amorphous and serve as a matrix embedding the cellulose microfibrils [28].

Figure 2.3 below illustrates hemicellulose's structure.

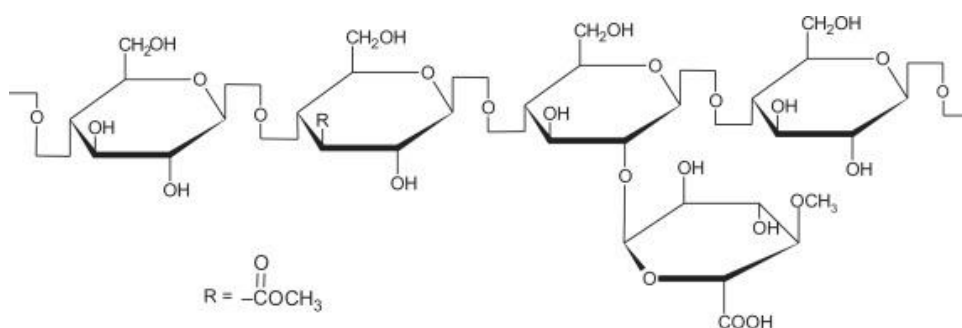


**Figure 2.3** Hemicellulose [29]

### 2.1.3 Lignin (15–20% of biomass)

A complex, amorphous polyphenolic polymer that acts as a natural adhesive, providing rigidity, hydrophobicity, and resistance to microbial attack [30-31]. Lignin adds flexibility, also aiding in the binding of the cellulose/hemicellulose matrices. It is regarded as nature's largest storehouse of aromatic molecules. Benzene rings containing methoxy, hydroxy, and propyl group make up the majority of the carbon-ring structures in the exceedingly random and chaotic molecular structure of lignin polymers, which are joined

by polysaccharides (sugar polymers). Lignin's ring structures offer a large number of possibilities as useful chemical intermediate compound. But lignin recovery and separation are challenging [29]. The structure of Lignin illustrated in Figure 2.4.

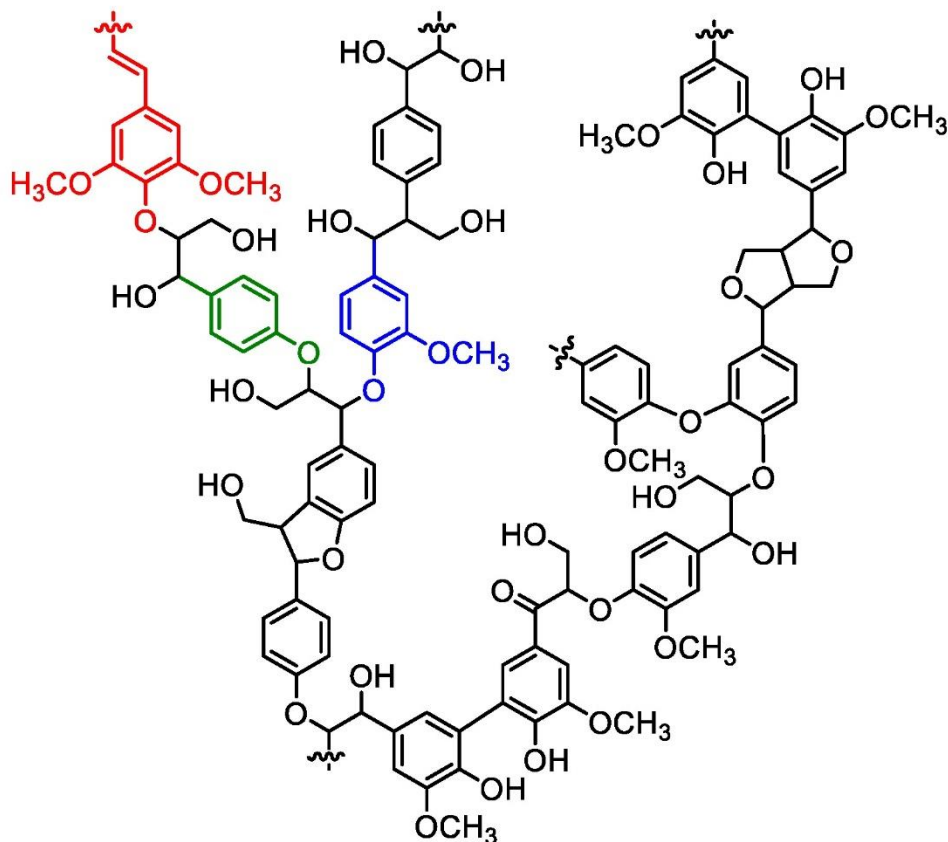


**Figure 2.4** Lignin macromolecule structure [32]

These three polymers are intricately bound together through interactions, forming a composite material that is difficult to deconstruct without pretreatment [33-34].

## 2.2 Importance for cellulose-based coatings

Among the constituents of lignocellulosic biomass, cellulose has become the most appealing option for the creation of sustainable coatings and composites because of its remarkable surface modifiability, high mechanical properties, and biodegradability, especially through chemical oxidation or grafting [35].

Additional benefits of nanocellulose, which is produced by carefully breaking down cellulose microfibrils, include a high specific surface area, superior barrier qualities, and, depending on the processing circumstances, the potential for transparency [36].

As such, nanocellulose is particularly well-suited for formulating next-generation bio-based coatings with customized features, including improved adhesion, barrier effects, and functional surface activity.

### **2.3 Nanocellulose: Properties and applications**

Nanocellulose refers to cellulose-based materials that exhibit at least one dimension in the nanometer range. Derived from natural lignocellulosic sources, nanocellulose possesses a unique combination of mechanical, barrier, and surface properties that make it highly attractive for a wide range of advanced material applications [37].

There are four main types of nanocellulose, distinguished by their morphology, production methods, and properties.

#### **2.3.1 Cellulose Nanocrystals (CNCs)**

Highly crystalline rod-like particles, typically obtained through acid hydrolysis of cellulose fibers. CNCs exhibit exceptional mechanical strength and high aspect ratios [38].

#### **2.3.2 Cellulose Nanofibers (CNFs)**

Long, flexible fibrils with both amorphous and crystalline regions, produced by mechanical shearing, often combined with enzymatic or chemical pretreatments (such as TEMPO-mediated oxidation). CNFs possess high entanglement ability and outstanding film-forming properties [39].

#### **2.3.3 Bacterial Nanocellulose (BNC)**

Pure nanocellulose produced by certain bacterial strains (e.g., *Gluconacetobacter xylinus*) through fermentation processes, characterized by extremely high purity and water-holding capacity [40].

### **2.3.4 Cellulose microfibrils (CMF)**

CMF are elongated, highly organized structures within plant cell walls that confer mechanical strength and rigidity. They comprise densely arranged cellulose chains featuring both crystalline and amorphous domains, reinforced by significant hydrogen bonding [38].

Cellulose nanofibers (CNFs) generated using TEMPO-mediated oxidation are particularly pertinent to this PhD project, as they provide an optimal combination of mechanical reinforcement, surface modifiability, and ecological sustainability for the development of bio-based coatings. The subsequent sections will provide a comprehensive analysis of several forms of nanocellulose and their preparation techniques [14].

### **2.3.5 Applications of Nanocellulose**

Thanks to its outstanding properties, nanocellulose has found applications across multiple fields. As a biodegradable barrier layer to replace petroleum-derived films in food packaging [41]. For imparting oxygen, grease, or UV-barrier properties to paper, wood, or plastic surfaces [42]. As scaffolds for tissue engineering, drug delivery carriers, and wound dressings [43]. As a mechanical reinforcement agent in polymers, rubbers, or hydrogels [44]. Transparent substrates for flexible electronics, supercapacitors, and batteries [45]. As filters or absorbents for water purification and pollutant capture [46].

Many of the beneficial qualities associated with cellulose, such as low density, nontoxicity, and high biodegradability, are also present in nanocellulose, which is either extracted from plant matter or biochemically generated in a laboratory. However, due to its distinctive shape, size, surface chemistry, and high degree of crystallinity, it also possesses special qualities, such as high mechanical strength, reinforcing powers, and tuneable self-assembly in aqueous media [47]. Nanocellulose find applications in wide spectrum of usage from the medical to industrial application. Figure 2.5 represents nanocellulose application in today's economy sector.

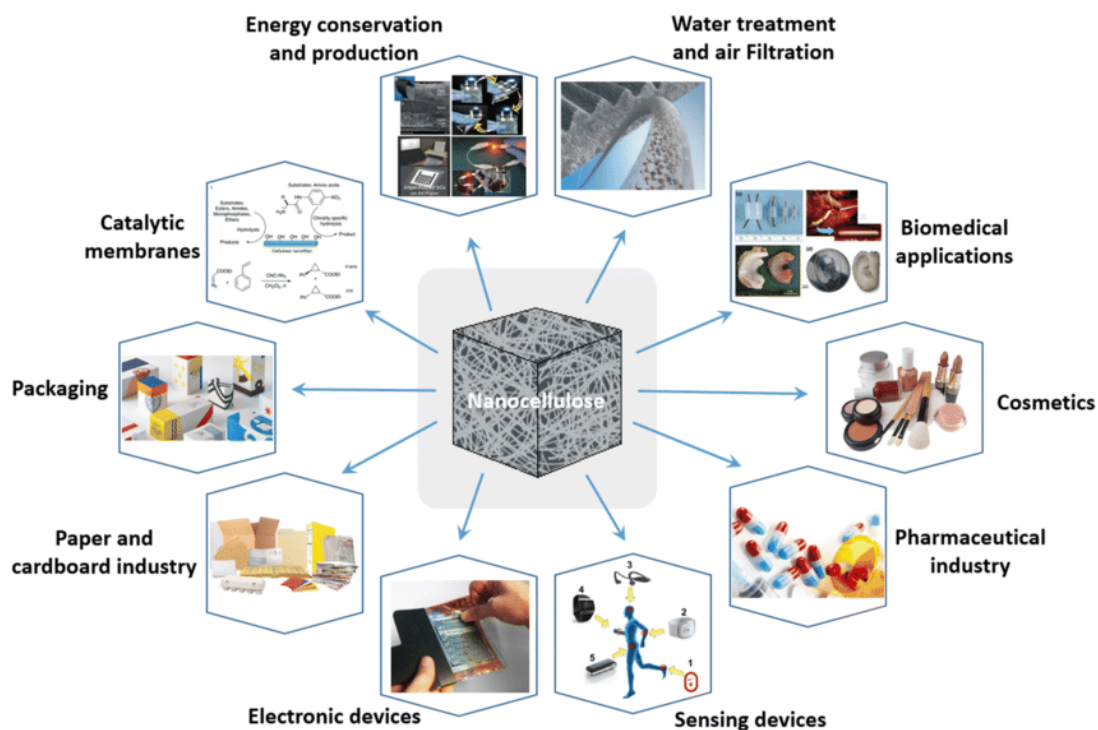


**Figure 2.5** Nanocellulose application [48]

In the context of this project, CNF serve as the primary bio-based matrix for developing functional coatings with targeted adhesion, conductivity, and barrier properties. Their high surface charge and fibrillar network structure provide an ideal platform for the integration of conductive polymers like polypyrrole and functional additives such as polyvinyl alcohol and glycerol.

## 2.4 Surface Modification Techniques for Nanocellulose

Although nanocellulose offers excellent intrinsic properties, its native surface is highly hydrophilic due to abundant hydroxyl groups, which limits its compatibility with hydrophobic materials and reduces its performance under high-humidity conditions. Therefore, surface modification techniques are often employed to tailor the physicochemical characteristics of nanocellulose for specific applications, such as enhancing barrier properties, introducing functional groups, improving dispersion in polymer matrices, or imparting electrical conductivity. Several chemical and physical approaches have been explored to modify nanocellulose surfaces. Among them, ionic group addition, hydrophobic functionalization, and grafting of polymers are widely used.

In this project, TEMPO-mediated oxidation was selected as the primary surface modification strategy due to its efficiency, selectivity, and suitability for aqueous processing [14].

Ionic charges can be added to the nanocellulosic surface via a variety of surface modification techniques, giving the surface a hydrophilic quality. Following Figure 2.6 show types of processes that can be taken into consideration based of the type of group to be attached.

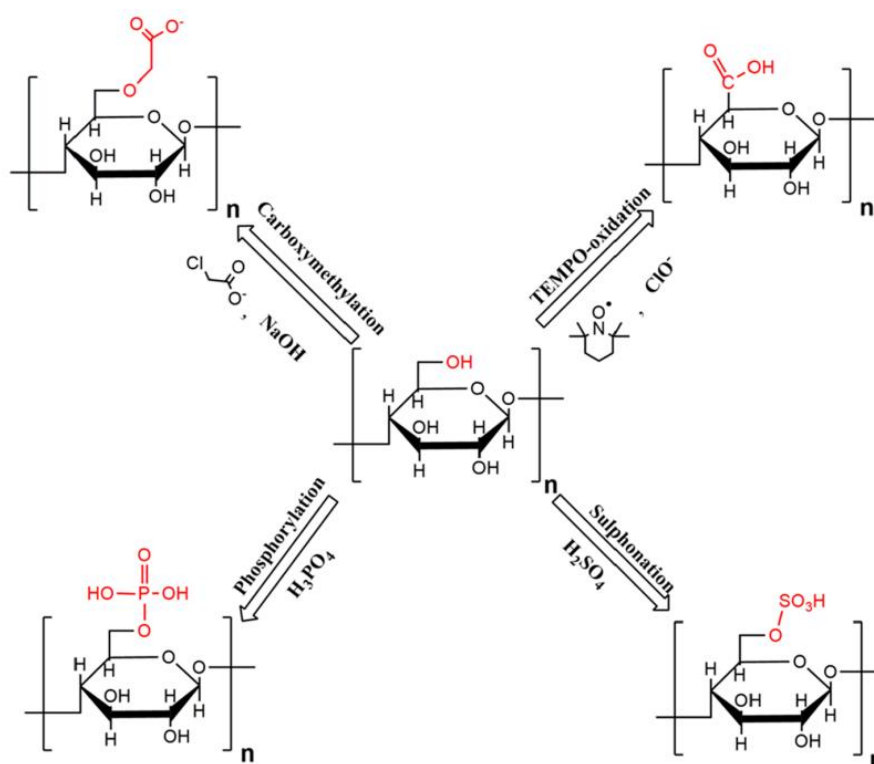


**Figure 2.6** Ionic group addition processes [47]

To replace halogen-based chemicals in flame-retardant composites, wood-derived cellulose can be improved. To do this, phosphorylation of nanocellulose was utilised to chemically modify sulfite-dissolving pulp fibres. The resulting material was then used to create cellulose nanofibrils (CNF), which had a width of about 3 nm [49]. The carboxymethylation method adds carboxymethyl groups to cellulose surfaces, making them negatively charged form. These charges produce electrostatic repulsions that help lignocellulosic fibres break down into nanoparticles. By homogenising

carboxymethylated cellulosic fibres, [50] developed NFCs, which had a diameter of 5–15 nm [47], [51]. Other approach for adding anionic charges to the surface of nanocellulose is sulfonation. The hydrolysis of the monomers is catalysed by concentrated sulfuric acid employed in CNC synthesis, which also facilitates the generation of sulphate half-esters from CNC hydroxyl groups. Stable colloidal suspensions of cellulose nanocrystals are produced as a result of sulfuric acid hydrolysis [47], [52]. With benefits for position-selective reaction at room temperature under aqueous conditions, 2,2,6,6-Tetramethylpiperidine-1-oxyl radical (TEMPO)-mediated oxidation is a special reaction to the native and regenerated celluloses. The C6-primary groups of hydroxy on crystalline cellulose microfibril surfaces are largely transformed to sodium C6-carboxylate groups when the TEMPO/NaBr/NaClO oxidation is applied to native celluloses in water at pH 10 [53].

#### **Key advantages of TEMPO-oxidized cellulose nanofibers (TOCNs):**

The augmented negative surface charge improves electrostatic stabilization in aqueous solutions, while the heightened reactivity facilitates additional functionalization, including the attachment of conductive polymers. These alterations enhance dispersion capability and film-forming characteristics, while also offering the potential for increased hydrogen bonding and ionic interactions with other polymers and substrates.

Moreover, in comparison to alternative techniques for adding carboxyl groups, TEMPO oxidation represents a milder and less aggressive approach, rendering it particularly appropriate for the production of TEMPO-oxidized nanocellulose. Moreover, our research group has developed a robust foundation on TOCN-PPy creation, which acts as a significant building block for the current effort [54-56].

#### **2.5 2,2,6,6,tetramethylpiperidine-1-oxyl (TEMPO)**

Being key element of (TEMPO)-mediated oxidation process, TEMPO provides a platform for the native celluloses for completely distributed in water to the level of individual nanofibrils or elementary fibrils. When polysaccharides are oxidised using the TEMPO process, sodium carboxyl groups are added to the surfaces of the elementary fibrils of

cellulose. TEMPO-induced oxidation causes electrostatic repulsion to arise between cellulose fibrils and inhibits the creation of potent interfibrillar hydrogen bonds. Additionally, cellulose crystallites exhibit no oxidation [57]. Figure 2.7 shows the structure of TEMPO.

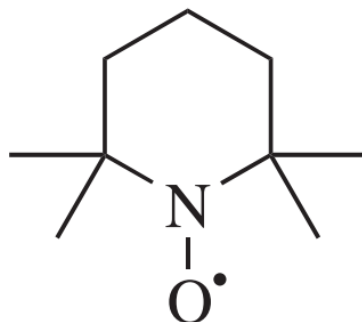


**Figure 2.7** Structure of TEMPO [58]

### 2.5.1 4-acetamido-TEMPO

The following Figure 2.10 illustrate the structure of 4-acetamido-TEMPO. A new TEMPO system that uses 4-acetamido-TEMPO and operates in the acidic to neutral pH range has been developed for the oxidation of both native and regenerated celluloses. The fundamental benefit of this new TEMPO system is that cellulose degradation is much reduced, making it possible to maintain the degree of polymerisation over a wide area after TEMPO adjustments [59]. Figure 2.8 illustrates the structure of 4-acetamido-TEMPO.

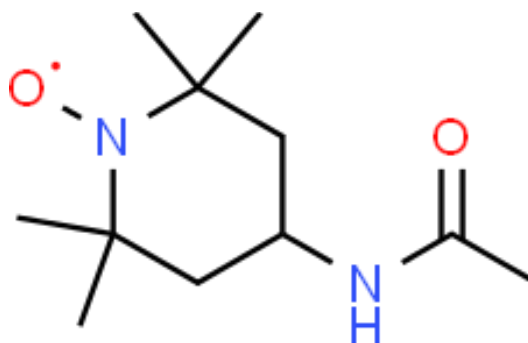


**Figure 2.8** Structure of 4-acetamido-TEMPO [60]

## 2.6 Polypyrrole (PPy) and Conductive Polymers

Polypyrrole (in Figure 2.9) is synthesized through the oxidative polymerization of pyrrole monomers ( $C_4H_5N$ ), leading to a conjugated polymer backbone with alternating single and double bonds that facilitate delocalization of electrons [61].

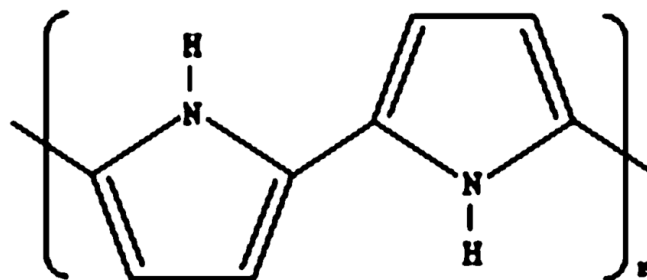


**Figure 2.9** Polypyrrole structure [62]

Key properties of PPy include are electrical conductivity, environmental stability, biocompatibility, processability, optical properties.

### 2.6.1 Alternative Conductive Polymers

While polypyrrole (PPy) was chosen as the conductive polymer for this project due to its easy synthesis, intrinsic black coloration, and environmental stability, other conductive polymers also been explored as potential alternatives for bio-based composite and coating applications. These polymers exhibit unique properties that could offer complementary or improved performance depending on the target applications.

#### 2.6.1.1 Polyaniline (PANI)

Polyaniline (PANI) is a well-established conductive polymer known for antibacterial properties, PANI can produce hydrogen peroxide during oxidation, contributing to antimicrobial action [63]. For barrier properties, PANI can reversibly switch between oxidation and reduction states, making it suitable for corrosion protection and barrier applications [64]. For electrical conductivity, PANI can be easily doped with acids to enhance its conductivity and shows good environmental stability [65].

### **2.6.1.2 Polythiophene**

Polythiophene and its derivatives are another class of conjugated polymers offering antibacterial properties, Polythiophene exhibits antibacterial properties in flexible film as dopant [66]. For barrier properties, Polythiophene structures provide robust environmental stability, aiding in protection against external stresses [67]. For electrical conductivity, Polythiophene typically exhibits conductivity greater than 100 S/cm and offers excellent thermal and chemical stability [68].

Among the available conductive polymers, pyrrole was selected over polyaniline, and polythiophene due to its unique combination of easy, scalable, and water-based synthesis, intrinsic black pigmentation, good environmental stability, and compatibility with nanocellulose matrices. Unlike polyaniline, which suffers from poor solubility and film brittleness, polypyrrole forms flexible, adherent coatings under mild oxidative conditions without requiring harsh dopants or acid treatments. Compared to polythiophene, which demands complex synthesis routes and costly precursors, pyrrole polymerizes rapidly and controllably using inexpensive oxidants like FeCl<sub>3</sub>. Furthermore, while polyfuran offers antioxidant activity, it typically exhibits lower electrical conductivity and weaker mechanical performance than polypyrrole. Thus, the choice of pyrrole enabled the development of sustainable, multifunctional coatings with optimized conductivity, barrier properties, and black pigmentation, while maintaining a low-cost, environmentally responsible processing pathway [69].

## **2.7 Current Status of Coating Technologies**

Coatings are essential in several industries for surface protection, aesthetic enhancement, and the provision of certain functional attributes. The majority of coatings have been derived from petroleum, utilizing synthetic polymers and organic solvents, which may pose environmental and health risks due to factors such as restricted biodegradability, volatility, and possible toxicity [70].

### **2.7.1 Conventional Petroleum-Based Coatings**

Traditional coatings are primarily formulated using synthetic polymers such as polyurethane, epoxy resins, polyvinyl chloride (PVC), and acrylics [71]. These coatings offer excellent durability, chemical resistance, and versatility. However, they come with several drawbacks as per [72], due to their dependence on non-renewable resources, substantial carbon emissions during manufacture, release of volatile organic compounds (VOCs), and overall non-biodegradability, they contribute to prolonged environmental accumulation [5-7]. Additionally, disposal and recycling of synthetic coatings remain challenging, with many coatings ending up in landfills or contributing to microplastic pollution [5].

### **2.7.2 Emerging Trends Toward Bio-Based Coatings**

#### **2.7.2.1 Focus on biobased approach**

The move towards bio-based polymers focuses on replacing petroleum-derived components with renewable alternatives, such as [73], including polysaccharides like cellulose, starch, and chitosan; proteins such as casein and soy protein; natural oils like linseed and tung oil; and biopolyesters such as polylactic acid and polyhydroxyalkanoates.

#### **2.7.2.2 Why biobased approach important?**

These bio-based systems aim to provide [72], providing benefits include biodegradability, reduced toxicity, reduced environmental impact, and enhanced resource circularity via the utilization of agricultural or forestry by-products.

#### **2.7.2.3 Challenges with biobased approach**

However, fully bio-based coatings still face several performance challenges, particularly in terms of [74], delivering critical performance attributes including mechanical strength, moisture and oxygen barrier capabilities, and resilience in adverse environmental conditions.

### **2.7.3 Solution via hybrid approach**

Consequently, current study increasingly investigates hybrid systems that integrate bio-based matrices with functional fillers, such as conductive polymers, to address existing performance constraints [54].

### **2.7.4 Nanocellulose in Coating Applications**

#### **2.7.4.1 Why nanocellulose component of interest?**

Nanocellulose has emerged as a promising bio-based component for coatings due to its [75], providing robust mechanical reinforcing properties and a significant capacity for surface modification to enable additional functionalization.

#### **2.7.4.2 Challenge with only nanocellulose in coating?**

However, pure nanocellulose coatings challenging as per [75], due to their high hydrophilicity, they often demonstrate inadequate water-vapor barrier efficacy and may occasionally be susceptible to cracking during the drying process.

#### **2.7.4.3 Strategic approach to solve this issue**

To overcome these issues, strategies such as surface modification, plasticizer addition, and combination with hydrophobic polymers have been explored — approaches directly relevant to the development of the TOCN-PPy-PVA-Gly coatings in this work [69].

#### **2.7.4.4 Conductive Bio-Based Coatings: Opportunities and Challenges**

The integration of electrical conductivity into bio-based coatings remains a relatively underexplored field. Conductive coatings can enable applications in having prospective uses in flexible electronics, antistatic surfaces, electromagnetic shielding, and biosensors or intelligent packaging [76].

Conductive polymers such as polypyrrole (PPy), polyaniline (PANI), and PEDOT: PSS have been investigated to impart conductivity [77]. Nonetheless, other obstacles persist, such as attaining homogeneous distribution of conductive components, preserving overall

mechanical integrity, and reconciling electrical conductivity with biodegradability and environmental compatibility.

In this project, the combination of TOCN (for mechanical and barrier support) and PPy (for conductivity and pigmentation), supplemented by PVA and glycerol (for adhesion and flexibility), represents an innovative approach to developing sustainable, multifunctional coatings [69].

### **2.7.5 Application of TOCN-PPy in Coatings**

The combination of TOCN and PPy offers a promising platform for the development of multifunctional, sustainable coatings. TOCN provides a renewable, biodegradable matrix with high mechanical strength and barrier potential, while PPy imparts electrical conductivity, black pigmentation, and additional functional properties. When properly formulated, TOCN-PPy composites can be applied as surface coatings with applications across multiple sectors, including packaging, electronics, antimicrobial surfaces, and functional protective layers [16-17], [54], [56], [78].

### **2.7.6 Coating application via TOCN-PPy**

The three major aspects that previous work in our research group which investigated serve as the foundation for this thesis, propose application in a practical context, and address the difficulties associated with using TOCN-PPy film as a coating. The three components under conductivity, antibacterial nature, and barrier rigid support qualities that were studied are as follows:

#### **2.7.6.1 Conductivity nature**

Bideau et al. (2016) illustrated in order to graft on the carboxyl groups of CNFo, the 1-(2-cyanoethyl)pyrrole was first converted to N-(3-aminopropyl)pyrrole. Onto the grafted N-(3-aminopropyl)pyrrole, polypyrrole (Ppy) underwent oxidative polymerization in an iron(III) chloride (FeCl<sub>3</sub>) solution. By strengthening the potential connections across units of the conducting polymer and the cellulose fibres, the grafting of 1-(2-cyanoethyl)pyrrole was a key factor in improving these qualities. The results demonstrate that the coating of

PPy nanoparticles on the grafted films improves several properties of our composite, including wettability, mechanical properties, thermal protection, and most significantly, electrical conductivity, which has been enhanced by a  $10E5$  factor in contrast to the uncoated films. This nanostructure could be considered for creating high-performance electrodes for sensors, batteries, and supercapacitors, among other uses [79].

#### **2.7.6.2 Barrier rigid support nature**

Given this kind of packaging is renewable and reusable, it is of high interest. Benoit et al. (2018) illustrated the benefits of covering such paperboard with polypyrrole (PPy) and (2,2,6,6-Tetramethylpiperidin-1-yl)oxyl (TEMPO) oxidised cellulose nanofibres (TOCN). The strong network created by TOCN and polypyrrole particles considerably enhanced the coated paperboard's (CPb) mechanical characteristics and decreased gas permeability. These findings imply that polypyrrole surface coating may be used to produce multilayer paperboard containers in industrial settings, reducing the amount of packaging waste produced by the often-used traditional plastic [80].

#### **2.7.6.3 Antibacterial nature**

Gram-positive *B. subtilis* and Gram-negative bacteria *E. coli*, which are occasionally present in food, were used to test the nanocomposites' antibacterial abilities by Benoit et al. (2016). As seen by the decrease of 5.2 log colony forming units (CFU) for *B. subtilis* and 6.5 log CFU for *E. coli*, the results reveal that the nanocomposites are efficient against all of the bacteria examined. resulting in the complete annihilation of the germs under study. The exact match between the surface area of the composite and the ensuing inhibition zone has shown that our composite was contact active with only a minor leaching of PPy. Composite destroyed bacteria upon touch, it proved effective as an active packing on meat (liver), it can make application for preventing the spread of potential infections [81].

#### **2.7.6.4 Challenges**

The key challenge addressed via [81], of leaching must be addressed because it will play key role in the coating application in food packaging industry. Another problem is getting

TOCN-PPy to stick to the surface; this can be improved by using varied amounts of copolymer (e.g., PVA). Since customers prefer to see their products and prefer visibility in food packaging, the black colours of TOCN-PPy film are also a problem. The essential improvement that can be achieved with TOCN-PPy is to introduce it in a field where colour is not a real concern, or even if it can be a benefit. In this instance, a UV spectrometry test will be used, and if it is appropriate, TOCN-PPy, which has antibacterial properties as well as UV protection, can be introduced to large-scale packaging.

#### **2.7.6.5 Summary**

Prior research indicates that TOCN-PPy composites possess considerable potential; nevertheless, it has also underscored difficulties concerning adhesion, practical application efficacy, long-term durability, and environmental evaluation. This study directly tackles these deficiencies by modifying polymers using PVA and glycerol, optimizing formulations, conducting extensive environmental assessments, and pursuing application-focused development with an emphasis on barrier efficacy. The objective is to link essential material comprehension with the development of effective and sustainable coating solutions.

### **2.8 Potential Application Areas**

The advancement of multifunctional coatings based on TOCN-PPy composites has substantial prospects in industrial and environmental domains. These coatings effectively combine mechanical strength, barrier performance, electrical conductivity, flexibility, and natural black coloring, meeting the increasing demand for sustainable, practical, and environmentally responsible materials. The primary application domains with the greatest potential for TOCN-PPy-based coatings are delineated below:

#### **2.8.1 Food Packaging Coatings**

Sustainable food packaging materials are in high demand to replace petroleum-based plastics and to address issues of biodegradability, food safety, and barrier performance. TOCN-PPy-based coatings can contribute by providing oxygen and grease barrier layers

for paper-based packaging, enhancing mechanical strength and surface protection against moisture or handling damage, and offering antistatic or antimicrobial potential through polypyrrole integration (future studies). The black coloration could also be desirable for specific packaging designs (e.g., protective inner layers, specialty foods requiring light shielding).

### **2.8.2 Functional Surface Coatings for Wood and Rigid Materials**

TOCN-PPy-PVA-Gly coatings, especially on plywood and wood surfaces, offer: Improved surface adhesion and flexibility; Enhanced moisture resistance compared to untreated wood; Functional conductive properties for potential smart furniture or anti-static surfaces.

Such coatings could be applied to: Decorative panels; Protective furniture coatings; Indoor applications requiring both aesthetics and light functionality.

### **2.8.3 Sustainable Paints and Pigmented Coatings**

The deep black coloration of TOCN-PPy composites naturally suits applications requiring pigmented paints and coatings: Exterior and interior paints; Anti-corrosion primers; Decorative surface treatments.

Replacing synthetic black pigments (e.g., carbon black) with bio-derived, conductive pigments could provide both environmental and functional benefits.

## **2.9 Environmental and Toxicological Considerations**

Environmental safety and material end-of-life behavior are crucial factors when developing bio-based coatings intended for sustainable applications. The integration of polypyrrole (PPy) and the use of iron-based oxidants ( $\text{FeCl}_3$ ) in the TOCN-PPy coatings necessitate a careful evaluation of elemental leaching, biodegradability, and material stability under realistic conditions.

Specific environmental and toxicological investigations were carried out, focusing on Fe leaching, soil biodegradation behavior, and polypyrrole leaching phenomena.

## **2.10 Perspectives from External Research Groups and Innovation Positioning**

Significant research into high-performance bio-based coatings has been prompted by the global trend toward sustainable material systems [42]; advancements in this field have included metallic nanoparticles [82], natural polymers [83], lignin derivatives [84], nanocellulose [41], [54], and inorganic–organic hybrid coatings [85]. Numerous approaches have been provided by outside research teams with the goal of giving coating matrices mechanical strengthening [86], barrier improvement [87], antibacterial activity [88-89], and functional responsiveness [87]. Notwithstanding notable advancements, the current corpus of work is still dispersed and frequently concentrates on individual qualities or uses non-renewable components that restrict environmental compatibility. The advancements and weaknesses that drive the creation of more integrated, multipurpose, and sustainable coating systems are highlighted in a summary of these contributions.

### **2.10.1 Metal-nanoparticles based coating**

Metal-nanoparticle-based coatings, especially those that contain silver nanoparticles (AgNPs), are one extensively studied route [90-91]. Because of their potent and well-established antibacterial qualities, silver nanoparticles have drawn a lot of interest and are being researched for use in a variety of coating systems. AgNPs exhibit antibacterial action through a number of mechanisms, such as the release of silver ions, the production of reactive oxygen species (ROS), and the disruption of intracellular processes and microbial membranes, according to numerous external investigations. AgNPs offer efficient defense against a wide range of bacteria and fungi when they are embedded, chemically attached, or surface grafted into matrices including cellulose, chitosan, or synthetic polymers [91].

### **2.10.2 Chitosan based coating**

Because of its inherent antibacterial activity, potent film-forming capacity, and advantageous barrier qualities against UV light, gasses, and moisture, chitosan—a biodegradable cationic polysaccharide produced from crustacean exoskeletons—is frequently utilized in films, coatings, and membranes. Because of its mechanical strength, translucency, and versatility in processing through solvent casting, extrusion, electrospinning, thermoplastic

processing, layer-by-layer assembly, spraying, and dipping, it can be used in a wide range of food packaging and preservation applications. By lowering microbial contamination and increasing shelf life, it effectively protects fruits, vegetables, meat, seafood, dairy products, and other perishables. To improve chitosan's flexibility, water resistance, anti-oxidant activity, and antibacterial activity, its composition can be changed or new ingredients added. Beyond food systems, systematic research demonstrates that chitosan's antimicrobial and anti-adhesive efficacy for preventing implant-associated infections is greatly enhanced when combined with enzymes, antimicrobial peptides, or polymers. This highlights chitosan's wide potential as a functional, biocompatible coating material in both food and biomedical applications [92-94].

### **2.10.3 Lignin based coating**

The most prevalent polyaromatic biopolymer, lignin, has a rich and adaptable chemistry that makes it possible to use it in functional coatings and films. It can be used to replace polymers derived from fossil fuels and to create new material functionalities like improved barrier performance, oxygen scavenging, UV blocking, and antimicrobial activity. The pulp and paper industry already produces large amounts of technical lignin, and future biorefineries are expected to diversify further. Current research highlights lignin's applicability in polymer coatings, adsorbents, paper-sizing additives, wood veneers, food packaging, biomaterials, fertilizers, corrosion-resistant layers, and antifouling membranes. Lignin nanoparticles (LNPs) have also received a lot of attention because their formation is highly dependent on the structural heterogeneity of lignin. Research indicates that differences in residual fatty acids, carbohydrate content, and aliphatic hydroxyl groups affect LNP size, morphology, and the development of hollow structures, highlighting the need for a deeper understanding of the connection between lignin structure and nanoparticle formation mechanisms. Advanced manufacturing techniques have made it possible to employ lignin-derived functional composites in 3D printing, nanomaterials, hydrogels, biodegradable composites, and electrochemical systems, making them more promising eco-efficient materials than nanoparticles. While ongoing research continues to address structural bottlenecks and explore opportunities for developing next-generation biobased materials through green chemistry and sustainable processing, these lignin-based composites

have shown promise in environmental applications, biomedicine, sensing technologies, functional packaging, and energy storage [95-97].

#### **2.10.4 Multifunctional hybrid coating**

Multifunctional hybrid coatings intended to overcome material constraints in specialized applications like bioresorbable implants and stone conservation are the subject of another area of external research. Studies have created hybrid PEO-based structures for magnesium systems that combine polycaprolactone matrices with halloysite nanotubes loaded with corrosion inhibitors with porous ceramic-like layers to improve corrosion protection and regulate degradation behavior. These studies show how coating construction and performance verification have advanced, but they also highlight the need for a better comprehension of degradation mechanisms and long-term resorption management. For hydrophobic and biocidal stone-protection treatments, bio-based epoxy–silica hybrids containing plant-derived epoxy precursors, silica-forming additives, ionic liquids, essential oils, and functional nanoparticles have been studied concurrently. Systems enhanced by nanoparticles retain beneficial thermo-mechanical and hydrophobic properties and show effective microbial suppression, but certain additions interfere with network development and decrease thermal stability. When taken as a whole, these investigations highlight the difficulties associated with formulation stability, additive compatibility, and guaranteeing constant multifunctional performance while also demonstrating the promise of hybrid material techniques [98-99].

#### **2.10.5 The current work's position in relation to the state of the art**

The current study distinguishes itself in this broader scientific framework by tackling significant constraints seen in external systems. The TOCN–PPy system, in contrast to AgNP-enhanced coatings, employs conductive polymer mechanisms to provide antibacterial functionality while avoiding the use of metallic agents, thereby minimizing toxicity, lowering environmental risks, and conforming to circular biomaterial principles. While chitosan gives antibacterial activity, TOCN provides much greater modulus, dimensional stability, and network connection. The inclusion of PPy further compensates for functional limitations that chitosan can only overcome through synthetic additions or nanoparticles.

The homogeneity and optical constraints present in lignin-based films are overcome by the well-defined fibrillar structure of TOCN (-COOH), which permits controlled PPy deposition and a homogeneous hybrid network. The TOCN-PPy approach simultaneously enables rigidity, barrier enhancement, antibacterial behavior, and electrical conductivity, placing it among the most multifunctional bio-based coatings described to date. By omitting petroleum-based additives, non-biodegradable synthetic binders, or high-impact metallic nanoparticles that are included in many external alternatives, the system maintains its bio-origin at its core.

## **Chapter 3 - Research project development and methodology**

Building upon the insights gained from the literature, the research project was structured to develop functional TOCN-Polypyrrole optimized for antibacterial, conductive, and barrier properties which was developed by our research group's previous PhD student (Benoit Bideau), here we are introducing the binder and plasticiser for making paint and provide detailed characterisation. This chapter details the experimental development, including material fabrication, coating procedures, characterization methods, and preliminary findings. It also critically analyzes the challenges encountered during the project and proposes strategies to overcome them for advancing bio-based coating applications.

### **3.1 Project Overview and Research Framework**

The main aim of this research project was to create multifunctional coatings and paints utilizing TOCN and PPy as structural additives and pigments, respectively, alongside copolymers like PVA as a binder and glycerol as a plasticizer, with water as the primary solvent for application on rigid substrates. This study addresses the limitations found in prior research, including those concerning adhesion, leaching, and color restrictions, by employing targeted methodologies that incorporate copolymers and modify functional properties.

The project was structured in three main phases.

**Phase 1:** Material synthesis and formulation optimization of biobased paint. Surface coating trials and performance characterization

**Phase 2:** Environmental impact and toxicity evaluation

**Phase 3:** Application aspect in terms of barrier properties as well as LCA

The fundamental hypothesis underlying this project was that the incorporation of appropriate copolymers (PVA and Glycerol) into the TOCN-PPy matrix would improve adhesion to rigid surfaces.

Key research questions included, such as how does the addition of copolymers affect the adhesion and surface uniformity of TOCN-PPy coatings on rigid substrates? Can the hydrophobicity and barrier properties (e.g., moisture resistance) of TOCN-PPy based coatings be improved without compromising their structural integrity? What are the environmental implications of TOCN-PPy coatings in terms of biodegradability and potential ecotoxicity?

### **3.2 Fabrication of TOCN Nanocellulose**

By TEMPO (2,2,6,6-tetramethylpiperidine-1-oxyl radical)-mediated oxidation and subsequent moderate disintegration in water, native wood celluloses can be transformed into individual nanofibers 3–4 nm wide and at least several microns in length. Without altering the initial crystallinity (74%) or crystal width of wood celluloses, TEMPO-mediated oxidation selectively forms large amounts of C6 carboxylate groups on each cellulose microfibril surface. TOCN films exhibit high tensile strengths of 200–300 MPa and elastic moduli of 6-7 GPa. They are flexible and transparent. The TEMPO-mediated oxidation of natural cellulose fibres produced novel cellulose-based nanofibers that have the potential to be employed in high-tech sectors as new bio-based, environmentally friendly nanomaterials [100]. The C6-primary hydroxy groups on crystalline cellulose microfibril surfaces are largely transformed to sodium C6-carboxylate groups when the TEMPO/NaBr/NaClO oxidation is applied to native celluloses in water at pH 10 [53]. The TEMPO oxidation and sonication processes will be used to create the TOCN gel from bleached Kraft wood pulp, furthermore determination of the carboxylate content will be evaluated as described [101]. Overall, TEMPO oxidation process illustrated in Figure 3.1.

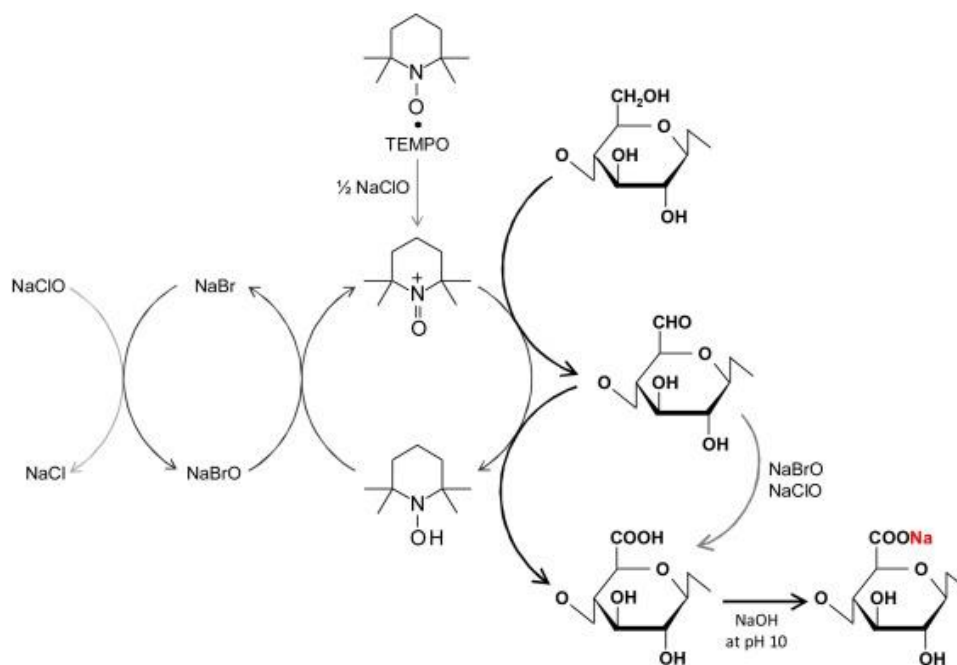


**Figure 3.1** TEMPO Oxidation [53]

Following the reaction, the oxidized graft pulp rinsed three to four times with deionised water before being collected in a plastic bag. The carboxylate concentration was estimated to be approximately to 1600 mmol/kg. IKA method is used after collecting of over 50 grammes of dry oxidised graft pulp. Below Figure 3.2 shows different steps taken during TEMPO oxidation.

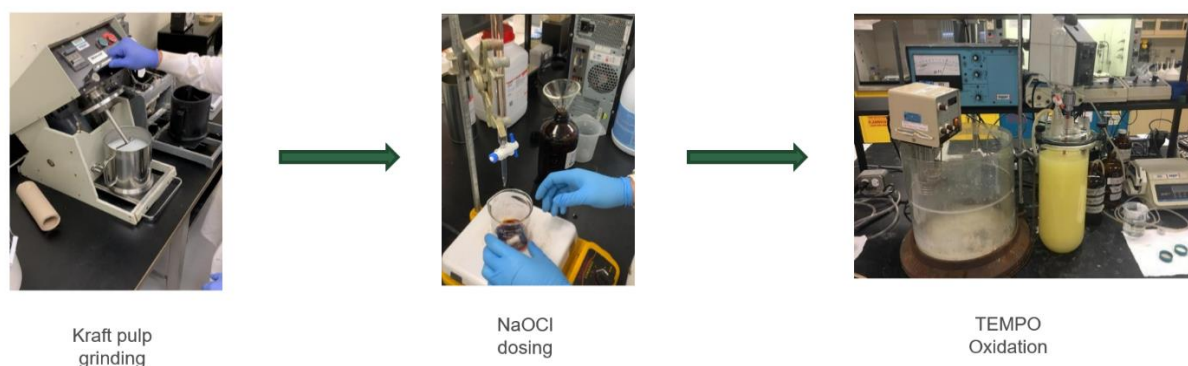


**Figure 3.2** Pictures taken during TEMPO oxidation process

The TEMPO-mediated oxidation was conducted using a 4 L reaction vessel, a motorized mechanical agitator for uniform mixing, a pH probe for continuous reaction monitoring,

and an automated dosing system with two pumps for the precise addition of sodium hydroxide buffer solution and 0.1 M hydrochloric acid, maintaining the pH between 10 and 12 during the oxidation process.

### **3.2.1 Oxidation Protocol**

Preparation of the reaction mixture: Two liters of fibrous Kraft pulp suspension were added to the reaction vessel. Mechanical agitation was commenced to avert sedimentation and guarantee uniform dispersion. The pre-prepared TEMPO/NaBr solution was directly introduced into the agitated suspension. Systematic introduction of the oxidizing agent: Sodium hypochlorite (NaOCl) was administered dropwise via an addition funnel. The gradual and continuous addition enhances oxidation efficiency by providing adequate time for the synthesis of carboxylic acid groups, thus optimizing reaction performance. The stopwatch commenced following the addition of the initial drops of NaOCl to guarantee a cumulative reaction duration of 1 hour and 30 minutes.

### **3.2.2 pH Regulation**

Shortly after the initial introduction of NaOCl, the buffer solution dosing system was engaged to sustain the reaction pH within the ideal range of 10–12. The adjustment of pH may be executed either manually or mechanically.

### **3.2.3 Oxidation cessation**

Upon completion of the 1 hour and 30 minute reaction duration, the pumps and mechanical agitator were deactivated, and 75 mL of 30% hydrogen peroxide was introduced to the reaction mixture to neutralize any remaining oxidizing agents and conclusively terminate the process.

### **3.2.4 Conductometric Titration of Carboxylic Acids**

Following the filtering of the oxidized pulp, a conductometric titration was conducted to quantify the carboxylic acid content produced during the oxidation process. Three grams of oxidized pulp (dry basis) were combined with 0.1 M HCl for 45 minutes, then followed by filtering. The acid wash was conducted a second time. The objective of HCl treatment

is to protonate the carboxylate groups ( $\text{COO}^- \rightarrow \text{COOH}$ ), thereby facilitating precise measurement. The processed pulp was subsequently combined with 450 mL of deionized water and 10 mL of 0.1 M HCl, then homogenized with a mechanical mixer. A 0.1 M NaOH solution was employed to titrate the mixture while continuously monitoring the conductivity. The conductivity curve generated during NaOH addition was utilized to ascertain the concentration of carboxylic acid groups produced during oxidation.

A descending conductivity curve is first observed, corresponding to the neutralization of hydrochloric acid, followed by a plateau region indicative of the titration of carboxylic acid groups. Beyond this point, the curve exhibits an increasing slope, reflecting the excess addition of sodium hydroxide (NaOH). The proprietary software developed by Prof. Loranger processes the conductivity data to precisely determine the length of the plateau, thereby quantifying the carboxylic acid content of the oxidized cellulose. Following this characterization, the preparation of TEMPO-oxidized cellulose nanofibers (TOCN) is carried out using an IKA high-shear homogenizer. This equipment consists of a rotor-stator assembly that generates intense shear forces, enabling the mechanical defibrillation of cellulose fibers into nanofibrils. The system operates in a closed-loop configuration. Approximately 50 g of filtered, dried cellulose paste is dispersed in 2 L of deionized water, after which the agitator ensures initial homogenization. A pump continuously circulates the mixture through the rotor-stator chamber of the IKA unit. The suspension is simultaneously cooled by a water-based heat exchanger to prevent thermal degradation and maintain optimal processing conditions. The mechanical treatment is performed for 1 hour and 30 minutes at a frequency of 60 Hz. During this step, the suspension gradually becomes more viscous, which is a clear indicator of progressive nanofibrillation and effective fiber defibrillation. At the end of the process, a uniform nanocellulose gel is obtained and stored at low temperature to prevent microbial growth, ensuring the stability of the TOCN suspension for subsequent applications. At the end of this step, the nanocellulose is ready and kept cold to avoid the development of bacteria. Overall, IKA process illustrated in Figure 3.3. And our research group's lab scale IKA is in Figure 3.4.

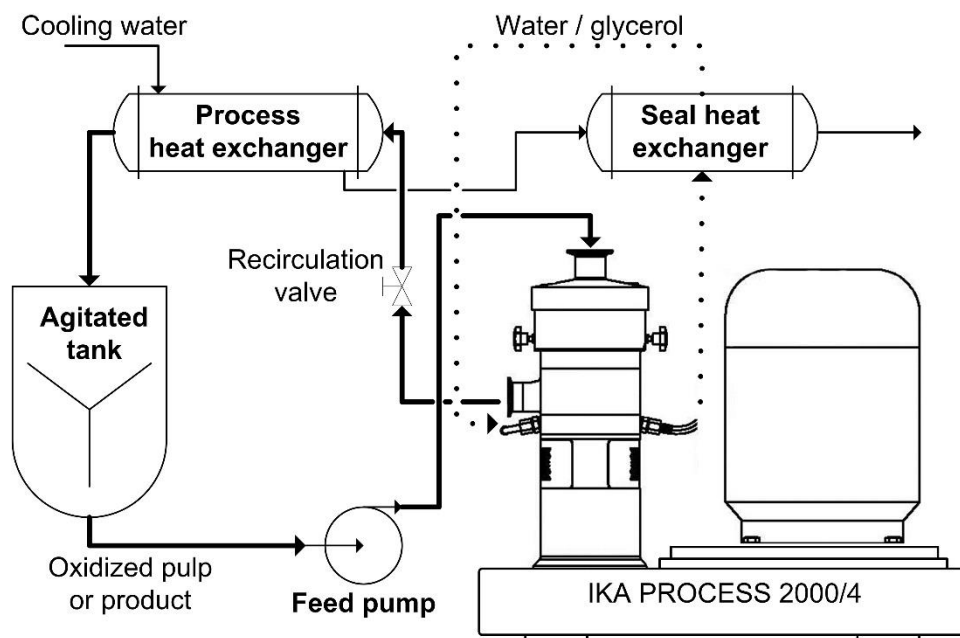


**Figure 3.3** IKA Process [102]

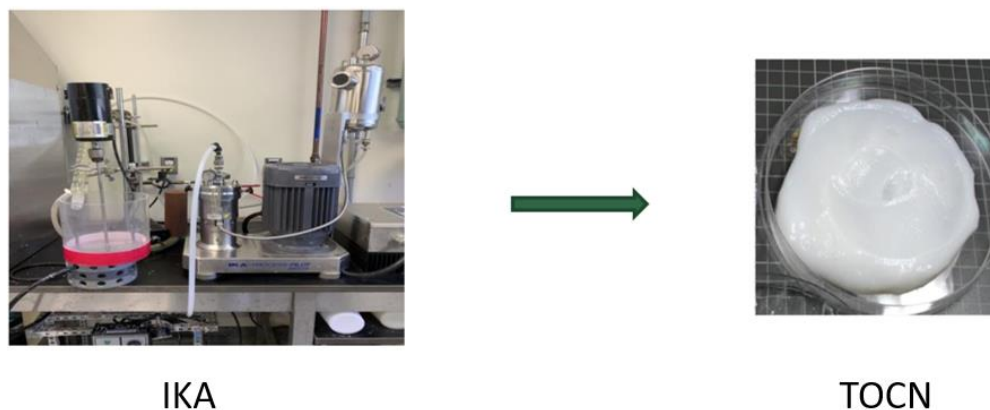


**Figure 3.4** IKA and TOCN formation

### 3.3 Synthesis of TOCN-PPy

TOCN – PPy formation: 80 ml of suspension of TOCN were combined with 2 ml of a pyrrole solution (98%). After 10 minutes of stirring, 10 ml of a 0.3 M oxidant solution ( $\text{FeCl}_3$ ) was added to the mixture in order to start the polymerization of pyrrole into PPy. After 30 minutes of continuous stirring, the fluid became black and began to exhibit

symptoms of pyrrole polymerization. After that, demineralized water was used to rinse the TOCN-PPy mix [80]. Figure 3.5, shown the formation of TOCN-PPy.

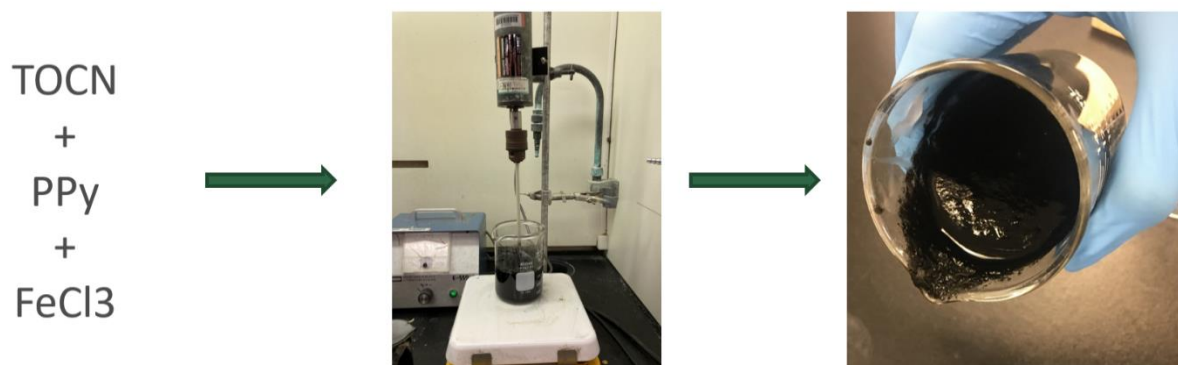


**Figure 3.5** Formation of TOCN-PPy

### 3.3.1 Polymerization Protocol

The synthesis procedure involved the following steps which are listed below.

**Preparation of the TOCN Suspension**, 100 mL of the prepared 0.45 wt% TOCN gel suspension was placed under constant magnetic stirring.

**Addition of Pyrrole Monomer**, 5 mL of freshly distilled pyrrole monomer (98% purity) was slowly added to the TOCN suspension under stirring. Pyrrole is highly sensitive to oxidation; therefore, it was handled under minimal exposure to air and light.

**Initiation of Polymerization**, after 10 minutes of stirring to allow uniform dispersion of the pyrrole monomer within the TOCN matrix, 25mL of a 0.3 M FeCl<sub>3</sub> aqueous solution was added dropwise to the mixture to initiate the oxidative polymerization process.

**Polymerization Process**, the reaction mixture was maintained under continuous stirring for 30 minutes. During this period, a noticeable color change from translucent white to dark black indicated the progressive formation of polypyrrole chains within the TOCN matrix.

**Post-Synthesis Washing**, after polymerization, the black-colored TOCN-PPy suspension was thoroughly rinsed several times with demineralized water to remove unreacted monomers, excess  $\text{FeCl}_3$ , and any byproducts. Washing continued until the conductivity of the wash water reached a baseline value, confirming minimal residual ionic species.

The resulting TOCN-PPy composite suspension displayed a stable colloidal state, with visibly uniform dispersion and an increased viscosity compared to the pristine TOCN gel.

### 3.3.2 Key Observations During Synthesis

The formation of the dark black color after the addition of  $\text{FeCl}_3$  was a critical visual indicator of successful pyrrole polymerization. Excessive polymerization time or high oxidant concentrations were carefully avoided to prevent overoxidation of PPy, which could degrade its conductive properties. Maintaining stirring during polymerization ensured homogeneous nucleation and minimized the formation of large PPy aggregates, promoting a more uniform coating material. The synthesized TOCN-PPy suspension served as the base material for further formulation modifications, coating trials, and performance testing, as described in the subsequent sections.

## 3.4 Coating development

While TOCN-PPy composites demonstrated promising functional properties such as conductivity and potential barrier effects, a major challenge encountered during preliminary coating trials was their limited adhesion to rigid substrates, such as steel and plywood. Poor adhesion manifested in peeling, cracking, and uneven surface coverage, severely limiting the applicability of the coatings for practical use. To address this limitation, strategies involving the incorporation of copolymers were implemented. The objective was to improve the mechanical bonding between the TOCN-PPy layer and the substrate without significantly impairing the composite's electrical or surface properties.

### 3.4.1 Surface Adhesion Challenges

Initial coating tests revealed multiple adhesion problems. The TOCN-PPy coatings exhibited inadequate wetting behavior on metallic surfaces like steel, partially detaching

during the drying process, whereas rust formation at the edges indicated potential chemical interactions or deficient barrier qualities at the interface. On hardwood substrates like plywood, the coatings exhibited non-uniform adhesion, resulting in uneven and fragile films during the drying process and mechanical manipulation. These observations necessitated the alteration of the formulation to enhance interfacial compatibility between the TOCN-PPy material and the underlying substrates.

### **3.4.2 Introduction of Copolymer Additives**

To improve adhesion and tune the surface properties of the TOCN-PPy coatings, formulation strategies were developed based on the incorporation of polyvinyl alcohol (PVA) and glycerol (Gly) as copolymer additives. PVA was selected due to its excellent film-forming capability, promoting strong adhesion to rigid surfaces, low cost and water solubility, aligning with sustainability objectives and ability to create hydrogen bonds with both nanocellulose and substrate surfaces. Glycerol was introduced as a plasticizer to: Enhance the flexibility of the coating films; Reduce brittleness upon drying; Improve the overall mechanical stability of the films. Based on these principles, four distinct formulations were developed, such as TOCN-PPy-PVA (without glycerol), TOCN-PPy-PVA-Gly (1ml) (low glycerol content), TOCN-PPy-PVA-Gly (2ml) (moderate glycerol content), TOCN-PPy-PVA-Gly (5ml) (high glycerol content). These formulations allowed systematic investigation of the effects of increasing glycerol concentration on the adhesion, conductivity, and surface hydrophobicity of the coatings.

Additionally, initial exploratory tests were performed using commercial PVA-based wood glue as an adhesive additive to evaluate rapid adhesion improvement strategies. However, its use raised concerns regarding potential negative impacts on conductivity and overall film uniformity.

### **3.4.3 Expected Impacts of Copolymer Addition**

The incorporation of PVA and glycerol into the TOCN-PPy matrix was expected to significantly modify the physical properties of the resulting coatings, particularly with regard to adhesion, flexibility, and surface characteristics. The expected effects were as

listed below. Adhesion improvement, by PVA's strong film-forming ability and capacity to form hydrogen bonds with both the TOCN nanofibers and substrate surfaces were anticipated to greatly enhance coating adhesion, reducing the occurrence of peeling and cracking upon drying. Flexibility enhancement, by addition of glycerol as a plasticizer was expected to improve the mechanical flexibility of the coatings, minimizing brittleness and promoting better durability during handling and drying processes. Surface hydrophobicity modification, depending on the ratio of PVA and glycerol, changes in surface hydrophobicity were anticipated. PVA alone may slightly increase hydrophilicity, while the combination with glycerol at controlled concentrations could modulate water absorption and improve moisture resistance. Impact on conductivity, it was recognized that the incorporation of non-conductive additives such as PVA and glycerol might slightly reduce the overall electrical conductivity of the coatings. Therefore, a balance needed to be achieved between enhancing adhesion and maintaining acceptable conductivity levels for intended applications. Barrier property optimization, the combination of PVA and glycerol was also expected to impact the barrier properties (e.g., Oxygen Transmission Rate [OTR] and Moisture Vapor Transmission Rate [MVTR]), potentially improving the coatings' resistance to gas and moisture permeation.

Thus, the strategic formulation of four different recipes—ranging from pure TOCN-PPy-PVA to TOCN-PPy-PVA-Gly (with 1ml, 2ml, and 5ml glycerol)—was designed to systematically evaluate and optimize the trade-offs between adhesion, flexibility, conductivity, hydrophobicity, and barrier functionalities.

#### **3.4.4 Surface Coating Trials and Observations**

Subsequent to the synthesis of TOCN-PPy and the formulation of copolymer-modified coatings, experimental applications were conducted predominantly on plywood panels to assess adhesion, surface uniformity, and overall aesthetic quality. Plywood was chosen as the primary rigid substrate due to its prevalent use in packaging, furniture, and structural applications, and the formulations demonstrated superior adhesion on cellulose-based surfaces. Initial considerations encompassed the potential for testing on steel substrates, however, these were ultimately excluded due to ongoing adhesion difficulties on metallic surfaces, which exceeded the parameters of the current study. Observations from the

plywood coating trials were meticulously recorded to facilitate formulation enhancement and optimization.

#### 3.4.4.1 Coating Behavior on Plywood Surfaces

When coated on plywood surfaces, the unmodified TOCN-PPy formulations presented significant limitations: Non-uniform spreading with patchy coverage, brittle film formation with cracking upon drying, and detach from surface after drying as observed in Figure 3.6.



**Figure 3.6** TOCN-PPy on plywood

The application of copolymer-modified formulations demonstrated a clear improvement, TOCN-PPy-PVA (containing no glycerol) exhibited superior surface wetting and increased adhesion relative to raw TOCN-PPy, despite the observation of slight surface contraction after drying. TOCN-PPy-PVA-Gly with 1 mL or 2 mL of glycerol demonstrated ideal performance regarding adhesion, flexibility, and surface uniformity; these coatings attached securely, displayed no significant cracking, and preserved excellent mechanical resistance. TOCN-PPy-PVA-Gly containing 5 mL of glycerol yielded very flexible films with superior adhesion; nevertheless, minor tackiness and surface deformation under pressure were observed, likely attributable to the elevated glycerol concentration, and the surface exhibited a propensity to collect moisture. Formulations with low to moderate glycerol additions (1–2 mL) attained an optimal equilibrium among coating flexibility, adhesion, and surface integrity, without resulting in excessive softness or stickiness.

#### 3.4.4.2 Summary of Observations

The coating trials on plywood surfaces clearly demonstrated that: The addition of PVA improves adhesion significantly compared to raw TOCN-PPy; The controlled addition of glycerol enhances flexibility and crack resistance; Higher glycerol content (5ml) can lead to surface softness and tackiness, which may not be desirable for certain end uses. These findings emphasized the importance of recipe optimization based on the intended application, balancing adhesion strength, mechanical durability, and surface properties.

### 3.5 Characterization Techniques Employed

A comprehensive set of characterization techniques was employed to evaluate the functional properties of the developed TOCN-PPy-PVA-Gly coatings. The primary objectives were to assess surface behavior, electrical conductivity, mechanical strength, barrier performance, and environmental degradation potential. Each formulation was systematically characterized using the following methodologies.

**Rheology** was employed to analyze the viscosity and flow behavior of the paint formulations. This analysis is crucial to assess their suitability for coating applications, as it provides insight into the pseudoplastic or shear-thinning nature of the system, which directly influences spreading, leveling, and film formation during application. The rheological properties of the paint formulations were assessed using a Rheologica Stresstech HR Rheometer (ATS RheoSystems) equipped with a C40 cone-plate geometry. All measurements were conducted at a regulated temperature of 25 °C, with shear rates ranging from 0.1 to 1000 s<sup>-1</sup>. The apparent viscosity ( $\eta_{app}$ ) was derived from the slope of the shear stress ( $\tau$ ) vs shear rate ( $\dot{\gamma}$ ) graph, utilizing the formula  $\eta_{app} = \tau / \dot{\gamma}$ . Each formulation underwent three measurements to guarantee reproducibility, and the published viscosity values reflect the average of these repeated assessments.

**Scanning Electron Microscopy (SEM)** was used to examine the surface morphology, and cross-sections of the films. SEM enabled us to visualize the homogeneity of the coatings, identify possible defects such as cracks or agglomerates, and evaluate the coverage on both rigid and paper substrates. Scanning Electron Microscopy (SEM)

analysis was performed utilizing a Hitachi SU1510 microscope. To reduce surface charging and enhance image clarity, non-conductive samples were sputter-coated with a thin layer of gold utilizing an International Scientific Instruments PS-2 coating machine. Imaging was conducted in secondary electron mode at an accelerating voltage of 15 kV and a beam current of 100  $\mu\text{A}$ , facilitating high-resolution observation of surface morphology.

**3D Surface Profilometry ( Alicona )** was applied to quantify the topographical features of the coatings, such as roughness parameters ( $S_a$ ,  $S_q$ ,  $S_p$ ,  $S_v$ ). These measurements allowed for the correlation between surface morphology by coating over UPM paper. The surface morphology of the biobased coating films consisting of TOCN-PPy-PVA and their glycerol-modified variants (Gly1, Gly2, Gly5) was analyzed using a high-resolution 3D optical profilometer ( Alicona InfiniteFocus G5 ), which utilizes focus-variation technology. This non-contact method offers intricate microscale areal topography, enabling the identification of nuanced surface characteristics. Profilometric scans were conducted across three representative locations for each dried film. Surface leveling and background curvature reduction were executed via best-fit plane correction in the Alicona analysis software. A collection of standard roughness metrics was obtained to characterize both amplitude and spatial attributes of the surface texture, comprising  $S_a$  (arithmetic mean height),  $S_q$  (root mean square height), and  $S_p$ ,  $S_v$ ,  $S_z$  (maximum peak height, maximum valley depth, and maximum height, respectively). This methodology facilitated a quantitative analysis of microstructural alterations across several formulations based on glycerol content.

**Raman Spectroscopy** was used to confirm the chemical structure of the composites and the presence of polypyrrole within the cellulose matrix. The technique provided molecular-level information on the conjugated structure of PPy and helped verify the interactions between PPy and TOCN through characteristic spectral peaks. Raman spectroscopy was conducted utilizing a Thermo Fisher DXR3 Raman Microscope to analyze the molecular composition and chemical structure of the paint films. The device used a 785 nm excitation laser and a comprehensive grating covering roughly 300–3000  $\text{cm}^{-1}$ . Spectral acquisition was enhanced by employing a laser power of 30 mW, an

exposure duration of 30 seconds each scan, and three accumulations. A 50  $\mu\text{m}$  slit aperture and a 10 $\times$  objective lens were employed to precisely focus the laser on the sample surface. Three spectra were obtained at various locations for each formulation to verify measurement uniformity. The instrument's automatic X-axis calibration enhanced the dependability and stability of the data collected.

**Thermal Analysis (TGA and DSC)** was conducted to determine the thermal stability, degradation onset, and residual mass of the formulations. TGA provided quantitative data on decomposition profiles and residue content (e.g., confirming iron and PPy content), while DSC gave insights into the thermal transitions and the influence of glycerol and PVA on material stability. Thermogravimetric analysis (TGA) was conducted on a PerkinElmer TGA-8000 (USA) to evaluate the thermal stability and compositional properties of the paint films. Samples were positioned in ceramic crucibles and examined in a nitrogen environment at a flow rate of 50 mL/min. The temperature protocol included an initial equilibration at 40 °C for 3 minutes, a ramp from 40 °C to 105 °C at a rate of 10 °C/min to eliminate adsorbed moisture, an isothermal hold at 105 °C for 20 minutes, followed by a heating phase to 900 °C at 10 °C/min for polymer decomposition and carbonization, an additional isothermal hold at 900 °C for 20 minutes, and concluding with a cooling phase to 40 °C at 200 °C/min. Data on continuous mass loss were gathered during the run to determine thermal behavior and composition. Differential Scanning Calorimetry (DSC) was conducted with a TA Instruments DSC 2500 to analyze thermal transitions in the paint films. Measurements were performed in a nitrogen atmosphere at a flow rate of 50 mL/min to prevent oxidative effects, with samples heated from 40 °C to 200 °C at a rate of 10 °C/min.

**Contact Angle Measurements** were performed to evaluate the surface wettability of the coatings. These measurements provided information on the hydrophilic or hydrophobic nature of the films, which is particularly important for packaging and barrier applications. The wettability of the coated wood surfaces was evaluated using contact angle measurements employing the sessile drop technique. The studies were conducted using a Microdrop Contact Angle Analyzer FTA4000 (First Ten Angstroms, USA). Five microliters of deionized water droplets were distributed onto the paint films via the

instrument's precision dosing system, and the droplet profiles were documented at room temperature with the integrated high-resolution camera. The software computed the contact angle at the liquid–solid–air interface using the acquired images. To guarantee measurement reliability and accommodate natural surface changes, five measurements were conducted at various locations on each sample, and the average contact angle was documented.

**Tensile Testing** was used to determine the mechanical performance of the TOCN–PPy–PVA–Gly films, including tensile strength, elongation at break, and stiffness. These results highlighted how glycerol acts as a plasticizer, modifying the flexibility and mechanical durability of the coatings. The tensile strength of the TOCN–PPy–PVA–Gly films were evaluated using a universal testing machine (Instron 4201, USA) under regulated laboratory conditions (25 °C and 50% relative humidity). Rectangular specimens measuring 30 mm by 15 mm were subjected to testing with a gauge length of 10 mm and a crosshead speed of 10 mm/min. Owing to the films' ultrathin characteristics, strain was determined using crosshead displacement instead of utilizing an extensometer, employing a methodology influenced by the TAPPI T494 standard for paper. This approach may marginally exaggerate elongation at break, although it yielded reliable and reproducible results across samples. Each formulation underwent testing in no fewer than six replicates, with the mechanical parameters presented as mean values accompanied by standard deviations. The principal characteristics assessed were tensile strength (MPa), which is the highest stress before failure; elongation at break (%), indicating the strain at fracture; and Young's modulus (GPa), calculated from the slope of the initial linear segment of the stress–strain curve.

**Oxygen Transmission Rate (OTR) and Water Vapor Transmission Rate (WVTR)** tests were performed to quantify the barrier properties of the coatings against gas and moisture permeation. These tests are critical for evaluating the suitability of the coatings for sustainable packaging applications, especially when glycerol content impacts water resistance. The performance of the oxygen barrier was assessed with a Systech Illinois M8001 oxygen permeation analyzer. One side of the film received pure oxygen (99.9%), while high-purity nitrogen served as the sweep gas on the opposing side. All

measurements were performed at 23 °C and 50% relative humidity, with uniform humidity conditions upheld on both sides of the specimens. Circular film samples were affixed to diffusion cells with an exposed area of 3.14 cm<sup>2</sup>, corresponding to a diameter of 2.0 cm, appropriate for the small size of the cast films. The instrument reported the oxygen transmission rate (OTR) in cm<sup>3</sup>/m<sup>2</sup>·day. Each formulation was analyzed in duplicate, with findings expressed as mean ± standard deviation. The water vapor transmission characteristics of the films were assessed at 23 ± 0.5 °C under two relative humidity conditions—50 ± 2% and 70 ± 2%—to investigate the impact of ambient moisture on vapor permeability. Circular film specimens were excised and affixed to the apertures of standard glass permeability cups (2.0 cm diameter, exposed area of 3.14 cm<sup>2</sup>). Each cup contains 2.0–2.5 g of anhydrous calcium chloride as the desiccant for moisture absorption. Silicone grease was put around the cup rim to maintain adequate sealing and avoid edge leakage, while O-rings were securely positioned over the film edges. The mass increase of each cup was recorded using a high-precision analytical balance with a resolution of ±0.001 mg, with measurements conducted twice daily over three consecutive days. The water vapor transmission rate (WVTR) was determined from the slope of the linear segment of the mass-gain versus time curve and normalized by the exposed surface area to yield the MVTR, given in g/m<sup>2</sup>·day. All formulations underwent triplicate testing, and results are presented as mean values accompanied by their respective standard deviations.

The **pH** of the washing solutions and reference materials was measured with a Thermo Scientific ORION Star A215 pH meter. Prior to measurements, the equipment was calibrated using standard buffer solutions at pH values of 4.00, 7.00, and 10.00. All pH measurements were conducted at ambient temperature under conventional laboratory settings.

**ICP-OES** was used to measure the release of iron ions from the PPy synthesis process, providing insight into the stability of the coatings and potential environmental risks. The liberation of iron (Fe) from TOCN-PPy and its polymer-modified composites was examined utilizing inductively coupled plasma optical emission spectroscopy (ICP-OES, Perkin Elmer AVIO 550) after 24 hours of sample immersion in 50 mL of deionized water. Numerous samples displayed concentrations at or near the instrumental detection

threshold; hence, any recorded values beneath 0.05 mg/L were documented as “Fe  $\leq$  0.05 mg/L,” in accordance with standard analytical reporting protocols. Iron measurement conformed to ASTM D1976-20, Standard Test Method for Elements in Water using Inductively Coupled Plasma Atomic Emission Spectroscopy. According to this standard, the instrumental detection limit (IDL) for iron was established at Fe  $\leq$  0.05 mg/L, with quantities below this threshold reported as “Fe  $\leq$  0.05 mg/L” in accordance with the ASTM process (ASTM International, 2020).

Complementary to this, **HPLC-MS/MS** enabled precise detection and quantification of residual pyrrole and glycerol in leachates, ensuring no harmful components migrated into water. Analyses were conducted utilizing an Agilent HPLC-MS/MS system featuring a Jet Stream ESI source. Chromatographic separation was performed using a Kinetex EVO C18 column (150  $\times$  4.6 mm, 5  $\mu$ m, 100 Å; Phenomenex), with an autosampler maintained at 4 °C and a column oven regulated at 30 °C. A 5  $\mu$ L aliquot from each vortex-mixed sample was injected. The mobile phases for pyrrole detection were water with 0.1% formic acid (A) and methanol with 0.1% formic acid (B), administered at a flow rate of 0.4 mL/min according to the following gradient: 0.00–4.00 min, 10% B; 8.00–10.00 min, 100% B; 10.40–12.00 min, reverting to 10% B. Glycerol detection employed mobile phases consisting of 10 mM ammonium acetate with 0.1% acetic acid (A) and acetonitrile (B), maintained at a same flow rate, with a gradient of 0.00–1.50 min at 80% B; 1.60–3.00 min at 10% B; and 5.00–10.00 min at 80% B. Pyrrole was examined in ESI+ mode, observing the [M+H]<sup>+</sup> ion at m/z 68 and fragments at m/z 41 and 39 (retention time: 9.861 min). Glycerol was identified in ESI<sup>-</sup> mode through the [M+Ac]<sup>-</sup> ion at m/z 151, with fragment ions at m/z 59 and 133 (retention time: 1.018 min). The mass spectrometry source parameters for pyrrole comprised a drying gas flow of 10 L/min, a gas temperature of 300 °C, a nebulizer pressure of 45 psi, a sheath gas flow of 11 L/min, a sheath gas temperature of 300 °C, a capillary voltage of 4000 V, and a nozzle voltage of 500 V. For glycerol, the same parameters were employed, with the exception of a drying-gas flow rate of 13 L/min, a sheath-gas temperature of 400 °C, and a capillary voltage of 3000 V.

A **soil biodegradation test** was conducted over 60 days, using quintuplicate samples of TOCN-PPy-PVA and its glycerol-modified variants (TOCN-PPy-PVA-Gly1, TOCN-

PPy-PVA-Gly<sub>2</sub>, and TOCN-PPy-PVA-Gly<sub>5</sub>), which were buried 10 cm deep in dry soil circumstances. The weight variations were documented prior to and subsequent to the test to assess the biodegradation characteristics of the samples.

**Hydrothermal Reusability Tests** were designed to study the recyclability and circularity potential of the materials. These tests involved controlled heating of the coated films to induce partial solubilization, allowing the recovery and reuse of the coating material. The hydrothermal recovery characteristics of the TOCN-PPy-PVA-Gly composite coating were evaluated by a film recovery test aimed at investigating paint reusability. A dry film fragment (about 1.83 g) was submerged in 50 mL of deionized water and heated at 75 °C for 35 minutes under continuous stirring.

Finally, a **Life Cycle Assessment (LCA)** was performed to evaluate the overall environmental footprint of the bio-based coatings, comparing them to conventional fossil-derived paint systems. This analysis identified the main contributors to the carbon footprint (such as PVA and PPy) and provided strategies for improving sustainability through material selection and process optimization. A initial life cycle assessment (LCA) was conducted following ISO 14040/44 standards utilizing the SimaPro software platform, with background data sourced from the Ecoinvent 3.10 database (Wernet et al., 2016). The functional unit was defined as a single A4-sized UPM paper sheet (0.062 m<sup>2</sup>) coated by a two-layer bar-coating method, in accordance with laboratory-scale application. The system boundaries included the manufacture of raw materials (TOCN, pyrrole, FeCl<sub>3</sub>, PVA, and glycerol), in-situ synthesis and mixing, paint formulation, coating application, washing, and drying processes. Each A4 page necessitated around 10 mL of paint, applied in two successive coats (5 mL + 5 mL). A standard batch of paint formulation yielded approximately 60 mL of usable material, adequate to cover six A4 sheets (Malik et al., 2025). The life cycle inventory for a single A4 sheet consisted of 10 mL of coating derived proportionally from a 100 mL formulation including 0.45 wt% TOCN suspension (about 0.45 g of dry TOCN), in addition to 5 g of PVA, 5 mL of pyrrole, and 25 mL of 0.3 M FeCl<sub>3</sub>. Glycerol was included in different quantities based on the formulation: 1 mL for Gly<sub>1</sub>, 2 mL for Gly<sub>2</sub>, and 5 mL for Gly<sub>5</sub>.

### **3.6 Key Problems Identified**

During preliminary experiments, several challenges were identified with the use of raw TOCN-PPy coatings, particularly when applied directly onto rigid surfaces such as plywood. These problems motivated the introduction of copolymer additives (PVA and glycerol) to systematically improve the performance and overcome the limitations observed. The key issues and corresponding improvement strategies are summarized below:

#### **3.6.1 Poor Adhesion to Rigid Surfaces**

Coatings exhibited poor adhesion to plywood substrates, resulting in peeling, cracking, and uneven surface coverage upon drying. The incorporation of PVA significantly improved adhesion by enhancing surface wettability and film-forming ability. Glycerol further contributed by improving coating flexibility and reducing internal stresses during drying.

#### **3.6.2 Brittleness and Cracking**

Films formed from unmodified TOCN-PPy were brittle, with low elongation at break and poor mechanical resilience under bending or handling. The addition of glycerol as a plasticizer imparted flexibility to the coatings. Formulations with 1–2 mL glycerol showed enhanced toughness and resistance to mechanical cracking without severely compromising structural strength.

#### **3.6.3 Surface Defects and Drying Instabilities**

Non-uniform spreading and the formation of surface defects such as wrinkles and microcracks were observed during the drying of unmodified coatings. PVA addition enabled smoother and more continuous film formation, while glycerol helped maintain surface integrity during the drying process by mitigating shrinkage stresses.

### **3.7 Proposed Strategies for Problem Solving**

Based on the preliminary results and the key challenges identified, several strategies were developed to optimize the TOCN-PPy-PVA-Gly coatings for specific applications. The focus was on achieving a balance between adhesion enhancement, conductivity retention, mechanical flexibility, and environmental stability. The proposed problem-solving approaches are outlined below:

#### **3.7.1 Fine-Tuning Copolymer and Plasticizer Content**

To address the trade-off between improved adhesion and decreased conductivity. Moderate glycerol additions (1–2 mL) were prioritized to optimize flexibility and adhesion without excessively disrupting the conductive polypyrrole network. It could be good for the places where humidity is high. Excessive glycerol content (5 mL), although improving flexibility, was avoided for formulations intended for applications requiring higher mechanical rigidity or conductivity. It could be good for environment where humidity is very less.

Tailoring the PVA and glycerol ratios for each formulation allowed better control over the final properties according to targeted use cases.

#### **3.7.2 Multi-Recipe Development Approach**

Recognizing that a single formulation could not satisfy all application requirements, a multi-recipe strategy was adopted. Low-glycerol formulations (1 mL) for applications prioritizing conductivity and surface hardness (e.g., functional coatings, packaging). Moderate-glycerol formulations (2 mL) for applications requiring balanced flexibility and moisture resistance (e.g., packaging films). Higher-glycerol formulations (5 mL) only for highly flexible, low-conductivity needs where mechanical deformation resistance is critical (for dry environment application). This application-specific adaptation allowed greater versatility of the developed coating system.

### **3.7.3 Process Optimization**

Several practical adjustments were proposed to improve coating performance. Slow and controlled drying under ambient conditions could minimize crack formation and surface defects. Applying thin successive layers rather than a single thick coating could help reduce internal stresses and prevent cracking during drying. In bar coating in article 3, we did 2 layer bar coating.

### **3.7.4 Long-Term Environmental Testing**

To validate the coatings' real-world performance, it was proposed to conduct extended aging tests under controlled humidity and temperature conditions, (by WVTR), and to perform accelerated soil burial degradation tests to assess composability and environmental fate. These strategies would ensure that the developed coatings meet both functional and environmental sustainability criteria.

## **Chapter 4 - Scientific Article 1: Synthesis, formulation and characterization of paints based on TOCN–PPy–PVA–Gly**

### **4.1 Preface**

This part of the work was published in the peer-reviewed journal *Progress in Organic Coatings* (Elsevier, IF 7.3, DOI: <https://doi.org/10.1016/j.porgcoat.2025.109511>). The article entitled “*Synthesis, formulation, and characterization of a bio-based paint derived from TOCN and polypyrrole*” mainly focuses on the design and preparation of bio-based paints using TEMPO-oxidized cellulose nanofibers (TOCN) combined with polypyrrole (PPy) as the conductive phase, polyvinyl alcohol (PVA) as a binder, and glycerol as a plasticizer. The work emphasizes the optimization of formulation strategies to achieve stable paint dispersions and uniform coatings. This study represents the first step toward developing eco-friendly and functional paint systems derived from renewable cellulose nanofibers and conductive polymers, showcasing their potential for sustainable and technologically advanced coating applications.

### **Authors details**

#### **Aakash Malik, CPI, MSc**

Ph.D. Candidate, Sciences et génie des matériaux lignocellulosiques

I2E3 – Institut d’Innovations en Écomatériaux, Écoproduits et Écoénergies à base de biomasse

Université du Québec à Trois-Rivières,

P.O. Box 500, Trois-Rivières, Québec, Canada, G9A 5H7

Email: [aakash.malik@uqtr.ca](mailto:aakash.malik@uqtr.ca)

#### **Prof. Éric Loranger, Ph.D., ing.**

Research director and corresponding author

I2E3 – Institut d’Innovations en Écomatériaux, Écoproduits et Écoénergies à base de biomasse

Université du Québec à Trois-Rivières,

P.O. Box 500, Trois-Rivières, Québec, Canada, G9A 5H7

Email: [eric.loranger1@uqtr.ca](mailto:eric.loranger1@uqtr.ca)

**Prof. Simon Barnabé, Ph.D.**

Research Co-director

I2E3 – Institut d’Innovations en Écomatériaux, Écoproduits et Écoénergies à base de biomasse

Université du Québec à Trois-Rivières,

P.O. Box 500, Trois-Rivières, Québec, Canada, G9A 5H7

Email: [simon.barnabe@uqtr.ca](mailto:simon.barnabe@uqtr.ca)

**Author Contributions:**

**Aakash Malik:** Writing – original draft, Visualization, Validation, Methodology, Investigation, Formal analysis, Data curation, Conceptualization

**Simon Barnabé:** Writing – review & editing, Supervision

**Éric Loranger:** Writing – review & editing, Validation, Supervision, Project administration, Funding acquisition, Conceptualization

## 4.2 Résumé

Cette étude présente le développement d'une peinture biosourcée par l'intégration de nanofibres de cellulose oxydées TEMPO (TOCN) avec du polypyrrole (PPy) et l'incorporation d'alcool polyvinylique (PVA) comme liant et de glycérol comme plastifiant. Le composite TOCN-PPy a été synthétisé par polymérisation in situ, suivie d'un lavage pour garantir la pureté de la composition. Un mélange à haut cisaillement et un traitement thermique contrôlé ont permis d'obtenir des formulations homogènes et stables. La microscopie électronique à balayage (MEB) a révélé un réseau de nanofibres bien dispersé, avec une teneur accrue en glycérol contribuant à une morphologie de surface plus lisse. Ceci pourrait être corrélé à une meilleure flexibilité observée lors de la manipulation. L'analyse Raman a confirmé la présence de polypyrrole et a révélé des

décalages spectraux associés à une meilleure dispersion du polymère et à des liaisons hydrogène influencées par le PVA et le glycérol. Les mesures d'angle de contact ont montré qu'une teneur plus élevée en glycérol augmentait la mouillabilité, réduisant l'hydrophobicité et améliorant l'adaptabilité aux applications de revêtement. L'analyse thermogravimétrique (ATG) a révélé une dégradation en plusieurs étapes, le polypyrrole améliorant la stabilité thermique. La flexibilité accrue observée dans les échantillons contenant du glycérol est attribuée à son effet plastifiant, comme en témoignent les observations morphologiques et de manipulation. La DSC a également été utilisée pour évaluer la transition vitreuse, la fusion et la décomposition thermique, ainsi que les tendances en matière de stabilité thermique. Ces résultats soulignent la modularité des revêtements TOCN-PPy, équilibrant l'intégrité structurelle, les performances thermiques et la mouillabilité pour diverses applications industrielles. Ils soulignent également le potentiel des composites TOCN-PPy en tant que revêtements hautes performances et respectueux de l'environnement, soutenant les innovations en chimie verte et en bioéconomie circulaire.

### 4.3 ABSTRACT

This study presents the development of a biobased paint by integrating TEMPO-oxidized cellulose nanofibers (TOCN) with polypyrrole (PPy) and incorporating polyvinyl alcohol (PVA) as a binder and glycerol as a plasticizer. The TOCN-PPy composite was synthesized via in-situ polymerization, followed by a washing process to ensure compositional purity. High-shear mixing and controlled thermal treatment produced homogeneous and stable formulations. Scanning Electron Microscopy (SEM) revealed a well-dispersed nanofiber network, with increased glycerol content contributing to smoother surface morphology. This may correlate with improved flexibility observed during handling. Raman analysis further confirmed the presence of polypyrrole and revealed spectral shifts associated with enhanced polymer dispersion and hydrogen bonding influenced by PVA and glycerol. Contact angle measurements showed that higher glycerol content increased wettability, reducing hydrophobicity and enhancing adaptability for coating applications. Thermogravimetric Analysis (TGA) revealed multi-stage degradation, with polypyrrole improving thermal stability. The enhanced flexibility

observed in glycerol-containing samples is attributed to its plasticizing effect, as evidenced by morphological and handling observations. DSC was also employed for glass transition, melting and thermal decomposition behavior, and thermal stability trends. These findings emphasize the tunability of TOCN-PPy coatings, balancing structural integrity, thermal performance, and wettability for various industrial applications. The results also highlight the potential of TOCN-PPy composites as high-performance, eco-friendly coatings, supporting innovations in green chemistry and the circular bioeconomy.

**Keywords:** Biobased paint, TEMPO-oxidized cellulose nanofibers (TOCN), Polypyrrole, Polyvinyl alcohol, Glycerol, Circular bioeconomy

#### 4.4 INTRODUCTION

The growing emphasis on bio-based coatings stems from the depletion of fossil resources and the environmental concerns associated with conventional petrochemical-based coatings. This shift is reflected in the increasing research on innovative binders derived from renewable sources such as plant oils, fatty acids, cellulose, and cardanol. As sustainability becomes a key driver of material innovation, the demand for eco-friendly alternatives to traditional coatings continues to rise (Chek & Ang, 2024). The widespread use of conventional plastics has led to significant environmental concerns, as their persistence contributes to pollution and greenhouse gas emissions from incineration. This has driven the search for biodegradable alternatives in many applications (Samir et al., 2022). Cellulose nanofibrils (CNFs) have emerged as promising bio-based nanomaterials for advanced composites due to their high aspect ratio, specific surface area, and mechanical properties. They also offer improved sustainability over synthetic reinforcements. However, their hydrophilicity complicates integration with hydrophobic polymers, often leading to agglomeration, void formation, and poor interfacial adhesion, which reduce composite performance. As a result, considerable research is focused on CNF surface functionalization to improve dispersion, minimize interfacial energy differences, and enhance fiber–matrix interactions for better mechanical integrity (Oesef et al., 2024). TEMPO-mediated oxidation functionalizes cellulose nanofibers (TOCNFs) with carboxyl groups and requires less energy than producing microfibrillated cellulose

(MFC) or cellulose nanocrystals (CNCs). The carboxyl groups enhance the physicochemical properties of TOCNFs, making them well-suited for applications in biomedicine, wastewater treatment, and bioelectronics (Tang et al., 2024). While CNFs themselves lack inherent conductivity, they are often used as sustainable substrates in combination with conductive additives for flexible and wearable electronics. Conductive polymers such as polypyrrole (PPy) and polyaniline (PANI) are commonly employed to impart conductivity to insulating matrices. Literature (Zheng et al., 2024) indicates that PPy-coated fabrics exhibit lower cytotoxicity than PANI-based ones, making PPy more favorable for biocompatible applications. Consequently, PPy is widely used for its electrical conductivity, biocompatibility, and environmental stability. Recent advances in electrospun cellulose followed by in-situ PPy polymerization have enabled the development of cellulose/PPy composites for flexible strain sensors and other advanced electronics (Zheng et al., 2024; Bideau, Bras, et al., 2016; Bideau, Loranger, et al., 2016).

Polyvinyl alcohol (PVA) is a distinctive water-soluble polymer extensively utilized in papermaking, textiles, and various coatings. Known for its biocompatibility, it serves as a scaffold for cell cultures, embolic materials, contact lenses, and wound dressings. Additionally, PVA is increasingly being applied in environmental engineering and electrical materials (Halake et al., 2014; Ayissi Eyebe et al., 2019; Eyebe et al., 2018). Glycerol has been demonstrated to be an effective plasticizer for polyvinyl alcohol (PVA), significantly enhancing its processability and ductility. Among various polyol plasticizers, glycerol-plasticized PVA exhibits the greatest reduction in Young's modulus, improved toughness, and the lowest melting temperature (195 °C). In Xie et al. (2024), structural analysis reveals that glycerol reduces crystallinity to 29% and increases the amorphous layer thickness to 7.76 nm, indicating a significant impact on PVA's structural transformation. Additionally, molecular dynamics studies show that glycerol-plasticized PVA has a two-dimensional structure and the most heterogeneous chain dynamics, with the lowest rigid amorphous fraction (RAF) of 0.507 in the interphase. These findings highlight glycerol's crucial role in modifying PVA's physical and mechanical properties (Xie et al., 2024).

Paints generally consist of a pigment for color, a binding medium, and various additives that influence optical properties and workability. Over time, the characteristics of paint change, beginning as a liquid-like film and gradually transforming into a solid-like paint film. This transition occurs through two primary mechanisms: drying, where solvents evaporate from the paint film, or curing, which involves crosslinking and other chemical reactions that enhance stiffness. The duration of these processes varies significantly, ranging from a few hours (as seen in acrylics) to months (alkyds) or even decades (oil-based paints). During this transformation, the stiffness of the paint film can increase by several orders of magnitude (dePolo et al., 2021). Based on previous work for various application of TOCN-PPy films (Bideau et al., 2017, 2018), we now explore the formulation of a biobased paint designed to unify conductivity, antibacterial activity, and moisture barrier properties in a single, surface-applicable system. This multifunctional paint is particularly suited for applications such as in smart wooden surfaces, antimicrobial indoor coatings, low-power conductive layers in sensors, and sustainable packaging solutions. Its film-forming capability, ease of application, and bio-based composition make it a promising candidate for eco-friendly coatings across electronics, furniture, and health-sensitive environments. Therefore, this study will aim to integrate TOCN with polypyrrole as a base additive and optimizing the composition using PVA (as binder), glycerol (as plasticizer) and water (as solvent). This work will focus on understanding the structural, thermal, and surface properties of the resulting composite coatings and access their potential for antibacterial and conductive applications. Through a combination of viscosity, scanning electron microscopy (SEM), Raman spectroscopy, contact angle measurements, thermogravimetric analysis (TGA), differential scanning calorimetry (DSC), and qualitative electrical conductivity testing, we have evaluated the material's performance and potential. While previous studies have focused on the development of TOCN-PPy composites as conductive films or coatings, these typically lacked optimization for real-world application as a paint-like formulation. In contrast, our work integrates TOCN and PPy within a fully water-based system, incorporating polyvinyl alcohol (PVA) as a binder and glycerol as a plasticizer. This formulation approach enables direct application to substrates, offering tunable viscosity, improved flexibility, and enhanced adhesion. By systematically varying glycerol content, we demonstrate how to

balance network cohesion and plasticity to achieve a versatile, eco-friendly coating. This novel bio-based paint formulation not only preserves the key functional properties of TOCN-PPy but also extends its practical applicability—representing a significant step forward in green coatings for smart surfaces and sustainable packaging.

## **4.5 MATERIALS AND METHODOLOGY**

### **4.5.1 Materials**

Pyrrole ( $C_4H_5N$ ), iron (III) chloride ( $FeCl_3$ ), poly(vinyl alcohol) and glycerol were procured from Sigma Aldrich and Fisher Scientific, and used without further purification. TOCN were prepared from a commercially available never-dried bleached Kraft wood pulp from a methodology developed by our research group (Loranger, Jradi, et al., 2012; Loranger, Piché, et al., 2012). From previous work, these treatments resulted in a typical carboxyl content of 1600 mmol/kg, facilitating nanofibers extraction from the oxidized cellulose matrix, and exhibited an estimated width of  $3.5 \pm 1.0$  nm and a length of  $306 \pm 112$  nm with a minor fraction of MFC remaining in the final material (Bideau, Cherpozat, et al., 2016).

### **4.5.2 Synthesis of TOCN-Polypyrrole (TOCN-PPy)**

To enhance the functional properties of the composite material, polypyrrole (PPy) was incorporated into the TOCN matrix through an in-situ oxidative polymerization process. The polymerization reaction commenced with the dispersion of 5 mL of pyrrole (4.835 g) in 100 mL of a 0.45 wt% TOCN suspension, followed by stirring for 10 minutes to mitigate premature polymerization, resulting in an approximate PPy:TOCN mass ratio of 10.7:1. Subsequently, 25 mL of a 0.3 M  $FeCl_3$  solution was gradually introduced under continuous stirring, initiating the polymerization process over a period of 30 minutes. Following polymerization, the TOCN-PPy composite underwent an extensive purification protocol to eliminate residual  $FeCl_3$ . During each washing cycle, the pH of the water was monitored, and washing was continued until the pH stabilized near the level of distilled water, indicating effective removal of  $FeCl_3$ . This involved four times sequential washing cycles with 1000 ml of deionized water over a filtration apparatus (Whatman filter paper,

Grade 202)) to ensure compositional purity, with pH stabilization being monitored as an indicator of  $\text{FeCl}_3$  removal.

### **4.5.3 Preparation of Paint Formulations Incorporating TOCN-PPy, PVA, and Glycerol**

The development of paint formulations utilized TOCN-PPy as a functional additive, polyvinyl alcohol (PVA) as a binder, glycerol as a plasticizer, and water as a solvent. The formulation process involved several key steps.

#### **4.5.3.1 Preparation of the PVA Base Formulation**

A homogeneous solution was prepared by dissolving 5 g of PVA in 100 mL of water, followed by the incorporation of the washed TOCN-PPy composite. High-shear mixing (Silverson L4RT-A, USA) was employed a period of 3 minutes at room temperature to ensure uniform dispersion of the composite within the PVA matrix.

#### **4.5.3.2 Incorporation of Glycerol**

To modify the mechanical and rheological properties of the paint, glycerol was introduced in varying concentrations: 1 mL (Gly1), 2 mL (Gly2) and 5 mL (Gly5). Each formulation was subjected again to high-shear mixing (Silverson L4RT-A, USA) for a period of 3 minutes at room temperature to achieve thorough integration of TOCN-PPy, PVA, water, and glycerol.

#### **4.5.3.3 Thermal Processing**

To facilitate complete dissolution of PVA and promote homogeneous blending of all components, the formulations were heated at  $75^\circ\text{C}$  for a duration of 50 minutes to 1 hour under continuous stirring. This thermal treatment ensured uniform dispersion of TOCN-PPy within the polymer matrix, yielding a stable and homogeneous paint formulation suitable for further applications.

#### 4.5.3.4 Experimental design for paints development

This structured approach, illustrated in Figure 4.1, has enabled composite synthesis and formulation development of TOCN-PPy into a paint system. In the developed paint formulations, each component plays a distinct functional role in achieving the desired material properties. The TOCN-polypyrrole serves as a functional additive, contributing to the active properties. Polyvinyl alcohol (PVA) functions as the binder, ensuring strong adhesion and film-forming capabilities essential for coating applications. Glycerol acts as a plasticizer, improving the flexibility and workability of the paint, thereby preventing brittleness and enhancing durability. Water serves as the solvent, enabling uniform dispersion of all components and facilitating efficient mixing and processing throughout the formulation. Together, these components create a stable and homogeneously blended paint system.

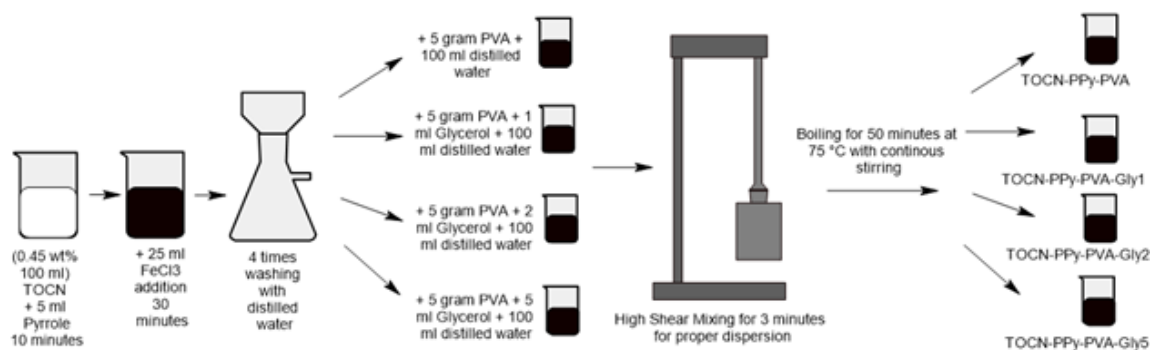


**Figure 4.1** Formation of TOCN-PPy-PVA-Glycerol based paints

#### 4.5.3.5 Making of Paint Films

The paint formulations were used to prepare films by casting 20–25 mL of the paint solutions into Fisherbrand disposable aluminum weighing pans (10 cm diameter). The samples were then left to dry at room temperature ( $23 \pm 2$  °C) for a period of two days, allowing complete solvent evaporation and film formation without thermal acceleration. Once fully dried, the films were carefully peeled from the pans and stored under ambient

conditions prior to characterization. This method yielded self-standing films suitable for structural, surface, thermal, and conductivity analyses.

#### **4.5.4 Substrate coating**

In this study, we evaluated the coating performance of various formulations, including TOCN-PPy, TOCN-PPy-PVA, TOCN-PPy-PVA-Gly1, TOCN-PPy-PVA-Gly2, and TOCN-PPy-PVA-Gly5, on wood substrates, the paints were applied via brush and let it dry over the period of 1 day at room temperature. While the TOCN-PPy formulation alone failed to adhere properly—forming a brittle film that detached from the wood surface upon drying—the inclusion of PVA and varying concentrations of glycerol significantly improved film formation and adhesion. The paint formulations containing PVA and glycerol remained well-adhered to the wood surface, demonstrating their potential for effective painting applications.

### **4.6 Characterisations**

The following sections are describing the apparatus and specific methodology used to characterise the suspension and films.

#### **4.6.1 Rheometer**

The rheological properties of the paint formulations were assessed using a Rheologica Stresstech HR Rheometer (ATS RheoSystems) equipped with a C40 cone–plate geometry. Measurements were conducted at a controlled temperature of 25 °C, with the shear rate ranging from 0.1 to 1000 s<sup>-1</sup>. Apparent viscosity ( $\eta_{\text{app}}$ ) was determined as the slope of the shear stress ( $\tau$ ) versus shear rate ( $\gamma$ ) curve, calculated using the relationship  $\eta_{\text{app}} = \tau/\gamma$ . Each formulation underwent three measurements to ensure data reliability, with average viscosity values reported.

#### **4.6.2 Scanning electron microscopy (SEM)**

Scanning Electron Microscopy (SEM) was performed using a Hitachi SU1510 microscope. Non-conductive samples were sputter-coated with a thin layer of gold using

an International Scientific Instruments PS-2 coating unit to prevent charging and enhance imaging quality. The SEM operated in secondary electron mode at an accelerating voltage of 15 kV and a beam current of 100  $\mu\text{A}$ , providing detailed imaging of surface features.

#### **4.6.3 Raman Spectroscopy**

Raman spectroscopy was conducted using a Thermo Fisher DXR3 Raman Microscope to analyze the molecular composition and chemical structure of the paint films. The instrument was equipped with a 785 nm excitation laser and a full-range grating covering approximately 300 to 3000  $\text{cm}^{-1}$ . Optimal spectral data were obtained by setting the laser power to 30 mW, utilizing an exposure time of 30 seconds per scan, and performing three accumulations. A 50  $\mu\text{m}$  slit aperture and a 10 $\times$  objective were employed to focus the laser on the sample surface. Three replicate measurements were collected for each sample at various locations to ensure data reliability. The DXR3 Raman Microscope features automatic X-axis calibration, enhancing measurement reliability and stability.

#### **4.6.4 Contact angle**

The wettability of the paint films applied to wood surfaces was evaluated through contact angle measurements using the sessile drop method. A Microdrop Contact Angle Analyzer FTA4000 (First Ten Angstroms, USA) was employed for this purpose. Deionized water droplets of 5  $\mu\text{L}$  were carefully deposited onto the coated wood surfaces using the analyzer's precision dispensing system. The contact angles were measured at ambient temperature by capturing the droplet profiles with the instrument's high-resolution camera. The instrument's software analyzed the droplet images to determine the contact angle at the liquid-solid-air interface. To ensure reliability and account for surface heterogeneity, measurements were performed at five different locations on each sample, and the average contact angle was reported.

#### **4.6.5 Thermogravimetric analysis**

Thermogravimetric analysis (TGA) was conducted using a Perkin Elmer TGA-8000 (USA) thermogravimetric analyzer to evaluate the thermal stability and composition of the paint films. Samples were placed in ceramic crucibles and subjected to a temperature

program under a nitrogen atmosphere with a flow rate of 50 mL/min. The program included equilibration at 40 °C for 3 minutes, heating from 40 °C to 105 °C at 10 °C/min to remove adsorbed moisture, an isothermal hold at 105 °C for 20 minutes, followed by heating to 900 °C at 10 °C/min for polymer decomposition and carbonization, an isothermal hold at 900 °C for 20 minutes, and finally cooling back to 40 °C at 200 °C/min. Weight changes were continuously recorded to assess the thermal stability and compositional characteristics of the samples.

#### **4.6.6 Differential scanning calorimetry**

Differential Scanning Calorimetry (DSC) was conducted using a TA Instruments DSC 2500 to analyze the thermal transitions of the paint films. Under a nitrogen atmosphere maintained at a flow rate of 50 mL/min to prevent oxidative degradation, the samples were heated from 40 °C to 200 °C at a rate of 10 °C/min.

#### **4.6.7 Qualitative Conductivity Analysis**

To qualitatively assess the electrical conductivity of the paint films, a simple circuit was constructed comprising a 9V battery and a LED bulb as an indicator. Initially, the circuit was tested in an open configuration without any connecting material; as expected, the bulb remained unlit, confirming that a continuous conductive path is necessary for current flow. An aluminum disk was then introduced into the circuit, completing the electrical pathway and causing the bulb to illuminate, thereby validating the setup's functionality. Subsequently, paint film samples measuring 30 mm in length and 15 mm in width were placed into the circuit in place of the aluminum disk. This result reinforces the reliability of the experimental setup and ensures that the observed conductivity in the TOCN-PPy-PVA-based composites was due to intrinsic material properties rather than experimental artifacts.

### **4.7 RESULTS AND DISCUSSION**

As the application of this study is develop a paint-like coating, measurements of the suspension properties and the resulting film was undergone.

#### 4.7.1 Rheological measurements (Suspensions)

Viscosity measurements on a rheometer enable determination of the viscosity values at a given shear rate but also accurate characterization of shear-dependent flow behavior. Figure 4.2 presents the flow behavior for all the TOCN-PPy-PVA-Glycerol formulations as described in the methodology; an apparent viscosity can be extracted from the data of the shear stress vs. shear rate curves (Table 4.1).

The variation in viscosity observed across the TOCN-PPy-PVA-glycerol system can be attributed to the complex interplay between hydrogen bonding, polymer chain mobility, and filler dispersion. In the base formulation containing TOCN, polypyrrole (PPy), and polyvinyl alcohol (PVA), the viscosity remains relatively low due to limited molecular entanglement and weak physical interactions. The incorporation of a small amount of glycerol (Gly1) results in a significant increase in viscosity, which is attributed to reduced polymer chain mobility by hydrogen bonding between PVA and TOCN nanofibers. This facilitates the formation of a more cohesive and entangled network, while also improving the dispersion of PPy within the matrix. The increase in viscosity observed with the addition of a small amount of glycerol (Gly1) is supported by the Abdullah et al., 2022 findings that glycerol enhances hydrogen bonding and decreases crystallinity, which reduces chain mobility and promotes polymer network cohesion, especially between PVA and other matrix components. As the glycerol content increases further (Gly2 and Gly5), it now assumes a dominant plasticizing role, disrupting interpolymeric hydrogen bonds and reducing the effective network density. Consequently, the viscosity decreases, although it remains higher than the PVA-only formulation. This nonlinear rheological behavior highlights glycerol's dual functionality, acting as a network enhancer at low concentrations and as a plasticizer at higher concentrations, enabling tunable viscosity. This biphasic effect has been documented in a study Kovtun et al., 2024 showed that adding 22% w/w glycerol to PVA initially increased crystallinity due to hydrogen bonding, while higher concentrations (36–55% w/w) disrupted the polymer network, reducing flow resistance. Similarly, another study Tathimongkon et al., 2024 found that while polyvinylpyrrolidone increased viscosity in transdermal patch formulations, increasing glycerol concentrations led to decreased viscosity due to its plasticizing effects.

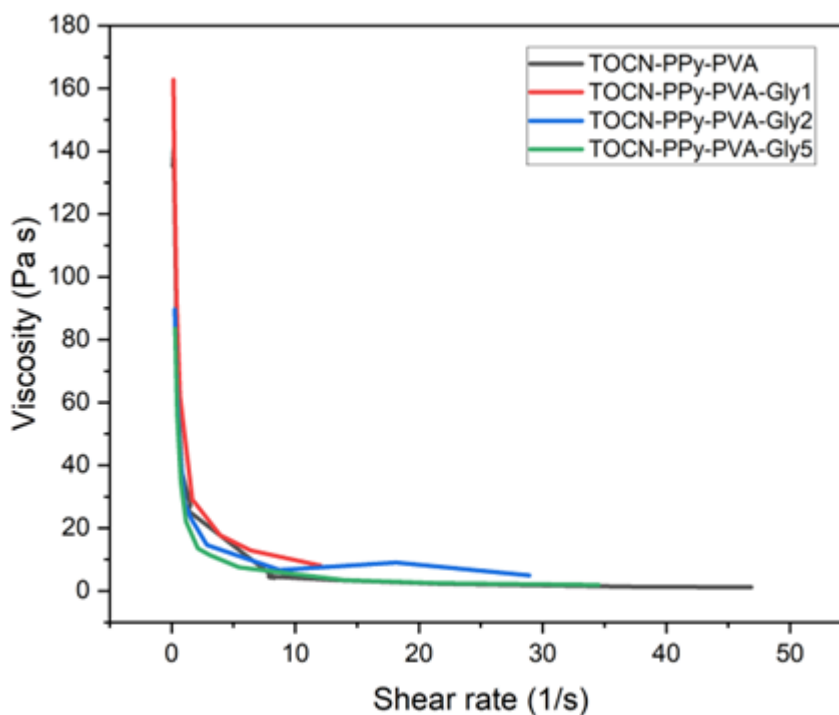


**Figure 4.2** Rheological behaviour of TOCN-PPy-PVA-Glycerol based paints

The rheological behavior of TOCN-PPy-PVA-Glycerol formulations exhibited typical shear-thinning characteristics observed from Figure 4.2, where viscosity decreased with increasing shear rate, demonstrating suitability for paint applications due to ease of application under shear and film stability at rest. The incorporation of glycerol significantly influenced viscosity, with the Gly1 formulation showing the highest viscosity due to enhanced hydrogen bonding and polymer network formation between TOCN, PVA, and glycerol. However, further addition of glycerol in Gly2 and Gly5 reduced the viscosity, as excess glycerol acted as a plasticizer, disrupting the hydrogen bonding network and increasing polymer chain mobility. This biphasic behavior highlights glycerol's dual role—initially strengthening the matrix at low concentrations and later reducing structural cohesion at higher concentrations—allowing tunable rheological properties for tailored coating performance. Furthermore, The viscosity measurements for the TOCN-PPy-PVA-Gly1 formulation (5.93, 10.2, 12.6 Pa·s) exhibit variability due to the inherent complexity and heterogeneity of the paint system. This

formulation contains multiple components (TOCN, PPy, PVA, and glycerol), which can lead to local differences in dispersion and microstructure in each replicate, impacting flow behavior. Additionally, as a non-Newtonian, shear-thinning fluid, slight variations in shear history and rest periods during rheological testing can cause differences in the reported viscosity values. Instrumental factors, such as torque resolution and sample loading, can also contribute to this normal experimental variability. Nevertheless, these differences do not affect the overall trends and conclusions from the rheological characterization.

The rheological profiles of the TOCN-PPy-PVA-Glycerol formulations (Figure 4.2) clearly exhibit shear-thinning behavior, characterized by a decrease in apparent viscosity with increasing shear rate. This behavior is typical of pseudoplastic fluids and is crucial for paints, as it facilitates ease of application under mechanical shear while enhancing stability at rest. Shear thinning in these formulations can be attributed to the alignment and disentanglement of polymer chains (TOCN, PVA, and PPy) and the disruption of transient hydrogen-bonded networks under shear forces. During shear application (e.g., brushing, mixing), viscosity decreased, enabling smooth application, and upon resting, the viscosity of the system appeared to partially recover—indicating reversible structural rebuilding. This is consistent with typical behavior of waterborne polymeric and nanocellulose-based paints, which exhibit structural network rebuilding driven by hydrogen bonding, polymer chain entanglement, and van der Waals interactions (as described by Sreekumar et al., 2012; Shi et al., 2017).

**Table 4.1** Viscosity of TOCN-PPy-PVA-Glycerol based paints

Sample	Viscosity (Pa.s)				
	Measure 1	Measure 2	Measure 3	Mean	Standard deviation
TOCN-PPy-PVA	0.73	0.59	0.59	0.64	0.08
TOCN-PPy-PVA-Gly1	5.93	10.20	12.60	9.58	3.40
TOCN-PPy-PVA-Gly2	2.77	4.76	3.35	3.63	1.00
TOCN-PPy-PVA-Gly5	0.87	0.95	0.86	0.90	0.05

Since the structure of the suspension is proving to be of importance, we want to investigate the structure of the final's products. Therefore, films were made from the above solutions of TOCN-PPy-PVA, TOCN-PPy-PVA-Gly1, TOCN-PPy-PVA-Gly2 and TOCN-PPy-PVA-Gly5.

#### 4.7.2 Scanning electron microscopy (Films)

The SEM micrographs reveal significant morphological variations across the TOCN-PPy-based composites, highlighting the structural influence of PVA and glycerol on the material. The Figure 4.3 shows the SEM for the surface of TOCN-PPy, TOCN-PPy-PVA, and TOCN-PPy-PVA-Gly2. The TOCN-PPy (Figure 4.3a) sample exhibits a highly rough, porous, and fibrous surface morphology, indicative of an interconnected polypyrrole (PPy) network embedded within the TOCN matrix. The presence of visible voids and irregularities suggests a high surface area, but could lead to increased mechanical fragility. Upon the incorporation of PVA (TOCN-PPy-PVA), Figure 4.3b, show that microstructure appears significantly smoother and more compact, suggesting improved polymer matrix integration, thus potential enhanced mechanical stability. PVA likely acts as a binder, reducing phase separation and improving structural cohesion.

However, minor surface irregularities may still imply localized polymer aggregation. In Figure 4.3c, further modification with glycerol (TOCN-PPy-PVA-Gly2) show an even more cohesive microstructure, characterized by a smooth morphology with visible fibrillar structures. The plasticizing effect of glycerol appears to enhance polymer blending, reducing surface roughness while maintaining an interconnected network. The presence of elongated streaks or fibrils suggests polymer chain alignment, potentially improving mechanical flexibility while preserving electric conductive pathways.

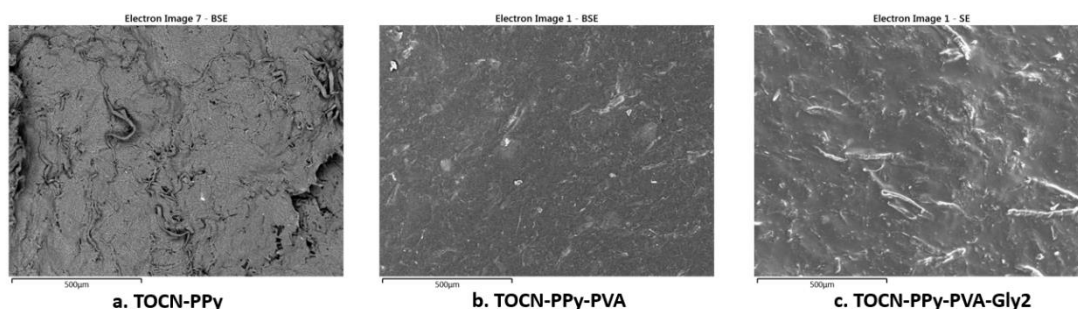


**Figure 4.3** Scanning electron microscopy for the TOCN-PPy, TOCN-PPy-PVA and TOCN-PPy-PVA-Gly2

#### 4.7.3 Raman Spectroscopy (Films)

The Raman spectra of TOCN-PPy, TOCN-PPy-PVA, and glycerol-modified composites (TOCN-PPy-PVA-Gly1, TOCN-PPy-PVA-Gly2, and TOCN-PPy-PVA-Gly5) were analyzed and compared with reported literature values to assess structural and electronic variations (Figure 4.4).

The key Raman peaks of interest observed in this study were at 922, 1042, 1230, 1318, 1408, 1507, and 1597  $\text{cm}^{-1}$ , corresponding to fundamental vibrational modes associated with polypyrrole (PPy) and its composites. The observed Raman bands were compared with previously reported assignments (Šetka et al., 2019; Ishpal & Kaur, 2013). The comparison suggests that the molecular structure and oxidation state of PPy were influenced by the presence of TOCN, PVA, and glycerol modifications.

Raman spectroscopic analysis of the TOCN-PPy-PVA composites revealed spectral shifts and peak broadening, indicating complex molecular interactions between the polypyrrole

(PPy) backbone, TOCN, polyvinyl alcohol (PVA), and glycerol. A notable shift is observed in the C–C ring deformation associated with bipolaron formation, where the peak appears at  $922\text{ cm}^{-1}$ , slightly downshifted from the reported  $933\text{--}939\text{ cm}^{-1}$  range (Šetka et al., 2019). This shift may be influenced by interactions between TOCN and PVA. Similarly, the C–H in-plane deformation associated with polaronic structures is observed at  $1042\text{ cm}^{-1}$ , downshifted from the typical  $1050\text{--}1056\text{ cm}^{-1}$  range (Ishpal & Kaur, 2013). The shift may be attributed to hydrogen bonding interactions between the polypyrrole chains and TOCN or PVA, which alter the local electronic environment and influence charge delocalization. Further modifications in conjugation are evident in the ring stretching and antisymmetric C–H bending modes, with a peak at  $1230\text{ cm}^{-1}$ , compared to the literature-reported  $1241\text{--}1253\text{ cm}^{-1}$  (Šetka et al., 2019). This shift suggests changes in electronic density along the PPy backbone, likely due to TOCN-PVA interactions. Similarly, the C–C in-ring and antisymmetric C–N stretching vibrations, detected at  $1318\text{ cm}^{-1}$  (compared to  $1330\text{--}1333\text{ cm}^{-1}$  in literature), indicate slight variations in conjugation length. These modifications may result from hydrogen bonding interactions or steric effects introduced by the polymeric matrix.

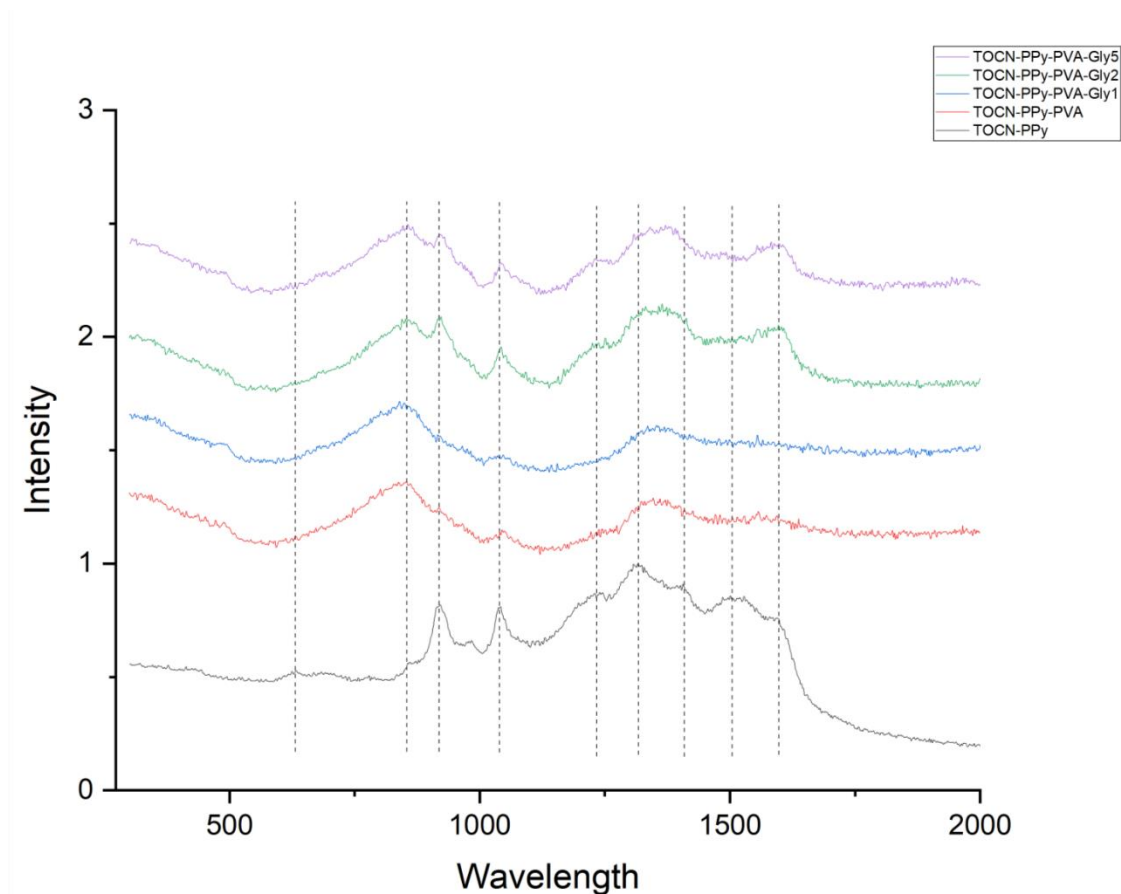


**Figure 4.4** Raman spectroscopy of TOCN-PPy-PVA-Glycerol based paints

A more pronounced shift is observed in the C–C in-ring, C–N stretching, and N–H bending vibrations, where the  $1408\text{ cm}^{-1}$  peak is significantly upshifted from the expected  $1372\text{--}1389\text{ cm}^{-1}$  range (Šetka et al., 2019). This shift suggests possible changes in the oxidation state of PPy, with increased oxidation levels typically leading to higher peak intensities in this region (Ishpal & Kaur, 2013). The presence of PVA and glycerol appears to influence the electronic charge distribution within the polypyrrole framework, potentially modifying its conductivity and charge transport properties. The C–C and C=N stretching vibrations, appearing at  $1507\text{ cm}^{-1}$ , align well with the literature values of  $1492\text{--}1498\text{ cm}^{-1}$  (Šetka et al., 2019), confirming the integrity of polypyrrole’s characteristic vibrational modes within the composite structure. Similarly, the C=C in-ring and C–C inter-ring stretching mode, observed at  $1597\text{ cm}^{-1}$ , remains consistent with reported values of  $1583\text{--}1609\text{ cm}^{-1}$  (Šetka et al., 2019). While these observations indicate that the main polypyrrole backbone remains intact, the small spectral shifts observed could be

associated with interactions between PVA, TOCN, and glycerol. However, minor shifts indicate that while PVA and glycerol modifications do not disrupt the primary PPy backbone, they do influence charge delocalization.

Finally, the Raman spectra show increased broadening in TOCN-PPy-PVA and TOCN-PPy-PVA-Gly1, particularly in the peaks around  $1408\text{ cm}^{-1}$  and  $1597\text{ cm}^{-1}$ . This broadening is indicative of enhanced molecular interactions, possibly due to increased hydrogen bonding or polymeric entanglement effects. The spectral broadening is more pronounced in Gly1, suggesting an initial increase in molecular disorder and charge delocalization due to glycerol incorporation. With Gly2 and Gly5, the peaks become more defined, indicating a stabilization effect as the glycerol content increases. This suggests that at higher glycerol concentrations, the molecular interactions become more structured, possibly leading to better charge transport properties.

#### 4.7.4 Contact angle (Wood painted surfaces)

While not being a chemical analysis, the water droplet contact angle give relevant information about the surface hydrophobicity. The results from Table 4.2 show how glycerol content affects the surface properties of TOCN-PPy-PVA composites, with a clear trend toward increased hydrophobicity and reduced wettability as glycerol concentration increase.

**Table 4.2** Contact angle measurement of TOCN-PPy-PVA-Glycerol based paints

Sample	Static Contact Angle (°)
TOCN-PPy-PVA	$85.40 \pm 4.22$
TOCN-PPy-PVA-Gly1	$93.09 \pm 6.50$
TOCN-PPy-PVA-Gly2	$86.46 \pm 5.23$
TOCN-PPy-PVA-Gly5	$79.89 \pm 4.09$

The control sample (TOCN-PPy-PVA) exhibits moderate hydrophobicity with a contact angle of  $85.40^\circ \pm 4.22$ . With the addition of glycerol, the contact angle increases to  $93.09^\circ \pm 6.50$  for the Gly1 sample, indicating enhanced hydrophobicity, though variability is observed due to higher standard deviation. For the Gly2 sample, the contact angle decreases to  $86.46^\circ \pm 5.23$ , suggesting a slight reduction in hydrophobicity and improved wettability. The highest glycerol content (Gly5) leads to the lowest contact angle ( $79.89^\circ \pm 4.09$ ), reflecting a shift toward hydrophilicity and enhanced wettability. Overall, as glycerol content increases, there is a consistent reduction in hydrophobicity and an increase in wettability, with lower variability observed at higher glycerol concentrations.

#### **4.7.5 Thermogravimetric Analysis (Films)**

Thermogravimetric analysis (TGA) was performed to investigate the thermal stability, decomposition behavior, and residual mass content of TOCN-based composites, including pure TOCN, TOCN-PPy, TOCN-PPy-PVA, and glycerol-modified composites (TOCN-PPy-PVA-Gly1, Gly2, Gly5). The thermogravimetric analysis (Figure 4.5) of TOCN-based composites revealed distinct thermal degradation profiles reflecting the influence of added components.

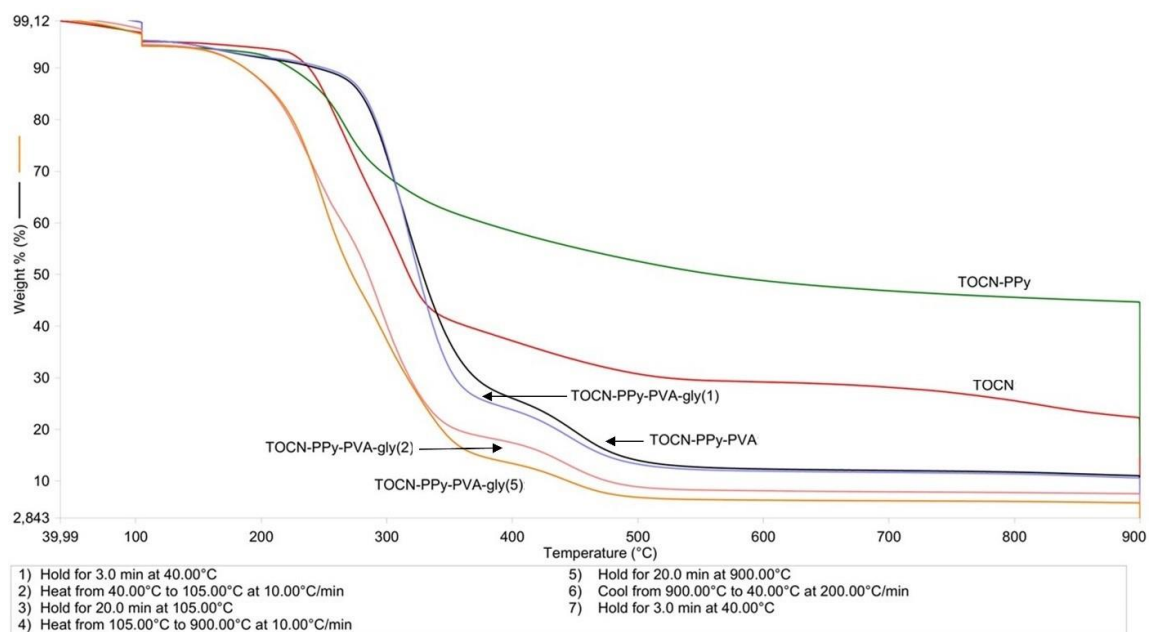


**Figure 4.5** Thermogravimetric analysis of TOCN-PPy-PVA-Glycerol based paints

Pure TOCN exhibited two main degradation stages: moisture loss below 105°C and cellulose decomposition between 200–350°C, leaving residue at 900°C. TOCN-PPy exhibited the highest thermal stability, with a residual mass of approximately 44% at 900°C, indicating the formation of a stable carbonaceous structure due to polypyrrole's conjugated aromatic backbone. Pure TOCN retained about 22%, reflecting typical cellulose char formation after thermal degradation. Incorporating PVA reduced the final residue to 11%, indicating a more complete thermal decomposition of the polymeric matrix. The introduction of glycerol further reduced thermal stability, with residual masses decreasing progressively to 10.5% (Gly1), 8% (Gly2), and 6.5% (Gly5). This trend is consistent with glycerol's known plasticizing effect, which lowers the thermal decomposition onset and enhances volatility, leading to lower char formation. These results underscore the trade-off between flexibility and thermal resistance, as the addition of glycerol improves processability but diminishes structural integrity under thermal stress. The enhanced char yield in PPy-containing samples confirms its role in improving high-temperature performance, crucial for applications requiring both conductivity and thermal durability. Glycerol lower decomposition temperature (~150–250°C) and high volatility result in significant mass loss at earlier stages and reduced carbonaceous residue. Incorporating polypyrrole (PPy) improved thermal stability, with a delayed onset of

degradation and increased residue due to stable carbonaceous content. The addition of polyvinyl alcohol (PVA) and glycerol introduced overlapping degradation steps and increased moisture loss at 105°C, highlighting their hydrophilic nature. In the end, glycerol reduced overall thermal stability due to its lower decomposition temperature, while PPy enhanced stability by delaying decomposition.

These results underscore the trade-off between flexibility, hydrophilicity, and thermal performance, critical for tailoring composites for applications in biobased coatings and packaging. The lower residual mass observed in the glycerol-modified composites (TOCN-PPy-PVA-Gly1, Gly2, and Gly5) indicates a greater degree of thermal degradation and reduced char yield compared to TOCN and TOCN-PPy, making them less suitable for high-temperature applications. Sreekumar et al., 2012 also observed that increasing glycerol concentrations led to a decrease in crystallinity and tensile strength, particularly at elevated temperatures. They also concluded that while glycerol acts as an effective plasticizer enhancing flexibility, it compromises the structural integrity of the material under thermal stress.

#### **4.7.6 Differential scanning calorimetry (Films)**

Differential Scanning Calorimetry (DSC) was conducted to evaluate the thermal behavior of TOCN, TOCN-Polypyrrole (TOCN-PPy), TOCN-PPy-PVA, and glycerol-modified composites (TOCN-PPy-PVA-Gly1, TOCN-PPy-PVA-Gly2, and TOCN-PPy-PVA-Gly5) (Figure 4.6). In Figure 4.6, the glass transition temperature ( $T_g$ ) is observed as a subtle deviation in the baseline, indicating molecular mobility changes in the polymer matrix. The pure TOCN sample exhibits a  $T_g$  at approximately 135°C, attributed to the amorphous fraction of cellulose nanofibers. Incorporation of polypyrrole (PPy) into TOCN (TOCN-PPy) results in a slight increase in  $T_g$  to ~140°C, suggesting enhanced thermal stability due to strong interfacial interactions between TOCN and PPy. With the addition of polyvinyl alcohol (PVA), the  $T_g$  becomes less defined, indicating a reduction in crystalline fraction and an increase in polymer chain flexibility. The glycerol-modified samples (TOCN-PPy-PVA-Gly1, TOCN-PPy-PVA-Gly2, and TOCN-PPy-PVA-Gly5) exhibit an even broader  $T_g$  transition due to the plasticizing effect of glycerol, which further increases polymer mobility and reduces the rigidity of the composite matrix.

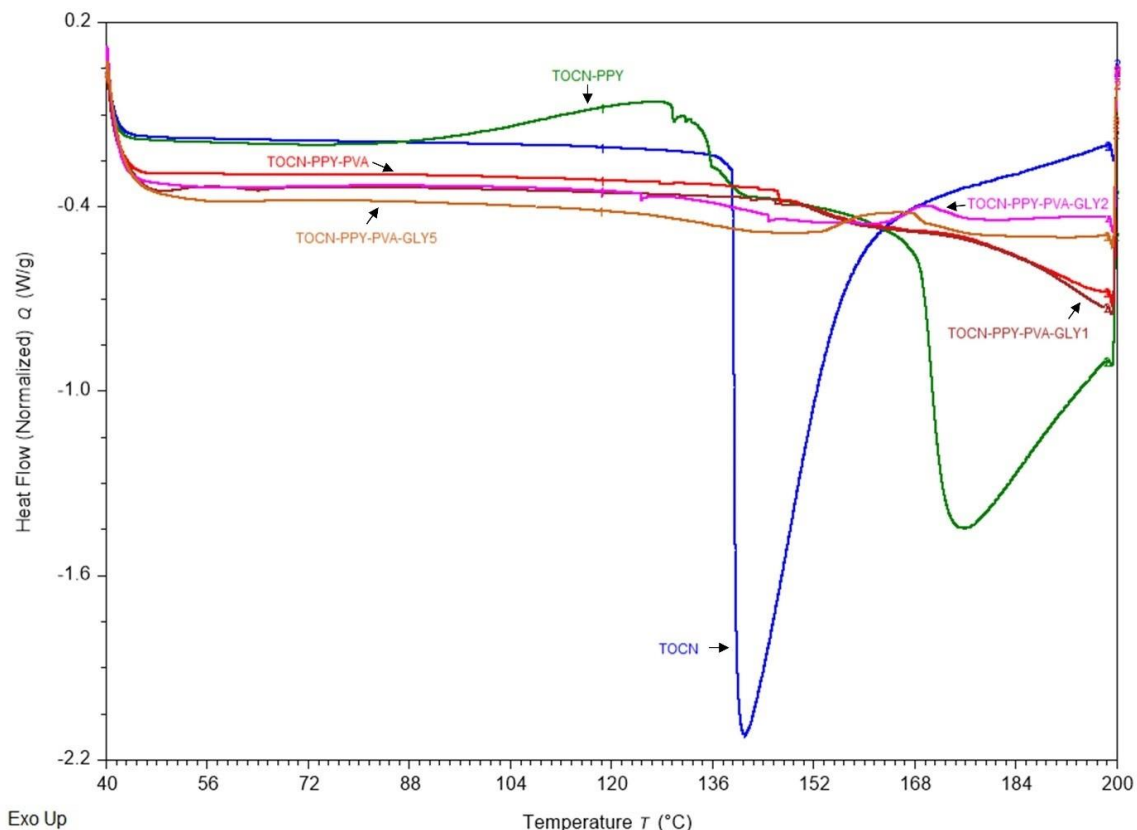


**Figure 4.6** Differential scanning calorimetry analysis of TOCN-PPy-PVA-Glycerol based paints

The DSC thermograms of Figure 4.6 also reveal significant endothermic peaks in the range of 130°C to 160°C, associated with melting or structural relaxation of the composite materials. The pure TOCN sample exhibits a sharp endothermic peak at ~140°C, corresponding to its degradation point. However, upon incorporating PPy, the transition shifts to a higher temperature (~175°C), demonstrating improved thermal stability (as in the TGA analysis) due to the presence of polypyrrole. The TOCN-PPy-PVA formulation shows a broader and less distinct endothermic peak (~145-160°C) compared to TOCN and TOCN-PPy, indicating increased amorphous content and enhanced thermal flexibility. The addition of glycerol further influences the thermal transitions by suppressing sharp melting peaks and broadening the transition region. This behavior is characteristic of plasticized polymer systems, where glycerol disrupts crystalline domains, increasing polymer chain mobility and reducing rigidity. As per (Kovtun et al., 2024), incorporating glycerol into PVA films affects their crystallinity. At low glycerol

concentrations, glycerol enhances the mobility of molecular chains, promoting ordering and crystallization. However, at higher concentrations, glycerol may aggregate and interact selectively with PVA chains at crystalline interfaces, potentially penetrating the crystals and disrupting molecular order. Interestingly, the TOCN-PPy-PVA-Gly2 and TOCN-PPy-PVA-Gly5 samples exhibit small exothermic peaks ( $\sim 160-175^{\circ}\text{C}$ ), suggesting possible molecular rearrangement or secondary crystallization before decomposition. These events may be attributed to 1- a structural Relaxation Phase as the presence of PVA and glycerol leads to weak crystalline reordering, causing an exothermic response, 2- weak Crosslinking or Secondary Crystallization – The polymer matrix, influenced by hydrogen bonding interactions, may undergo localized structural reorganization in response to heating or 3-, reorientation of Hydrogen Bonds – The hydroxyl groups in TOCN, PVA, and glycerol may undergo dynamic rearrangements, leading to minor exothermic energy release.

The polymer matrix, influenced by hydrogen bonding interactions, may undergo localized structural reorganization upon heating. Kovtun et al., 2024 have shown that the addition of glycerol to PVA films affects the crystalline structure, leading to changes in thermal transitions.

#### **4.7.7 Qualitative Conductivity Analysis (Films)**

In order to evaluate the electrical conductivity of the samples and confirm the continuous structure of the paints, a qualitative test was conducted using a basic electrical circuit. As explained in the methodology, the sample (in film factor) are used to close the circuit and evaluate the LED intensity (Figure 4.7). The aluminum disk was used as a control due to its well-established electrical conductivity and when integrated into the circuit, the bulb glowed brightly, indicating efficient current flow and confirming the material's high conductivity (Figure 4.7a). As expected, when the circuit was open (Figure 4.7b), the bulb did not illuminate, demonstrating the interruption of the electrical pathway. When TOCN-PPy-PVA-based composites, including TOCN-PPy-PVA, TOCN-PPy-PVA-Gly1, TOCN-PPy-PVA-Gly2, and TOCN-PPy-PVA-Gly5 (Figure 4.7c to Figure 4.7f), were introduced into the circuit, the bulb emitted a faint but noticeable glow. Although the brightness was significantly lower than that observed with the aluminum disk, the

consistent illumination across all samples indicated the presence of measurable electrical conductivity. The faint glow does confirm that the TOCN-PPy-PVA composites possess some level of electrical conductivity, which can be attributed to the incorporation of polypyrrole (PPy) within the matrix (Bideau, Cherpozat, et al., 2016). As a conductive polymer, PPy forms pathways that enable charge transport within the otherwise non-conductive TOCN, PVA, and glycerol-based network. The lower intensity of the bulb's glow compared to the aluminum disk underscores the fact that the conductivity of these polymer-based composites is considerably weaker than that of metals, which is expected for conductive polymers. Furthermore, the inclusion of glycerol in the modified samples (Gly1, Gly2, and Gly5) did not significantly hinder conductivity, as evidenced by the consistent bulb illumination. However, we acknowledge that these qualitative tests do not provide a rigorous quantification of electrical conductivity.

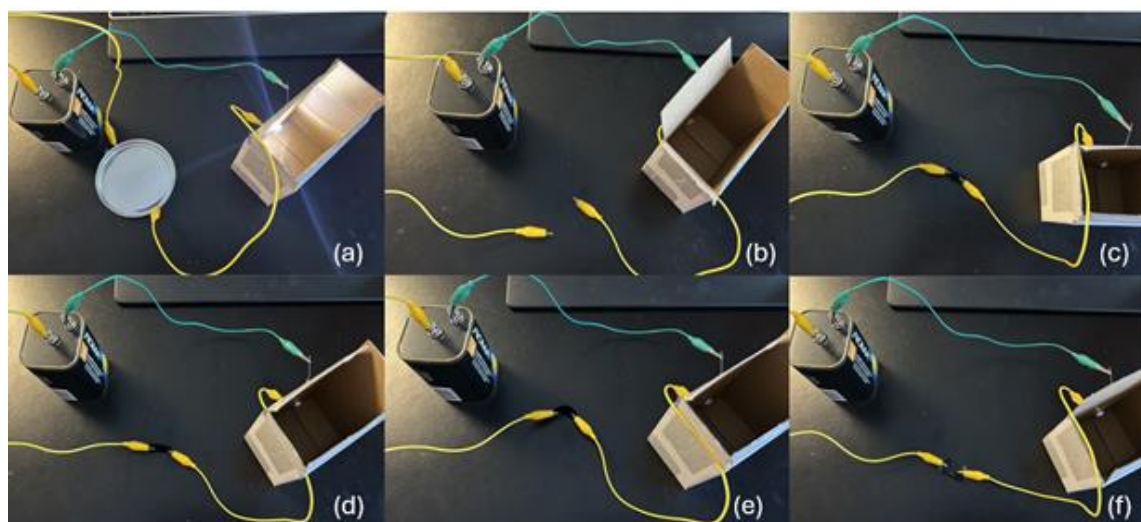


**Figure 4.7** (a) Circuit with aluminum disk, (b) open circuit, (c) with TOCN-PPy-PVA, (d) with TOCN-PPy-PVA-Gly2, (e) with TOCN-PPy-PVA-Gly2, (f) with TOCN-PPy-PVA-Gly5

#### 4.7.8 Proposed structure of TOCN-PPy, TOCN-PPy-PVA and TOCN-PPy-PVA-Gly

With the given analysis, we can make hypothesis on the structure of TOCN-PPy, TOCN-PPy-PVA and TOCN-PPy-PVA-Gly paints. Figure 4.8 illustrates the basic molecules while Figure 4.8(e) present a proposed structure of TOCN-PPy.

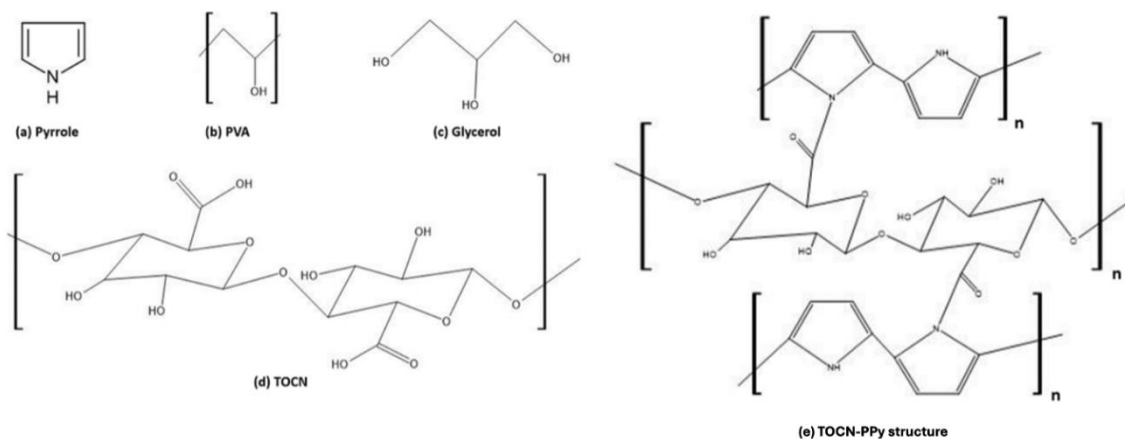


**Figure 4.8** (a) Pyrrole, (b) Polyvinyl alcohol, (c) Glycerol, (d) TOCN, (e) Proposed TOCN-PPy structure

The TOCN-PPy structure is primarily driven by electrostatic interactions between negatively charged carboxyl ( $-\text{COO}^-$ ) groups of TOCN and partially positively charged nitrogen ( $\text{N}^+\text{-H}$ ) sites in PPy, ensuring strong adhesion of PPy onto the TOCN surface. Raman spectroscopy did confirm polaronic and bipolaronic charge states, reinforcing this interaction. Additionally, hydrogen bonding between residual hydroxyl ( $-\text{OH}$ ) groups in TOCN and  $\text{N-H}$  sites in PPy provides further stabilization, enhancing dispersion and uniformity. The addition of glycerol (Gly) as a plasticizer induces further changes in the thermal degradation profiles, reflecting its plasticizing effect that enhances flexibility while reducing thermal stability. Together, the TGA and DSC analyses support the proposed structural model, emphasizing the distinct and synergistic interactions among TOCN, PPy, PVA, and Gly. These interactions modulate the composite paints' thermal transitions and residual stability, balancing flexibility with char-forming capacity

depending on the formulation. As demonstrated by Shi et al., 2017, glycerol disrupts hydrogen bonding within PVA, leading to enhanced flexibility (Figure 4.9). In the TOCN-PPy-PVA-Gly composite, this effect improves polymer chain mobility while maintaining the structural integrity provided by TOCN and PPy interactions.

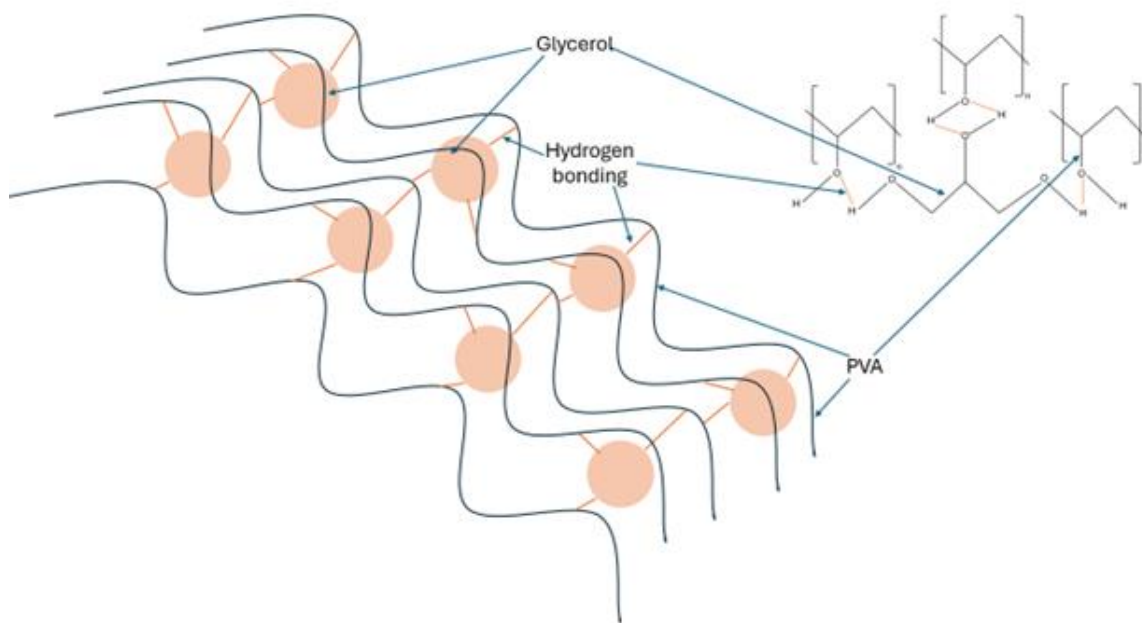


**Figure 4.9** PVA-Glycerol interaction

The TOCN-PPy-PVA structure is stabilized by electrostatic interactions and hydrogen bonding. The carboxyl ( $\text{-COO}^-$ ) groups of TOCN strongly bind to the  $\text{N}^+\text{-H}$  sites of PPy, ensuring uniform deposition. Polyvinyl alcohol (PVA) integrates through hydrogen bonding, primarily interacting with TOCN's hydroxyl ( $\text{-OH}$ ) and carboxyl ( $\text{-COO}^-$ ) groups, reinforcing structural stability. Additional PVA ( $\text{-OH}$ ) to PPy ( $\text{N-H}$ ) hydrogen bonding improves dispersion and prevents phase separation. This results in a well-integrated composite, where TOCN provides reinforcement, PPy imparts conductivity, and PVA enhances film uniformity, adhesion, and mechanical performance.

On the other hand, TOCN-PPy-PVA-Gly structure incorporates plasticization effects, in addition to electrostatic interactions and hydrogen bonding. While TOCN and PPy interact electrostatically, PVA binds through hydrogen bonding, stabilizing the matrix. Glycerol acts as a plasticizer, forming hydrogen bonds with PVA ( $\text{-OH}$ ) groups, disrupting PVA's

internal network, increasing polymer flexibility, and reducing crystallinity. A minor glycerol (-OH) interaction with TOCN (-OH) may enhance hydrophilicity, modifying the composite's wettability. This well-integrated structure enables TOCN to provide reinforcement, PPy to impart conductivity, PVA to enhance cohesion, and glycerol to improve flexibility, making the material suitable for coatings and functional applications.

#### 4.8 CONCLUSION

This study successfully developed a biobased paint and coating formulation by integrating TOCN with polypyrrole (PPy) in a matrix of polyvinyl alcohol (PVA) and glycerol. The observed nonlinear rheological behavior underscores glycerol's dual functionality: at low concentrations, it enhances network cohesion through hydrogen bonding, leading to increased viscosity; at higher concentrations, it acts as a plasticizer, disrupting interpolymeric interactions and reducing viscosity. Morphological analysis through SEM revealed a well-dispersed, cohesive structure, with glycerol contributing to flexibility and improved internal cohesion. Raman spectroscopy has verified polypyrrole integration by identifying its characteristic vibrational modes. The spectral analysis further validated molecular interactions within the composite, reinforcing its cohesive and stable structure. Additionally, qualitative conductivity testing demonstrated that the material exhibits measurable electrical conductivity, confirming the presence of polypyrrole within the composite. Contact angle measurements demonstrated that increasing glycerol content reduced hydrophobicity and enhanced wettability, indicating the tunability of surface properties for specific applications. Thermogravimetric analysis (TGA) revealed multi-stage thermal degradation, where polypyrrole improved thermal stability, and glycerol contributed to flexibility (which was further confirmed via DSC) by lowering the decomposition temperature. The proposed structure highlights the interaction between PVA and glycerol through hydrogen bonding, which contributes to the flexibility and integrity of the matrix. TOCN-PPy is incorporated into this network, where TOCN interacts with PVA and glycerol via hydrogen bonding, and PPy is expected to be well-dispersed within the matrix, supporting the overall stability and performance of the formulation. While earlier studies primarily explored TOCN-PPy composites as conductive films or coatings, they often lacked formulation strategies suitable for

practical, paint-like applications. In contrast, our work advances this field by developing a fully water-based system that combines TOCN and polypyrrole (PPy) with polyvinyl alcohol (PVA) as a binder and glycerol as a plasticizer, thus offering a more application-ready coating formulation. These findings underscore the balance between structural integrity, thermal performance, and adaptability, making the material suitable for diverse industrial and protective coating applications. Furthermore, these results highlight the potential of TOCN-PPy-PVA-Gly composites as a sustainable and high-performance paints. Future research should focus on assessing the antibacterial properties, biodegradability, UV resistance, substrate adhesion, humidity resistance, and gas permeation to explore real-world applications. Additionally, future work will include quantitative electrical conductivity testing, mechanical testing to validate the observed improvements in flexibility, and barrier property analysis to establish comprehensive structure–property correlations and confirm the multifunctional performance of these bio-based coatings.

#### **4.9 CRediT (CONTRIBUTOR ROLES TAXONOMY)**

Aakash Malik was responsible for Conceptualization, Data Curation, Formal Analysis, Investigation, Methodology, Project Administration, Validation, Visualization, and Writing – Original Draft; Éric Loranger contributed to Funding Acquisition, Project Administration, Supervision, Validation, and Writing – Review & Editing; Simon Barnabé contributed to Supervision and Writing – Review & Editing.

#### **4.10 Declaration of generative AI and AI-assisted technologies in the writing process**

During the preparation of this work the author(s) did not use any generative or AI related tools.

#### 4.11 ACKNOWLEDGEMENTS

This research project is funded by the Natural Sciences and Engineering Research Council of Canada (Discovery grant RGPIN-2021-02861) and Municipal Research Chair for Sustainable Cities (UQTR – Victoriaville).

#### 4.12 REFERENCES

- Abdullah, A. M., Aziz, S. B., Brza, M. A., Saeed, S. R., Al-Asbahi, B. A., Sadiq, N. M., Ahmed, A. A. A., & Murad, A. R. (2022). Glycerol as an efficient plasticizer to increase the DC conductivity and improve the ion transport parameters in biopolymer based electrolytes: XRD, FTIR and EIS studies. *Arabian Journal of Chemistry*, 15(6). <https://doi.org/10.1016/j.arabjc.2022.103791>
- Ayissi Eyebe, G. F. V., Bideau, B., Loranger, É., & Domingue, F. (2019). TEMPO-oxidized cellulose nanofibre (TOCN)films and composites with PVOH as sensitive dielectrics for microwave humidity sensing. *Sensors and Actuators, B: Chemical*, 291, 385–393. <https://doi.org/10.1016/j.snb.2019.04.070>
- Bideau, B., Bras, J., Adoui, N., Loranger, E., & Daneault, C. (2017). Polypyrrole/nanocellulose composite for food preservation: Barrier and antioxidant characterization. *Food Packaging and Shelf Life*, 12, 1–8. <https://doi.org/10.1016/j.fpsl.2017.01.007>
- Bideau, B., Bras, J., Saini, S., Daneault, C., & Loranger, E. (2016). Mechanical and antibacterial properties of a nanocellulose-polypyrrole multilayer composite. *Materials Science and Engineering C*, 69, 977–984. <https://doi.org/10.1016/j.msec.2016.08.005>
- Bideau, B., Cherpozat, L., Loranger, E., & Daneault, C. (2016). Conductive nanocomposites based on TEMPO-oxidized cellulose and poly(N-3-aminopropylpyrrole-co-pyrrole). *Industrial Crops and Products*, 93, 136–141. <https://doi.org/10.1016/j.indcrop.2016.06.003>

- Bideau, B., Loranger, E., & Daneault, C. (2016). Comparison of Three Polypyrrole-Cellulose Nanocomposites Synthesis. *Journal of Advances in Nanomaterials*, 1(2). <https://doi.org/10.22606/jan.2016.12007>
- Bideau, B., Loranger, E., & Daneault, C. (2018). Nanocellulose-polypyrrole-coated paperboard for food packaging application. *Progress in Organic Coatings*, 123, 128–133. <https://doi.org/10.1016/j.porgcoat.2018.07.003>
- Chek, Y. W., & Ang, D. T. C. (2024). Progress of bio-based coatings in waterborne system: Synthesis routes and monomers from renewable resources. In *Progress in Organic Coatings* (Vol. 188). Elsevier B.V. <https://doi.org/10.1016/j.porgcoat.2023.108190>
- dePolo, G., Walton, M., Keune, K., & Shull, K. R. (2021). After the paint has dried: a review of testing techniques for studying the mechanical properties of artists' paint. In *Heritage Science* (Vol. 9, Issue 1). Springer Science and Business Media Deutschland GmbH. <https://doi.org/10.1186/s40494-021-00529-w>
- Eyebe, G. A., Bideau, B., Loranger, E., Boubekeur, N., & Domingue, F. (2018). Novel TOCNPVOH Dielectric Composite Sheets with Low Ecological Footprint for Microwave Humidity Sensing. *IEEE Sensors Letters*, 2(4). <https://doi.org/10.1109/LSENS.2018.2869155>
- Halake, K., Birajdar, M., Kim, B. S., Bae, H., Lee, C. C., Kim, Y. J., Kim, S., Kim, H. J., Ahn, S., An, S. Y., & Lee, J. (2014). Recent application developments of water-soluble synthetic polymers. In *Journal of Industrial and Engineering Chemistry* (Vol. 20, Issue 6, pp. 3913–3918). Korean Society of Industrial Engineering Chemistry. <https://doi.org/10.1016/j.jiec.2014.01.006>
- Ishpal, & Kaur, A. (2013). Spectroscopic investigations of ammonia gas sensing mechanism in polypyrrole nanotubes/nanorods. *Journal of Applied Physics*, 113(9). <https://doi.org/10.1063/1.4793994>

- Kovtun, G., Casas, D., & Cuberes, T. (2024). Influence of Glycerol on the Surface Morphology and Crystallinity of Polyvinyl Alcohol Films. *Polymers*, 16(17). <https://doi.org/10.3390/polym16172421>
- Loranger, E., Jradi, K., & Daneault, C. (2012). Nanocellulose production by ultrasound-assisted TEMPO oxidation of Kraft pulp on laboratory and pilot scales. *IEEE International Ultrasonics Symposium, IUS*, 953–956. <https://doi.org/10.1109/ULTSYM.2012.0238>
- Loranger, E., Piché, A. O., & Daneault, C. (2012). Influence of high shear dispersion on the production of cellulose nanofibers by ultrasound-assisted tempo-oxidation of kraft pulp. *Nanomaterials*, 2(3), 286–297. <https://doi.org/10.3390/nano2030286>
- Nachlas, W. O., Bushmaker, S., & Sasson, E. (2023). X-ray Spectroscopy of Nitrogen in Jarosite, Ammoniojarosite, and other NH<sub>4</sub>-Bearing Sulfate Minerals. *Microscopy and Microanalysis: The Official Journal of Microscopy Society of America, Microbeam Analysis Society, Microscopical Society of Canada*, 29(1), 862–864. <https://doi.org/10.1093/micmic/ozad067.427>
- Oesef, K., Cranston, E. D., & Abdin, Y. (2024). Current advances in processing and modification of cellulose nanofibrils for high-performance composite applications. In *Materials and Design*. Elsevier Ltd. <https://doi.org/10.1016/j.matdes.2024.113417>
- Samir, A., Ashour, F. H., Hakim, A. A. A., & Bassyouni, M. (2022). Recent advances in biodegradable polymers for sustainable applications. In *npj Materials Degradation* (Vol. 6, Issue 1). Nature Publishing Group. <https://doi.org/10.1038/s41529-022-00277-7>
- Šetka, M., Calavia, R., Vojkůvka, L., Llobet, E., Drbohlavová, J., & Vallejos, S. (2019). Raman and XPS studies of ammonia sensitive polypyrrole nanorods and nanoparticles. *Scientific Reports*, 9(1). <https://doi.org/10.1038/s41598-019-44900-1>
- Shi, S., Peng, X., Liu, T., Chen, Y. N., He, C., & Wang, H. (2017). Facile preparation of hydrogen-bonded supramolecular polyvinyl alcohol-glycerol gels with excellent thermoplasticity and mechanical properties. *Polymer*, 111, 168–176. <https://doi.org/10.1016/j.polymer.2017.01.051>

- Sreekumar, P. A., Al-Harhi, M. A., & De, S. K. (2012). Effect of glycerol on thermal and mechanical properties of polyvinyl alcohol/starch blends. *Journal of Applied Polymer Science*, 123(1), 135–142. <https://doi.org/10.1002/app.34465>
- Tang, Z., Lin, X., Yu, M., Mondal, A. K., & Wu, H. (2024). Recent advances in TEMPO-oxidized cellulose nanofibers: Oxidation mechanism, characterization, properties and applications. In *International Journal of Biological Macromolecules* (Vol. 259). Elsevier B.V. <https://doi.org/10.1016/j.ijbiomac.2023.129081>
- Tathimongkon, J., Chaijaruwanich, A., Nakkiew, W., & Wattanutchariya, W. (2024). Effects of PVA, PVP, and Glycerol on the Viscosity of a Transdermal Patch. *Advances in Science and Technology*, 143, 27–34. <https://doi.org/10.4028/p-ZZvd6u>
- Xie, J., Jin, X., Cheng, H., Chen, W., Yu, W., & Wang, L. (2024). Molecular origin of the plasticizing effect difference of glycerol with other polyols on plasticizing polyvinyl alcohol (PVA) as elucidated by solid-state NMR. *Industrial Crops and Products*, 220. <https://doi.org/10.1016/j.indcrop.2024.119246>
- Zheng, Q., Li, Y., Liang, Y., Chen, T., Li, F., Zhu, P., & Tang, Y. (2024). In-situ polymerization of pyrrole on cellulose nanofiber film: Structure characterization and electrochemical properties. *Industrial Crops and Products*, 222. <https://doi.org/10.1016/j.indcrop.2024.120068>

## **Chapter 5 - Scientific Article 2 : Environmental fate of TOCN–PPy–PVA–Gly paint coatings**

### **5.1 Preface**

This part of the work is presented in the article entitled “*Assessment of the environmental fate of a bio-based TOCN–PPy–PVA–Glycerol coating by leaching, biodegradation and hydrothermal reusability.*” This article investigates the environmental behavior and circularity potential of a fully biobased coating system composed of TEMPO-oxidized cellulose nanofibers (TOCN), polypyrrole (PPy), polyvinyl alcohol (PVA), and glycerol. The study focuses on evaluating the multifunctional coating through a series of environmental performance tests, including aqueous leaching assessments, soil biodegradability analysis, and hydrothermal reusability trials. Altogether, the work provides a comprehensive understanding of the environmental interactions of TOCN–PPy–PVA–Gly coatings and explores their potential for integration into closed-loop and low-impact material cycles. The article has been submitted to the journal *Materials Today Communications* (Elsevier, IF 4.5) and is currently under consideration.

### **Authours details**

#### **Aakash Malik, CPI, MSc**

Ph.D. Candidate, Sciences et génie des matériaux lignocellulosiques

I2E3 – Institut d’Innovations en Écomatériaux, Écoproduits et Écoénergies à base de biomasse

Université du Québec à Trois-Rivières,

P.O. Box 500, Trois-Rivières, Québec, Canada, G9A 5H7

Email: [aakash.malik@uqtr.ca](mailto:aakash.malik@uqtr.ca)

#### **Prof. Éric Loranger, Ph.D., ing.**

Research director and corresponding author

I2E3 – Institut d’Innovations en Écomatériaux, Écoproduits et Écoénergies à base de biomasse

Université du Québec à Trois-Rivières,  
P.O. Box 500, Trois-Rivières, Québec, Canada, G9A 5H7  
Email: [eric.loranger1@uqtr.ca](mailto:eric.loranger1@uqtr.ca)

**Prof. Simon Barnabé, Ph.D.**

Research Co-director  
I2E3 – Institut d’Innovations en Écomatériaux, Écoproduits et Écoénergies à base de biomasse  
Université du Québec à Trois-Rivières,  
P.O. Box 500, Trois-Rivières, Québec, Canada, G9A 5H7  
Email: [simon.barnabe@uqtr.ca](mailto:simon.barnabe@uqtr.ca)

**Author Contributions:**

**Aakash Malik:** Writing – original draft, Visualization, Validation, Methodology, Investigation, Formal analysis, Data curation, Conceptualization

**Simon Barnabé:** Writing – review & editing, Supervision

**Éric Loranger:** Writing – review & editing, Validation, Supervision, Project administration, Funding acquisition, Conceptualization

## 5.2 Résumé

Cette étude présente une compréhension de l’évaluation environnementale d’un système de revêtement entièrement biosourcé composé de nanofibres de cellulose oxydées TEMPO (TOCN), de polypyrrole (PPy), d’alcool polyvinylique (PVA) et de glycérol. Ce revêtement multifonctionnel a été évalué pour son comportement à la lixiviation, sa biodégradabilité dans les sols, sa réutilisabilité hydrothermale et son potentiel de circularité. Des cycles de lavage aqueux séquentiels des films TOCN–PPy ont réduit l’acidité résiduelle (pH d’environ 2,3 à environ 4,7) et ont significativement abaissé la teneur en fer de 11,3 mg/L à 1,2 mg/L, telle que déterminée par ICP-OES. L’incorporation de PVA et de glycérol dans la matrice a supprimé la lixiviation du fer en dessous des

limites de détection ( $\leq 0,05$  mg/L), indiquant une stabilisation améliorée. Les analyses HPLC-MS/MS ont confirmé l'immobilisation complète du pyrrole dans toutes les formulations et ont démontré une libération de glycérol dépendante de la formulation, la lixiviation augmentant proportionnellement à la teneur initiale en glycérol. Les tests d'enfouissement dans le sol ont révélé une biodégradabilité ajustable, avec une perte de poids passant de 8,1 % pour la formulation non plastifiée à 54,6 % pour la teneur en glycérol la plus élevée, attribuée à une hydrophilie et une accessibilité microbiennes accrues. De plus, un traitement hydrothermal doux (75 °C, 35 min) a permis une solubilisation et une récupération complètes du film sans dégradation structurelle, soulignant sa réutilisabilité en boucle fermée. Ces résultats font du système TOCN–PPy–PVA–Gly une plateforme prometteuse pour des applications de revêtement durables, alliant sécurité environnementale, dégradation contrôlée et recyclabilité. Ces résultats contribuent à la conception rationnelle de revêtements biosourcés de nouvelle génération, conformes aux principes de l'économie circulaire et de la chimie verte.

### 5.3 ABSTRACT

This study presents an understanding of the environmental assessment of a fully biobased coating system composed of TEMPO-oxidized cellulose nanofibers (TOCN), polypyrrole (PPy), polyvinyl alcohol (PVA), and glycerol. The multifunctional coating was evaluated for its leaching behavior, soil biodegradability, hydrothermal reusability, and circularity potential. Sequential aqueous washing cycles of TOCN–PPy films reduced residual acidity (pH from  $\sim 2.3$  to  $\sim 4.7$ ) and significantly lowered iron content from 11.3 mg/L to 1.2 mg/L, as determined by ICP-OES. Incorporation of PVA and glycerol into the matrix suppressed iron leaching below detection limits ( $\leq 0.05$  mg/L), indicating enhanced stabilization. HPLC-MS/MS analyses confirmed the complete immobilization of pyrrole in all formulations and demonstrated a formulation-dependent release of glycerol, with leaching increasing in proportion to initial glycerol content. Soil burial tests revealed tunable biodegradability, with weight loss increasing from 8.1% for the unplasticized formulation to 54.6% for the highest glycerol content, attributed to increased hydrophilicity and microbial accessibility. Furthermore, a mild hydrothermal treatment (75 °C, 35 min) enabled full solubilization and recovery of the film without structural

degradation, highlighting its closed-loop reusability. These results establish the TOCN–PPy–PVA–Gly system as a promising platform for sustainable coating applications, combining environmental safety, controlled degradation, and recyclability. The findings contribute to the rational design of next-generation bio-based coatings aligned with circular economy and green chemistry principles.

**KEYWORDS:** Soil biodegradation testing; Reusability; Sustainable packaging; Leaching analysis; Circular bioeconomy

## 5.4 INTRODUCTION

The quest for environmentally friendly and high-performance coatings has intensified in recent years, driven by concerns over environmental degradation and the depletion of petroleum-based resources (Zhao et al., 2023). Bio-based coatings, derived from renewable feedstocks, have attracted significant attention as sustainable alternatives to conventional polymer coatings (Rastogi & Samyn, 2015). Among these, cellulose nanofibers (CNFs) and their oxidized derivatives, such as TEMPO-oxidized cellulose nanofibers (TOCN), offer unique advantages including high aspect ratios, biodegradability, and mechanical reinforcement capabilities (Djafari Petroudy et al., 2021; Isogai et al., 2011). The incorporation of functional fillers like polypyrrole (PPy) into CNF-based matrices can impart electrical conductivity and antibacterial properties, expanding their potential applications in packaging, sensors, and barrier coatings (Bideau et al., 2016; Hou et al., 2024; Malik et al., 2025). However, the environmental fate and safety of such composite materials must be carefully assessed, especially given the potential for leaching of metal ions and monomer residues during use and disposal (Mohanrasu et al., 2025). To address processability and mechanical flexibility, polyvinyl alcohol (PVA) and plasticizers like glycerol are often used as matrix modifier (Jamali et al., 2024). Glycerol, a widely used plasticizer, enhances flexibility but can also influence water uptake and biodegradation behavior (Ben et al., 2022; Heydari et al., 2014). These additives modify the physicochemical interactions within the composite, which can impact not only mechanical properties but also environmental behavior such as degradation (Wang et al., 2021).

The environmental safety of bio-based coatings thus hinges on understanding their behavior under relevant conditions, including water exposure, soil burial, and potential for recycling or recovery. Leaching of components like Fe (from oxidative polymerization processes) can raise concerns regarding ecological and human health risks if uncontrolled (Health Canada, 2024). Moreover, assessing the biodegradation of these bio-based materials in soil is crucial for validating their biodegradation claims, as incomplete biodegradation can lead to persistent microplastic pollution (Withana et al., 2025).

This study aims to provide an understanding of the environmental behavior of TOCN-PPy-based coatings modified with PVA and glycerol. We systematically examine the pH and Fe release during washing, quantify potential leaching of pyrrole and glycerol using HPLC-MS/MS, and evaluate biodegradability under soil burial conditions. Finally, the feasibility of coating recovery and recyclability under mild hydrothermal conditions is explored to align with circular economy principles (Arruda et al., 2021). However, despite the expanding functional potential of CNF-PPy-based films, focusing on parameters such as electrical conductivity, mechanical strength, and moisture barrier properties, there remains a critical gap in understanding their environmental interactions, particularly their leaching behavior, biodegradability, and end-of-life management. In most studies, their environmental behavior remains significantly underexplored or conducted under limited, less representative conditions. (Bideau et al., 2016) For instance, conducted a leaching study using Total Organic Carbon (TOC) analysis and reported that a TOCN-PPy composite released only  $0.2 \times 10^{-3}$  mol/L of PPy after 48 hours of water immersion ( $\pm 5.2 \times 10^{-6}$  mol/L), suggesting minimal solubilization of the conductive phase. TOC-based measurements offer only a bulk estimate of organic content. More detailed and compound-specific methods, such as HPLC-MS/MS and ICP-OES, are needed to quantify specific leached species and better understand their environmental behavior. (Bideau et al., 2016). Another challenge in previous literature is the limited consideration of plasticizers and matrix modifiers in these systems. Binder like polyvinyl alcohol (PVA) and glycerol are incorporated with TOCN-PPy used to improve film flexibility and processability (Malik et al., 2025). Yet, their influence on environmental safety (e.g., migration, reusability, and degradation) is also unexplored in combination with TOCN-PPy matrices. (Bideau et al., 2016) Furthermore, the environmental safety of conductive polymer composites,

especially regarding potential iron or pyrrole leaching from oxidative polymerization, has not been systematically investigated in a real-world context. Moreover, the potential for film reusability and recovery under low-energy aqueous conditions remains an underutilized opportunity in the context of circular material design.

This study thus aims to bridge these knowledge gaps by evaluating the environmental fate of TOCN–PPy–PVA–Glycerol coatings through three key indicators: (i) leaching behavior of residual iron and glycerol/pyrrole, (ii) soil biodegradability under dry burial conditions, and (iii) hydrothermal reusability at mild temperatures. By integrating these tests across systematically varied glycerol formulations, we demonstrate how additive tuning can balance functional performance with environmental integrity. The findings support the development of next-generation, bio-based coatings tailored for sustainable packaging and eco-compatible applications.

As such, this study investigates the environmental behavior and recovery potential of TOCN–PPy-based composite coatings modified with polyvinyl alcohol (PVA) and glycerol. By integrating aqueous leaching analysis, soil biodegradation testing, and hydrothermal reusability assessment, this work provides a comprehensive evaluation of the coatings' environmental fate, an aspect that has been largely overlooked in previous studies. The results demonstrate that the inclusion of PVA and glycerol markedly improves the stability, biodegradability, and reusability of TOCN–PPy composites. This integrated approach not only advances understanding of bio-based conductive coatings but also contributes to the development of sustainable materials designed for circular-use pathways.

## **5.5 MATERIALS AND METHODOLOGY**

### **5.5.1 Materials**

The TOCN-PPy-PVA and TOCN-PPy-PVA-Gly coatings used in this study were prepared as described in our previous work (Malik et al., 2025). Briefly, TOCN was synthesized via TEMPO-mediated oxidation of cellulose nanofibers (Loranger et al., 2012; Paquin et al., 2013), followed by in-situ oxidative polymerization (iron chloride) of

polypyrrole (PPy) within the TOCN matrix. Polyvinyl alcohol (PVA) and glycerol (at varying concentrations) were incorporated as film-forming and plasticizing agents, respectively, to enhance flexibility and processability. The detailed formulation parameters, including component ratios and processing conditions, are provided in (Malik et al., 2025). All chemicals were from Sigma Aldrich and use as received.

### 5.5.2 Experimental Strategy

To evaluate the environmental behavior of the TOCN–PPy–PVA–Glycerol paint system, experimental trials were developed, targeting three core indicators: leaching potential, biodegradation, and reusability. The influence of glycerol content, used as a plasticizer, was investigated using four distinct formulations as in Table 5.1.

**Table 5.1** Experimental Design: Formulations of TOCN–PPy–PVA–Glycerol Coatings with Varying Glycerol Content

Code	Description
<b>W0</b>	Initial washing of TOCN-PPy
<b>W1</b>	Second washing of TOCN-PPy
<b>W2</b>	Third washing of TOCN-PPy
<b>W3</b>	Fourth washing of TOCN-PPy
<b>W4</b>	Fifth washing of TOCN-PPy
<b>TOCN-PPy-PVA</b>	TOCN–PPy–PVA (no glycerol)
<b>TOCN-PPy-PVA-Gly1</b>	TOCN–PPy–PVA–Gly1 (1 mL glycerol)
<b>TOCN-PPy-PVA-Gly2</b>	TOCN–PPy–PVA–Gly2 (2 mL glycerol)
<b>TOCN-PPy-PVA-Gly5</b>	TOCN–PPy–PVA–Gly5 (5 mL glycerol)

As also show on Figure 5.1, the study was structured around testing of washing of TOCN-PPy and then four formulations with increasing glycerol content. Each formulation was subjected to aqueous immersion for chemical leaching analysis, soil burial for degradation assessment, and mild hydrothermal treatment for recyclability testing.

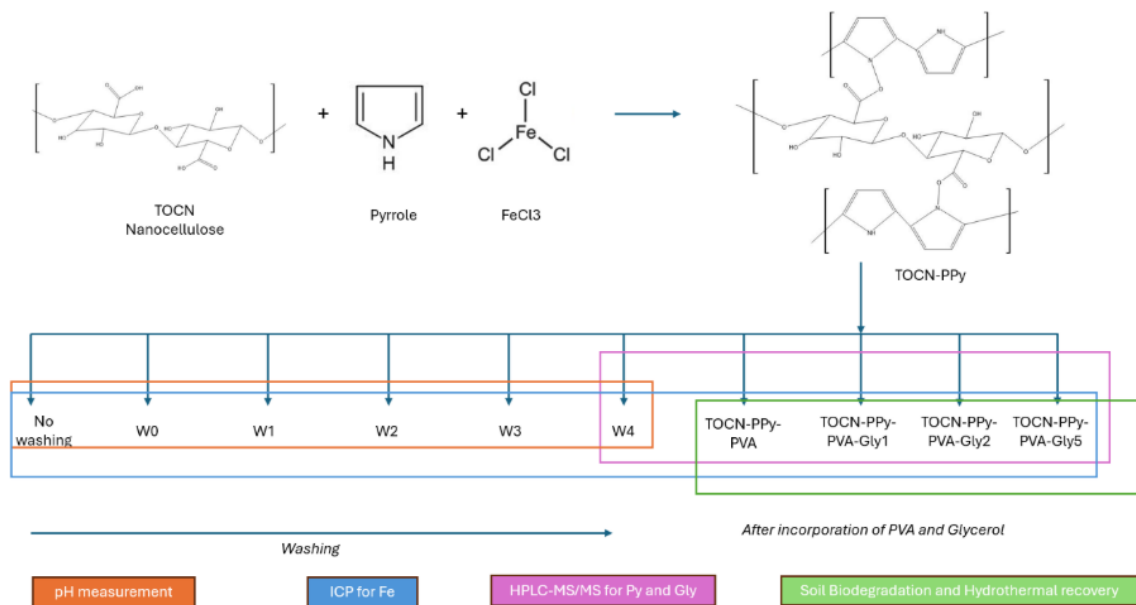


**Figure 5.1** Experimental workflow for evaluating the environmental behavior of TOCN–PPy–PVA–Glycerol coatings.

### 5.5.3 Leaching characterisations

#### 5.5.3.1 pH measurement via Thermo Scientific ORION Star A215 pH meter

The pH of the washing solutions and reference materials was measured using a Thermo Scientific ORION Star A215 pH meter. Prior to analysis, the instrument was calibrated with standard buffer solutions at pH 4.00, 7.00, and 10.00. Measurements were performed at room temperature under standard laboratory conditions.

#### 5.5.3.2 Inductively Coupled Plasma Optical Emission Spectroscopy (ICP-OES)

The release of iron (Fe) from TOCN-PPy and its polymer-modified composites was evaluated by inductively coupled plasma optical emission spectroscopy (ICP-OES, Perkin Elmer AVIO 550) after 24-hour immersion of samples in 50 ml deionized water. Low concentrations close to the detection limit were observed for some samples; therefore, concentrations below 0.05 mg/L were reported as “Fe ≤ 0.05 mg/L” in accordance with standard analytical conventions.

Iron quantification was in accordance with ASTM D1976-20: Standard Test Method for Elements in Water by Inductively Coupled Plasma Atomic Emission Spectroscopy. The method's instrumental detection limit (IDL) for Fe was  $\text{Fe} \leq 0.05 \text{ mg/L}$ ; therefore, concentrations below this threshold were reported as " $\text{Fe} \leq 0.05 \text{ mg/L}$ ", following standard analytical conventions established by the ASTM D1976-20 procedure (ASTM International, 2020).

To ensure accurate quantification of iron release, a calibration curve was established using standard solutions ranging from 0.5 to 16 mg/L, as summarized in Figure 5.2. Both emission lines (Fe 238.204 and Fe 259.939 nm) showed near-perfect linearity ( $R^2 \approx 1.000$ ).

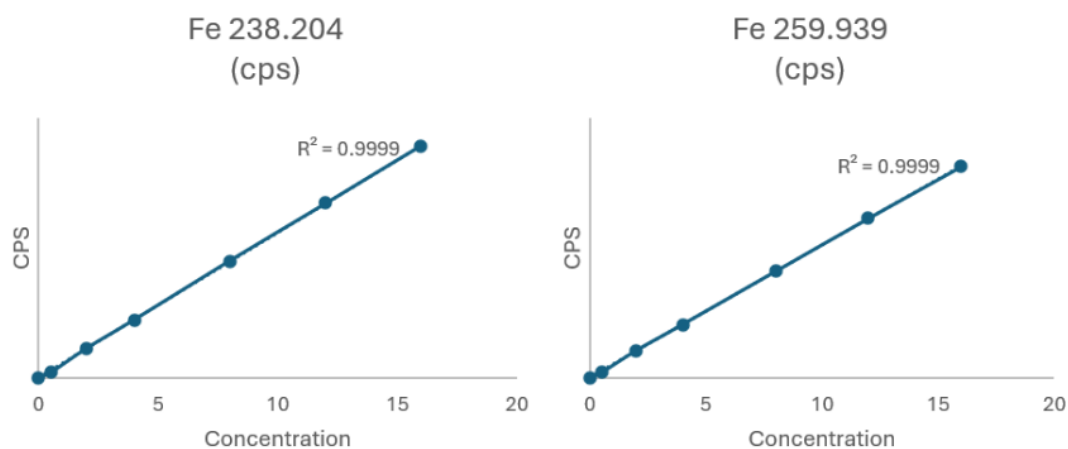


**Figure 5.2** Calibration standards (Concentration (PPM) vs CPS) for ICP-OES analysis of Fe at two emission lines (Fe 238.204 and Fe 259.939)

### 5.5.3.3 High-Performance Liquid Chromatography coupled with tandem Mass Spectrometry (HPLC-MS/MS)

HPLC-MS/MS analyses analytical runs included injections of blanks (mobile phase and acetonitrile) to verify the absence of background contamination and/or carryover, and standards of pyrrole and glycerol at 100 mg/L were injected to establish detection parameters. Signals were considered valid when a signal-to-noise ratio (SNR) greater than 3.0 was obtained in each monitored MRM transition. Compound identification was based

on comparison with authentic standards' retention times and characteristic MRM transitions. Prior to analysis, the samples were immersed in 50 mL of deionized water at room temperature for 24 hours under static conditions. The aqueous extracts were analyzed directly without dilution to simulate practical exposure scenarios and assess any migration of target compounds.

The HPLC-MS/MS, a high-performance liquid chromatography system coupled with a tandem mass spectrometer, from Agilent Technologies (USA) was equipped with an Agilent Jet Stream electrospray ionization (ESI) source. Chromatographic separation was achieved on a Kinetex EVO C18 column (150 × 4.6 mm, 5 μm, 100 Å; Phenomenex, Torrance, USA) using a binary solvent delivery system, an autosampler maintained at 4 °C, and a thermostated column compartment set at 30°C. Each sample was vortexed and injected without dilution, with an injection volume of 5 μL. For pyrrole detection, the mobile phases consisted of solvent A (Milli-Q water containing 0.1% v/v formic acid) and solvent B (methanol containing 0.1% v/v formic acid), delivered at a flow rate of 0.4 mL/min. The gradient program was as follows: 0.00–4.00 min, 10% B; 8.00-10.00 min, 100% B; 10.40-12.00 min, 10% B. For glycerol detection, the mobile phases were ammonium acetate 10 mM with acetic acid 0.1% v/v (A) and acetonitrile (B). They were delivered at a flow rate of 0.4 mL/min using the following gradient program: 0.00-1.50 min, 80% B; 1.60-3.00 min, 10% B; 5.00-10.00 min, 80% B.

Pyrrole detection was conducted in positive electrospray ionization mode (ESI+), monitoring the [M+H]<sup>+</sup> ion at m/z 68 and fragment ions at m/z 41 and 39, with an expected retention time of 9.861 minutes. Glycerol detection was conducted in negative electrospray ionization mode (ESI<sup>-</sup>), monitoring the [M+Ac]<sup>-</sup> ion at m/z 151 with fragment ions at m/z 59 and 133, and an expected retention time of 1.018 minutes. The MS/MS source parameters were set as follows for pyrrole detection: drying gas flow rate 10 L/min, gas temperature 300°C, nebulizer pressure 45 psi, sheath gas flow rate 11 L/min, sheath gas temperature 300°C, capillary voltage 4000 V in ESI<sup>+</sup> mode, and nozzle voltage 500 V. Same source parameters were used for glycerol detection, except drying gas flow rate was 13 L/min, sheath gas temperature was 400°C and capillary voltage was 3000 V in ESI<sup>-</sup> mode. Data acquisition was carried out using Agilent

MassHunter Data Acquisition software (version 1.2), and data processing was performed using MassHunter Qualitative Analysis (version 10.0).

#### **5.5.4 Soil Biodegradation Testing**

A homemade soil biodegradation test was performed over 60 days, where quintuplicate samples of TOCN-PPy-PVA and its glycerol-modified formulations (TOCN-PPy-PVA-Gly1, TOCN-PPy-PVA-Gly2, and TOCN-PPy-PVA-Gly5) were buried 10 cm deep in dry soil conditions. The weight changes were recorded before and after the test to evaluate the biodegradation behavior of the samples.

#### **5.5.5 Hydrothermal Reusability Assessment**

The homemade test was prepared for evaluating the hydrothermal recovery behavior of the TOCN-PPy-PVA-Gly composite coating was evaluated through a film recovery test to explore paint reusability. A fragment of the dried coating film, weighing approximately 1.83 grams, was immersed in 50 mL of deionized water and subjected to heating at 75 °C for 35 minutes under static conditions. After the thermal treatment, the system was cooled to room temperature, and the material was recovered by filtration. The recovered sample was subsequently dried under ambient conditions and visually inspected to assess its integrity and potential degradation.

### **5.6 RESULTS AND DISCUSSION**

#### **5.6.1 pH testing (for washing impact of TOCN-PPy)**

The samples included extracts from the TOCN-PPy films after immersion, washing solutions, a FeCl<sub>3</sub> reference solution, and pure deionized water. Each film sample (T1, T2, T3) corresponds to independent replicates. The evolution of pH during successive washings is detailed in Figure 5.3. Initially, the extract (W0) was highly acidic (~pH 2.3), indicating the presence of residual FeCl<sub>3</sub> or acidic by-products. With each washing (W1–W4), the pH progressively increased and stabilized around 4.7, indicating the effective removal of residual acidic species.

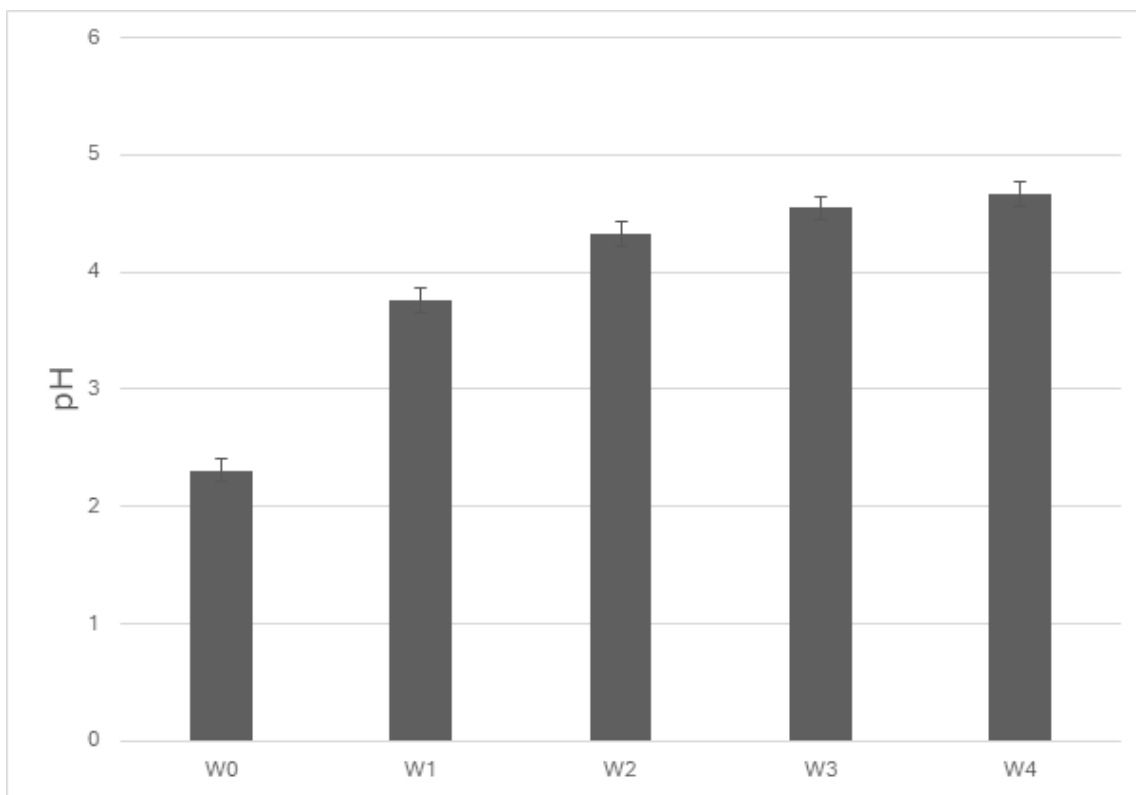


**Figure 5.3** pH values of water collected after each washing cycle (W0–W4) for TOCN-PPy films. Measurements were taken in triplicate

The first washing solution (W0) exhibited a highly acidic pH, with values around 2.30–2.32, suggesting the presence of residual acidic species, likely associated with unreacted  $\text{Fe}^{3+}$  ions or remaining by-products from the synthesis process. As successive washings (W1 to W4) were performed, a progressive increase in pH was observed. After the second washing (W1), the pH rose significantly to approximately 3.64–3.85. Further washing steps (W2 to W4) continued to gradually increase the pH, stabilizing around 4.62–4.74 by the fourth wash. This trend indicates the effective removal of free acidic impurities from the TOCN-PPy films with each successive washing cycle. The stabilization of pH after W4 suggests that most of the acidic residues were eliminated by this stage, leading to a more neutral aqueous phase. Comparatively, the pH of the  $\text{FeCl}_3$  solution used as a reference was 1.37, confirming its strong acidity, while the deionized water had a pH of 5.43, slightly acidic but much closer to neutrality. Since we don't reach the final pH of the washing water, residual iron may remain (to be confirmed with ICP-OES). However, the

initial washing solutions were significantly more acidic than the deionized water, reinforcing the contribution of residual synthesis components to the initial pH values.

Overall, these observations confirm that multiple washing steps are necessary to ensure the chemical purification of the TOCN-PPy films, reducing the risk of residual acidity that could influence material performance in subsequent applications.

### 5.6.2 Iron release and regulatory context via ICP-OES

The purification of the TOCN-PPy composite followed the procedure described by Malik et al. (2025). After polymerization, the film was subjected to five sequential washing cycles (W0–W4) using 1000 mL of deionized water per cycle through a filtration setup equipped with Whatman filter paper (Grade 202). The pH of the filtrate was monitored after each cycle, and washing was continued until the pH stabilized near that of distilled water, indicating complete removal of residual FeCl<sub>3</sub>. For the modified formulations (TOCN-PPy, TOCN-PPy-PVA, and TOCN-PPy-PVA-Gly1, Gly2, and Gly5), the films were soaked in 50 mL of deionized water for 24 hours under gentle agitation to remove any remaining surface residues prior to further analysis. Although photographs of the washing solutions were not taken, the light-yellow coloration observed in the initial washes disappeared with repeated cycles, confirming efficient Fe<sup>3+</sup> removal as verified by pH evaluation. The unwashed TOCN-PPy sample exhibited a high iron release of approximately 11.3 mg/L. Through sequential washing (W0–W4), the Fe concentration progressively decreased from 2.88 mg/L to 1.20 mg/L, indicating substantial but incomplete removal of loosely associated iron species trapped inside the matrix of TOCN. In comparison, polymer-modified samples incorporating polyvinyl alcohol (PVA) and glycerol (TOCN-PPy-PVA, TOCN-PPy-PVA-Gly1, TOCN-PPy-PVA-Gly2, and TOCN-PPy-PVA-Gly5) exhibited iron release below the detection limit ( $\text{Fe} \leq 0.05 \text{ mg/L}$ ), demonstrating the effectiveness of matrix stabilization in suppressing metal ion leaching. In consideration, the residual pH can then be attributed to trace amounts of iron. Figure 5.4 summarizes the iron leaching data for unwashed, sequentially washed, and polymer-modified TOCN-PPy samples. Unwashed TOCN-PPy released high Fe levels (~11.3 mg/L), which declined across washing steps to 1.2 mg/L after W4. PVA- and glycerol-containing films, however, exhibited Fe levels below 0.05 mg/L, indicating successful

stabilization of the composite matrix. For all formulations incorporating PVA and glycerol, Fe concentrations were below the detection limit of 0.05 mg/L, as defined by ICP–OES analytical conventions. A fixed liquid-to-sample ratio was maintained across all tests to ensure comparability between formulations. Importantly, the non-detectable levels ( $< 0.05$  mg/L) are well below guideline values for environmental relevance, and therefore no additional concentration steps were pursued.

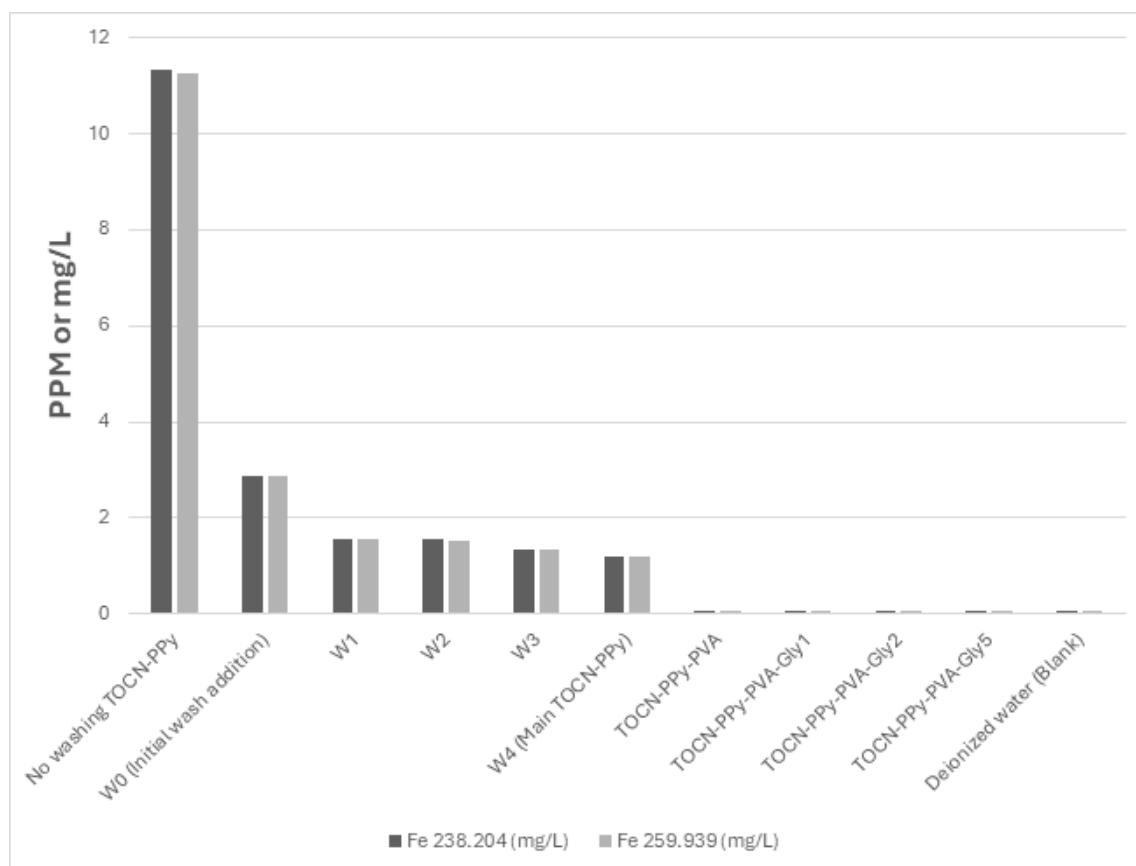


**Figure 5.4** Iron concentrations (mg/L) in washing solutions from various TOCN-PPy-based formulations measured by ICP-OES

These results hold important implications when compared against established drinking water standards. However, a recent draft guideline update proposes a stricter aesthetic objective (AO) of  $\leq 0.1$  mg/L, based on minimizing discolouration, metallic taste, and the accumulation of iron oxides which may also adsorb hazardous metals such as arsenic and lead (Health Canada, 2024). Similarly, in the United States, the Minnesota Department of Health considers iron concentrations above 0.3 mg/L as aesthetically objectionable

(Minnesota Department of Health, 2023). Notably, no health-based guideline for iron has been established, as current evidence does not associate iron in drinking water with adverse human health effects at typical environmental levels. When placed in this context, the initial iron leaching observed from unwashed TOCN-PPy (11.3 mg/L) substantially exceeds both the former (0.3 mg/L) and the proposed (0.1 mg/L) aesthetic thresholds. Even after four washings (1.2 mg/L), the iron concentration remains above recommended limits for drinking water aesthetic quality. Conversely, the iron release from the TOCN-PPy-PVA and TOCN-PPy-PVA-Gly formulations falls below 0.05 mg/L, which is significantly lower than both the existing and proposed guidelines, ensuring compliance with drinking water quality standards concerning iron.

The ability of the PVA- and glycerol-modified composites to limit iron leaching highlights their potential suitability for applications requiring environmental safety and material stability in aqueous environments. In particular, materials maintaining iron concentrations below 0.1 mg/L are advantageous for potential packaging applications, thereby enhancing consumer acceptance and public health protection.

### **5.6.3 HPLC-MS/MS analysis of pyrrole and glycerol leaching**

#### **5.6.3.1 Pyrrole Detection Results (ESI+)**

The detection of pyrrole ( $[M+H]^+$  at  $m/z$  68, fragments at  $m/z$  41 and 39) was assessed in all samples following immersion. The absence of pyrrole migration from all coatings, including TOCN-PPy and its modified formulations, is shown in Table 5.2. No signal corresponding to pyrrole or its fragments was detected above the method's signal-to-noise threshold, confirming its immobilization in the matrix. No pyrrole was detected in any sample after 24 hours of immersion. This result demonstrates the effective immobilization of pyrrole within the polypyrrole polymer network. The lack of detectable migration suggests that the conductive phase remains chemically integrated within the coating matrix under aqueous conditions. Such stability is critical for ensuring the environmental safety and long-term durability of TOCN-PPy-based coatings, particularly for water-contact applications such as barrier materials and bio-based conductive films.

**Table 5.2** Pyrrole detection in water extracts after 24 h immersion via HPLC-MS/MS. All samples showed non-detectable levels

<b>Sample</b>	<b>Pyrrole Detection</b>	<b>Retention Time (min)</b>	<b>Observation</b>
<b>Water</b>	Not detected (ND)	N/A	Pyrrole not detected
<b>TOCN-PPy</b>	Not detected (ND)	N/A	Pyrrole not detected
<b>TOCN-PPy-PVA</b>	Not detected (ND)	N/A	Pyrrole not detected
<b>TOCN-PPy-PVA-Gly1</b>	Not detected (ND)	N/A	Pyrrole not detected
<b>TOCN-PPy-PVA-Gly2</b>	Not detected (ND)	N/A	Pyrrole not detected
<b>TOCN-PPy-PVA-Gly5</b>	Not detected (ND)	N/A	Pyrrole not detected

### 5.6.3.2 Glycerol Detection Results (ESI<sup>-</sup>)

Glycerol presence was assessed by monitoring the  $[M+Ac]^-$  ion at  $m/z$  151 and fragment ion at  $m/z$  59. As seen in Table 5.3, glycerol leaching was clearly detected in Gly2 and Gly5 formulations, with retention times matching the analytical standard ( $\sim 0.96$  min). The absence of glycerol in control samples further confirms controlled and formulation-dependent migration behavior.

**Table 5.3** Glycerol detection in water extracts using HPLC-MS/MS. Detection was observed only in Gly2 and Gly5 samples, increasing with glycerol loading

<b>Sample</b>	<b>Glycerol Detection</b>	<b>Retention Time (min)</b>	<b>Observation</b>
<b>Water</b>	Not detected (ND)	N/A	Glycerol not detected
<b>TOCN-PPy</b>	Not detected (ND)	N/A	Glycerol not detected
<b>TOCN-PPy-PVA</b>	Not detected (ND)	N/A	Glycerol not detected
<b>TOCN-PPy-PVA-Gly1</b>	Not detected (ND)	N/A	Glycerol not detected
<b>TOCN-PPy-PVA-Gly2</b>	Detected	0.960	Moderate glycerol signal detected
<b>TOCN-PPy-PVA-Gly5</b>	Detected	0.957	Strong glycerol signal detected

No glycerol was detected in the water blank, TOCN-PPy, or TOCN-PPy-PVA, confirming the absence of background interference or glycerol release from non-plasticized samples. Clear glycerol detection was observed in TOCN-PPy-PVA-Gly2, and TOCN-PPy-PVA-Gly5, with signal intensity correlating to the initial glycerol content. Retention times for glycerol peaks were tightly grouped around the standard value, between 0.957 and 0.985 minutes, ensuring analytical consistency. These results demonstrate controlled migration of glycerol in plasticized coatings, with leaching proportional to the amount incorporated during formulation.

As seen in Gly2 and Gly5, increasing glycerol content promotes leaching, which can compromise film stability in water (after 24 hours residence time). The TOCN-PPy-PVA matrix, however, effectively mitigates this effect, improving suitability for food packaging.

#### 5.6.4 Soil biodegradation testing

The results from the soil biodegradation testing methodology are shown in Figure 5.5. The pure TOCN-PPy-PVA sample exhibited minimal weight loss over the 60-day testing period, indicating its high stability in dry soil conditions. This result can be attributed to the inherent resistance of polypyrrole and the robust intermolecular bonding within the TOCN-PPy-PVA matrix. Such low biodegradation rates suggest that the material is not easily susceptible to microbial or environmental breakdown in arid soil environments.

Soil burial tests were conducted for 60 days, after which the samples were recovered, cleaned, and weighed to determine mass loss. Due to the experimental design, intermediate sampling (e.g., at 15 or 30 days) was not possible without disturbing the soil environment and affecting the microbial dynamics. For this reason, the data reported correspond to the 60-day end point.

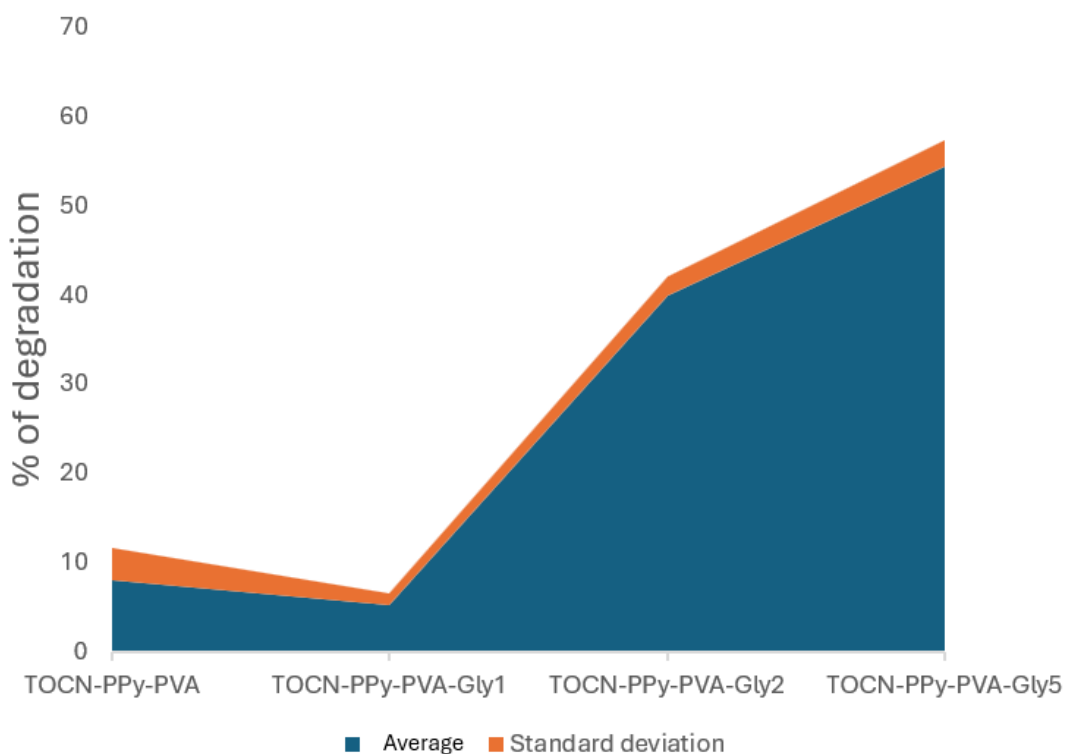


**Figure 5.5** Percent weight loss of TOCN-PPy-based coatings after 60 days of soil burial. Weight loss increased with glycerol content

Upon incorporating glycerol into the TOCN-PPy-PVA matrix, a progressive increase in weight loss was observed with higher glycerol content. At a lower glycerol content (TOCN-PPy-PVA-Gly1), the weight loss was reduced to 5.21%, indicating that glycerol acted as a stabilizing agent, initially reducing the matrix's susceptibility to degradation. As the glycerol content increased (TOCN-PPy-PVA-Gly2, TOCN-PPy-PVA-Gly5), the weight loss percentages rose steadily (39,9 and 54,6%). The composite with Gly5 (5 mL of glycerol) is showing the most substantial weight loss among the glycerol-modified samples. This behavior suggests that glycerol enhances the material's hydrophilicity, thereby increasing its interaction with soil moisture and microbial activity. The controlled increase in weight loss with higher glycerol concentrations reflects the material's tunable biodegradation properties, which can be leveraged to meet specific environmental or application requirements. While TOCN-PPy-PVA is inherently resistant to degradation, the addition of glycerol effectively modulates its environmental degradation behavior. These findings provide valuable insights into tailoring the biodegradability of TOCN-PPy-PVA composites through glycerol incorporation. By optimizing glycerol content, the material's durability and biodegradability can be balanced to meet specific application requirements, such as biobased packaging or environmentally friendly coatings.

#### **5.6.5 Hydrothermal Reusability Assessment**

During the hydrothermal treatment, the TOCN-PPy-PVA-Gly film exhibited progressive solubilization into the aqueous phase. The film gradually disintegrated and dispersed into the 50 ml deionised water during the 35-minute exposure at 75 °C, leading to the formation of a homogeneous dispersion by the end of the heating period. After cooling to room temperature, the resulting solution, approximately 30–35 ml in volume, could be reused directly as a solvent for preparing a fresh TOCN-PPy-PVA-Gly formulation. This behavior reflects the partial water solubility of the material under moderate hydrothermal conditions, primarily attributed to the presence of polyvinyl alcohol (PVA) and glycerol within the matrix. Both PVA and glycerol are hydrophilic components that facilitate swelling, dispersion, and reformation in aqueous environments without significant

chemical degradation. Therefore, the process shown in Figure 5.6 is therefore a result itself.

All formulations were subjected to hydrothermal treatment at 75 °C for 35 min. After treatment, the dried coating films readily disintegrated and redispersed in water under mild magnetic stirring, forming stable and homogeneous suspensions without visible clumps or sedimentation. Although photographs are not included, the dispersion quality was consistent across all formulations, and the recovered suspensions appeared visually indistinguishable from the original ones. Importantly, the recovered suspensions could be directly reintroduced into the coating preparation process. When mixed with the original paint recipe, the dispersions blended uniformly, producing continuous films upon drying that retained flexibility and good surface coverage. This demonstrates that the recycling process not only restores the material to a usable form but also enables its practical reintegration into new coating formulations. These observations confirm that TOCN–PPy–PVA–glycerol coatings possess hydrothermal reusability under mild conditions.

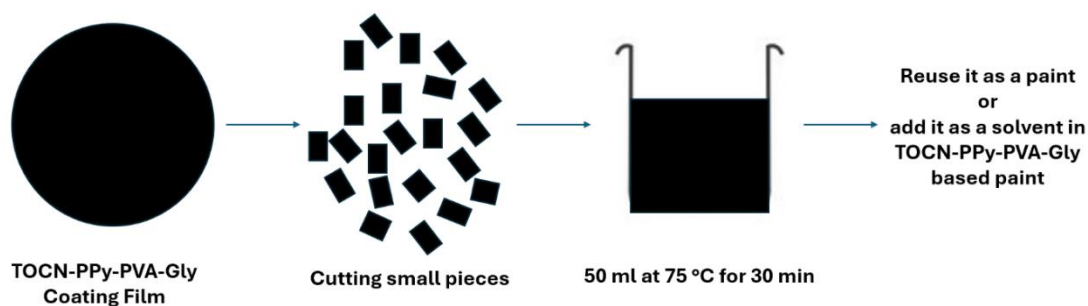


**Figure 5.6** Schematic of the hydrothermal recovery process used to evaluate recyclability of TOCN-PPy-PVA-Gly coatings

The observed behavior aligns strongly with the principles of the circular economy, promoting material recovery, reuse, and recyclability through low-energy, water-based processes. Unlike traditional materials that require harsh chemical treatments for recycling, TOCN-PPy-PVA-Gly can be reprocessed under mild conditions, thereby minimizing environmental impact and resource consumption. This property offers opportunities for the development of bio-based coatings and films that can be easily recovered and repurposed after use, fitting sustainable product life cycles. The water

sensitivity at elevated temperatures can be advantageous for temporary coatings, bio-based packaging, and controlled degradable systems where post-use material recovery is desirable. However, for applications requiring greater hydrothermal stability, formulation strategies such as crosslinking or the incorporation of hydrophobic components could be considered to fine-tune the balance between durability and reprocessability. Overall, the reversible solubilization and recovery behavior of TOCN-PPy-PVA-Gly highlights its strong potential for integration into circular material systems, contributing to the advancement of environmentally responsible material innovations.

## 5.7 CONCLUSION

This study assessed the environmental behavior and recovery potential of bio-based TOCN-PPy-PVA-glycerol coatings by integrating aqueous leaching, soil biodegradability, and hydrothermal reusability analyses. Unmodified TOCN-PPy films released measurable amounts of iron and exhibited acidic pH after immersion, whereas incorporation of PVA and glycerol markedly improved stability. Iron release fell below the detection limit by ICP-OES, pyrrole migration was undetectable by HPLC-MS/MS, and glycerol leaching followed a concentration-dependent trend. Successive washing cycles efficiently removed residual acidic and iron species from TOCN-PPy, as evidenced by pH stabilization around 4.7. The marked reduction of Fe release from 11.3 mg/L to 1.2 mg/L after five washes. Incorporation of PVA and glycerol further stabilized the composite matrix, reducing iron leaching below detection limits ( $\leq 0.05$  mg/L) and achieving values well within regulatory thresholds for aqueous safety. HPLC-MS/MS analyses confirmed complete immobilization of pyrrole across all formulations, while controlled glycerol migration was detected only in Gly2 and Gly5, increasing proportionally with glycerol content. Although elevated glycerol loading promoted leaching, the TOCN-PPy-PVA network effectively limited migration, preserving material integrity and supporting its suitability for food-contact applications. Soil burial tests confirmed that glycerol also enhanced biodegradability, with weight loss increasing from 8.1% in unplasticized films to 54.4% in the most plasticized formulation after 60 days. This tunable degradation behavior suggests the possibility of tailoring film persistence based on specific application requirements. Furthermore, all formulations

were recoverable under mild hydrothermal treatment (75 °C, 35 min), demonstrating their potential for low-energy recycling through redispersion in water. In conclusion, our work shows that adding PVA and glycerol to TOCN–PPy-based coatings makes them more stable, biodegradable, and recyclable. The primary contribution is the amalgamation of leaching analysis, biodegradation performance, and hydrothermal recovery into a unified framework, thus providing a thorough assessment of environmental fate that has been neglected in prior research. Future research should enhance glycerol content to achieve a balance between durability and degradation, extend testing to natural soils and aquatic habitats, and examine long-term performance in practical applications to further substantiate their viability as sustainable coatings.

### **5.8 CRediT (CONTRIBUTOR ROLES TAXONOMY)**

Aakash Malik was responsible for Conceptualization, Data Curation, Formal Analysis, Investigation, Methodology, Project Administration, Validation, Visualization, and Writing – Original Draft; Éric Loranger contributed to Funding Acquisition, Project Administration, Supervision, Validation, and Writing – Review & Editing; Simon Barnabé contributed to Supervision and Writing – Review & Editing.

### **5.9 Declaration of generative AI and AI-assisted technologies in the writing process**

During the preparation of this work the author(s) did not use any generative or AI related tools.

### **5.10 ACKNOWLEDGEMENTS**

This research project is funded by the Natural Sciences and Engineering Research Council of Canada (Discovery grant RGPIN-2021-02861) and Municipal Research Chair for Sustainable Cities (UQTR – Victoriaville).

## 5.11 REFERENCES

- ASTM International, ASTM D1976-20: Standard Test Method for Elements in Water by Inductively Coupled Plasma Atomic Emission Spectroscopy, ASTM International, 2020. DOI: 10.1520/D1976-20
- Arruda, E. H., Melatto, R. A. P. B., Levy, W., & de Melo Conti, D. (2021). Circular economy: A brief literature review (2015–2020). *Sustainable Operations and Computers*, 2, 79–86. <https://doi.org/10.1016/j.susoc.2021.05.001>
- Ben, Z. Y., Samsudin, H., & Yhaya, M. F. (2022). Glycerol: Its properties, polymer synthesis, and applications in starch based films. *European Polymer Journal*, 175, 111377. <https://doi.org/10.1016/j.eurpolymj.2022.111377>
- Bideau, B., Bras, J., Saini, S., Daneault, C., & Loranger, E. (2016). Mechanical and antibacterial properties of a nanocellulose-polypyrrole multilayer composite. *Materials Science and Engineering C*, 69, 977–984. <https://doi.org/10.1016/j.msec.2016.08.005>
- Djafari Petroudy, S. R., Chabot, B., Loranger, E., Naebe, M., Shojaeiarani, J., Gharehkhani, S., Ahvazi, B., Hu, J., & Thomas, S. (2021). Recent advances in cellulose nanofibers preparation through energy-efficient approaches: A review. In *Energies* (Vol. 14, Issue 20). MDPI. <https://doi.org/10.3390/en14206792>
- Health Canada. (2024). Guidelines for Canadian Drinking Water Quality: Guideline Technical Document – Iron. Health Canada. <https://www.canada.ca/en/health-canada/services/publications/healthy-living/guidelines-canadian-drinking-water-quality-guideline-technical-document-iron.html>
- Heydari, A., Alemzadeh, I., & Vossoughi, M. (2014). Influence of glycerol and clay contents on biodegradability of corn starch nanocomposites. *International Journal of Engineering, Transactions B: Applications*, 27(2), 203–214. <https://doi.org/10.5829/idosi.ije.2014.27.02b.05>

- Hou, R., Xie, Y., Song, R., Bao, J., Shi, Z., Xiong, C., & Yang, Q. (2024). Nanocellulose/polypyrrole hydrogel scaffolds with mechanical strength and electrical activity matching native cardiac tissue for myocardial tissue engineering. *Cellulose*, 31(7), 4247–4262. <https://doi.org/10.1007/s10570-024-05874-0>
- Isogai, A., Saito, T., & Fukuzumi, H. (2011). TEMPO-oxidized cellulose nanofibers. *Nanoscale*, 3(1), 71–85. <https://doi.org/10.1039/C0NR00583E>
- Jamali, A. R., Shaikh, A. A., & Dad Chandio, A. (2024). Preparation and characterisation of polyvinyl alcohol/glycerol blend thin films for sustainable flexibility. *Materials Research Express*, 11(4). <https://doi.org/10.1088/2053-1591/ad4100>
- Loranger, E., Piché, A. O., & Daneault, C. (2012). Influence of high shear dispersion on the production of cellulose nanofibers by ultrasound-assisted tempo-oxidation of kraft pulp. *Nanomaterials*, 2(3), 286–297. <https://doi.org/10.3390/nano2030286>
- Malik, A., Barnabe, S., & Loranger, E. (2025). Synthesis, formulation, and characterization of a bio-based paint derived from TOCN and polypyrrole. *Progress in Organic Coatings*, 208, 109511. <https://doi.org/10.1016/J.PORGCOAT.2025.109511>
- Minnesota Department of Health, U. (2023). Iron in Well Water. <https://www.health.state.mn.us/communities/environment/water/wells/waterquality/iron.html>.
- Mohanrasu, K., Manivannan, A. C., Rengarajan, H. J. R., Kandaiah, R., Ravindran, A., Panneerselvan, L., Palanisami, T., & Sathish, C. I. (2025). Eco-friendly biopolymers and composites: a sustainable development of adsorbents for the removal of pollutants from wastewater. *Npj Materials Sustainability*, 3(1), 13. <https://doi.org/10.1038/s44296-025-00057-9>
- Paquin, M., Loranger, É., Hannaux, V., Chabot, B., & Daneault, C. (2013). The use of Weessler method for scale-up a kraft pulp oxidation by TEMPO-mediated system

from a batch mode to a continuous flow-through sonoreactor. *Ultrasonics Sonochemistry*, 20(1), 103–108. <https://doi.org/10.1016/j.ultsonch.2012.08.007>

Rastogi, V. K., & Samyn, P. (2015). Bio-based coatings for paper applications. In *Coatings* (Vol. 5, Issue 4, pp. 887–930). MDPI AG. <https://doi.org/10.3390/coatings5040887>

Wang, W.-H., Huang, C.-W., Tsou, E.-Y., Ao-Ieong, W.-S., Hsu, H.-C., Wong, D. S.-H., & Wang, J. (2021). Characterization of degradation behavior of poly(glycerol maleate) films in various aqueous environments. *Polymer Degradation and Stability*, 183, 109441. <https://doi.org/https://doi.org/10.1016/j.polymdegradstab.2020.109441>

Withana, P. A., Yuan, X., Im, D., Choi, Y., Bank, M. S., Lin, C. S. K., Hwang, S. Y., & Ok, Y. S. (2025). Biodegradable plastics in soils: sources, degradation, and effects. In *Environmental Science: Processes and Impacts*. Royal Society of Chemistry. <https://doi.org/10.1039/d4em00754a>

Zhao, X., Wang, Y., Chen, X., Yu, X., Li, W., Zhang, S., Meng, X., Zhao, Z. M., Dong, T., Anderson, A., Aiyedun, A., Li, Y., Webb, E., Wu, Z., Kunc, V., Ragauskas, A., Ozcan, S., & Zhu, H. (2023). Sustainable bioplastics derived from renewable natural resources for food packaging. In *Matter* (Vol. 6, Issue 1, pp. 97–127). Cell Press. <https://doi.org/10.1016/j.matt.2022.11.006>

## **Chapter 6 - Scientific article 3 : Barrier and mechanical properties of TOCN–PPy–PVA–Gly films with LCA of paint on UPM paper**

### **6.1 Preface**

This part of the work is presented in the article entitled “Sustainable packaging enabled by TOCN–PPy–PVA–Glycerol coatings and paints with optimized barrier, mechanical, and environmental performance.” The research was conducted during a 3-month international research stay at LGP2 – CNRS – Grenoble INP – Université Grenoble Alpes under the PEPR B-BEST mobility fellowship program offered by ANR France to Aakash Malik. The article focuses on the development and characterization of bio-based coatings and films derived from TEMPO-oxidized cellulose nanofibers (TOCN), polypyrrole (PPy), polyvinyl alcohol (PVA), and glycerol for application in sustainable packaging. To complement the material performance analysis, a preliminary life cycle assessment (LCA) was conducted to evaluate the environmental footprint of the developed coatings, focusing on the impact of key components such as TOCN, PPy, and PVA. The article is currently being finalized for an eventual submission to *Surface and Coatings Technology* (Elsevier, IF 6.1, CiteScore 10.2).

### **Authors details**

#### **Aakash Malik, CPI, MSc**

Ph.D. Candidate, Sciences et génie des matériaux lignocellulosiques  
I2E3 – Institut d’Innovations en Écomatériaux, Écoproduits et Écoénergies à base de biomasse

Université du Québec à Trois-Rivières,

P.O. Box 500, Trois-Rivières, Québec, Canada, G9A 5H7

Email: [aakash.malik@uqtr.ca](mailto:aakash.malik@uqtr.ca)

#### **Prof. Éric Loranger, Ph.D., ing.**

Research director and corresponding author

I2E3 – Institut d’Innovations en Écomatériaux, Écoproduits et Écoénergies à base de biomasse

Université du Québec à Trois-Rivières,

P.O. Box 500, Trois-Rivières, Québec, Canada, G9A 5H7

Email: [eric.loranger1@uqtr.ca](mailto:eric.loranger1@uqtr.ca)

**Prof. Simon Barnabé, Ph.D.**

Research Co-director

I2E3 – Institut d’Innovations en Écomatériaux, Écoproduits et Écoénergies à base de biomasse

Université du Québec à Trois-Rivières,

P.O. Box 500, Trois-Rivières, Québec, Canada, G9A 5H7

Email: [simon.barnabe@uqtr.ca](mailto:simon.barnabe@uqtr.ca)

**Prof. Julien Bras, Ph.D.**

International Host Supervisor and Collaborator

LGP2 – CNRS – Grenoble INP – Université Grenoble Alpes, France

Institut Universitaire de France (IUF), Paris, France

Email: [julien.bras@grenoble-inp.fr](mailto:julien.bras@grenoble-inp.fr)

**Author Contributions:**

**Aakash Malik:** Writing – original draft, Visualization, Validation, Methodology, Investigation, Formal analysis, Data curation, Conceptualization

**Simon Barnabé:** Writing – review & editing, Supervision

**Éric Loranger:** Writing – review & editing, Validation, Supervision, Project administration, Funding acquisition, Conceptualization

**Julien Bras:** International hosting, Writing – review & editing, Supervision

## 6.2 Résumé

Cette étude examine les performances fonctionnelles et les caractéristiques de surface de films biosourcés TOCN–PPy–PVA–Glycérol, en se concentrant plus particulièrement sur leur aptitude à l'emploi comme matériaux de revêtement pour des emballages durables. Les propriétés barrières ont été évaluées par des mesures du taux de transmission de l'oxygène (OTR) et du taux de transmission de la vapeur d'eau (WVTR), tandis que les performances mécaniques ont été évaluées par des essais de traction. Toutes les formulations, y compris les films modifiés au glycérol (Gly1, Gly2, Gly5), ont démontré une excellente performance barrière à l'oxygène avec des valeurs d'OTR inférieures aux limites détectables. Cependant, l'augmentation de la teneur en glycérol a significativement compromis la résistance à la vapeur d'eau, notamment en cas d'humidité élevée. Les essais mécaniques ont révélé une résistance à la traction et une flexibilité ajustables en fonction de la concentration en plastifiant. Afin d'évaluer la morphologie et de justifier le volume de revêtement appliqué dans des applications pratiques, une profilométrie de surface 3D (Alicona) et une microscopie électronique à balayage (MEB) ont été réalisées. Ces analyses ont montré qu'une augmentation de la charge en glycérol entraînait une rugosité de surface et une hétérogénéité du revêtement accrues, influençant ainsi l'interaction avec un substrat papier. Une analyse préliminaire du cycle de vie (ACV), basée sur l'application de 10 ml de revêtement sur une feuille de papier UPM de format A4, a identifié le TOCN, suivi du pyrrole et du PVA d'origine fossile comme la principale préoccupation environnementale. Les résultats soulignent le potentiel de ces formulations pour des revêtements barrières recyclables et éco-efficaces, soutenant ainsi les stratégies d'emballage circulaire.

## 6.3 ABSTRACT

This study investigates the functional performance and surface characteristics of biobased TOCN–PPy–PVA–Glycerol films, with a specific focus on their suitability as coating materials for sustainable packaging. Barrier properties were evaluated through oxygen transmission rate (OTR) and water vapor transmission rate (WVTR) measurements, while mechanical performance was assessed via tensile testing. All formulations, including

glycerol-modified films (Gly1, Gly2, Gly5), demonstrated excellent oxygen barrier performance with OTR values below detectable limits. However, increasing glycerol content significantly compromised water vapor resistance, particularly under high humidity. Mechanical tests revealed tunable tensile strength and flexibility depending on plasticizer concentration. To assess the morphology and justify the applied coating volume in practical applications, 3D surface profilometry ( Alicona ) and scanning electron microscopy ( SEM ) were performed. These analyses showed that increasing glycerol loading led to greater surface roughness and coating heterogeneity, thereby influencing the interaction with a paper substrate. A preliminary life cycle assessment ( LCA ), based on the application of 10 mL of coating over an A4-sized UPM paper sheet, identified TOCN, followed by pyrrole and fossil-based PVA as the primary environmental concern. The findings highlight the potential of these formulations for recyclable and eco-efficient barrier coatings, supporting circular packaging strategies.

## 6.4 INTRODUCTION

The increasing environmental burden posed by synthetic plastics has accelerated global efforts toward developing sustainable alternatives for coatings and packaging materials (Moshood et al., 2022). The concept of a circular bioeconomy, which emphasizes the valorization of renewable resources, waste minimization, and ecological resilience, has emerged as a strategic framework for material innovation in this domain (Nguyen et al., 2025). Packaging, in particular, represents a critical frontier, as it accounts for a large fraction of global plastic consumption and waste generation (Dokl et al., 2024). To meet both environmental regulations and functional performance requirements, there is an urgent need for bio-based materials that can rival conventional polymers in mechanical strength, barrier performance, and processing versatility (Barbhuiya et al., 2025; Wu et al., 2021).

Cellulose nanofibres (CNFs), and especially TEMPO-oxidized cellulose nanofibres (TOCN), have garnered significant interest as renewable nanomaterials capable of forming dense, high-strength networks (Isogai et al., 2011; Liu et al., 2021). The TEMPO-mediated oxidation introduces carboxyl groups that enhance dispersibility in water and

facilitate strong hydrogen bonding (Pratama et al., 2024), making TOCN a compelling candidate for barrier applications. However, these materials are inherently brittle and prone to moisture sensitivity, which limits their practical use under ambient or high-humidity conditions, especially in food packaging (Shimizu et al., 2016).

To address these challenges, hybridization with functional polymers has been explored. Among them, polypyrrole (PPy) stands out for its electrical conductivity, redox activity, and antibacterial potential (Bideau, Cherpozat, et al., 2016; Bideau et al., 2017, 2018; Bideau, Loranger, et al., 2016). As a conjugated polymer synthesized under mild aqueous conditions, PPy can be polymerized in situ onto TOCN networks, reinforcing the structure and introducing new functionalities such as moisture resistance and microbial inhibition. Yet, the rigidity of the resulting TOCN-PPy composite must be counterbalanced to maintain flexibility and processability, essential traits for coatings and packaging films (Bideau et al., 2018).

Polyvinyl alcohol (PVA) and glycerol are commonly used as water-soluble binders and plasticizers, respectively (Prabhakaran et al., 2009). When incorporated into TOCN-PPy systems, they enhance film cohesion, reduce brittleness, and allow tunability. PVA improves interfacial adhesion and structural uniformity, while glycerol imparts elasticity and reduces cracking during drying. Despite the synergistic potential of TOCN, PPy, PVA, and glycerol, there remains a lack of comprehensive studies that assess their combined performance as barrier coating applications (Malik et al., 2025).

Previous research on TOCN-PPy composites has predominantly focused on their intrinsic functionalities, such as electrical conductivity, thermal response, and antimicrobial activity. However, there remains a critical need to evaluate their application-specific performance parameters, particularly in the context of sustainable coating technologies. In this study, we expand upon our prior formulation work on TOCN-PPy-PVA-glycerol systems (Malik et al., 2025) by conducting a comprehensive evaluation of their physical and environmental performance. At the film level, we have assess key barrier properties, including water vapor transmission rate (WVTR) and oxygen transmission rate (OTR), alongside mechanical integrity through uniaxial tensile testing to determine their suitability for packaging applications. Furthermore, to translate laboratory-scale

formulations into practical applications, a cradle-to-gate life cycle assessment (LCA) is conducted for the paint applied over A4-sized UPM paper, quantifying environmental impacts associated with material production, formulation, and coating deposition. Surface topography of the coated films is characterized via 3D optical profilometry ( Alicona InfiniteFocus), while scanning electron microscopy (SEM) provides insights into the morphological features and layer integrity of both surface and cross-sectional regions before and after coating. This centralized approach enables a multidimensional understanding of the material's functional performance and environmental footprint, supporting its potential as a high-performance, bio-based alternative for barrier coatings in circular and active packaging systems.

## **6.5 MATERIALS AND METHODOLOGY**

### **6.5.1 Materials, synthesis, formulation, and casting of paint films**

This study employed pyrrole ( $C_4H_5N$ ), iron(III) chloride ( $FeCl_3$ ), poly(vinyl alcohol) (PVA), and glycerol, all procured from Sigma-Aldrich and Fisher Scientific and used without further purification. TEMPO-oxidized cellulose nanofibres (TOCNs) were synthesized in-house from commercially available never-dried bleached Kraft wood pulp, following the TEMPO-mediated oxidation protocol developed by our group. The resulting TOCNs had a carboxyl content of  $\sim 1600$  mmol/kg, enabling high dispersibility and nanofibril formation. Transmission electron microscopy (TEM) showed an average width of  $3.5 \pm 1.0$  nm and length of  $306 \pm 112$  nm, with minor microfibrillated cellulose residues (Bideau, Cherpozat, et al., 2016)

As per Malik et al., 2025, polypyrrole (PPy) was incorporated into the TOCN matrix via in situ oxidative polymerization. Specifically, 5 mL of pyrrole (4.835 g) was added to 100 mL of a 0.45 wt% TOCN aqueous dispersion under magnetic stirring for 10 minutes. This generated an approximate PPy:TOCN mass ratio of 10.7:1. Polymerization was initiated by the dropwise addition of 25 mL of 0.3 M  $FeCl_3$  under constant stirring at room temperature for 30 minutes. The resulting TOCN–PPy composite was purified by four successive washings with deionized water (1000 mL per cycle) using Whatman Grade 202 filter paper, monitoring pH after each wash to ensure  $FeCl_3$  removal and achieve near-

neutral pH. To formulate the bio-based coating, 5 g of PVA was dissolved in 100 mL of distilled water at 75 °C under continuous stirring for 50–60 minutes. The TOCN–PPy composite was incorporated into the hot PVA solution and homogenized via high-shear mixing (Silverson L4RT-A) for 3 minutes at room temperature. Glycerol was added as a plasticizer in three concentrations: 1 mL (Gly1), 2 mL (Gly2), and 5 mL (Gly5), followed by an additional 3 minutes of high-shear mixing. The final formulations included TOCN–PPy (functional filler), PVA (binder), glycerol (plasticizer), and water (solvent).

For film preparation, 20–25 mL of each formulation was poured into 10 cm-diameter aluminum dishes and dried at ambient conditions ( $23 \pm 2$  °C) for 48 hours. The dried self-standing films were then peeled and stored at room temperature for further characterization.

### **6.5.2 Mechanical Characterization**

The tensile properties of the TOCN–PPy–PVA–Gly films were evaluated using a universal testing machine (Instron 4201, USA) under controlled environmental conditions (25 °C and 50% relative humidity). Rectangular film strips (30 mm × 15 mm) were tested with a 10 mm gauge length and a constant crosshead speed of 10 mm/min. Given the ultra-thin nature of the samples, strain was calculated from the crosshead displacement rather than using an extensometer. A method inspired of TAPPI T494 test method for paper that may slightly overestimate elongation at break but ensured consistent and reproducible measurements. Each formulation was tested in at least six replicates, and results were reported as mean  $\pm$  standard deviation. Key mechanical parameters included tensile strength (MPa), defined as the maximum stress before failure; elongation at break (%), representing the strain at fracture; and Young's modulus (GPa), determined from the slope of the initial linear portion of the stress–strain curve.

### **6.5.3 Barrier Properties Measurements**

#### **6.5.3.1 Oxygen Transmission Rate (OTR)**

Oxygen barrier properties were measured with a Systech Illinois M8001 oxygen permeation analyzer. Pure oxygen (99.9%) was introduced on one side of the film, while

high-purity nitrogen flowed on the other side as a sweep gas. Measurements were done at 23 °C and 50% RH, with the same humidity on both sides of the films. Circular specimens were mounted over dedicated diffusion cells with an exposed area of 3.14 cm<sup>2</sup> (corresponding to a 2.0 cm diameter) to accommodate the small-sized cast films. The OTR was given by the device in cm<sup>3</sup> /m<sup>2</sup> ·day. Each formulation was tested in duplicate, and results are presented as mean ± standard deviation.

### **6.5.3.2 Moisture Vapor Transmission Rate (MVTR)**

Water vapor properties of the films were measured at 23 ± 0.5 °C. Two distinct relative humidity conditions, 50 ± 2% and 70 ± 2%, were employed depending on the test batch to evaluate environmental effects on vapor permeability. Circular specimens were carefully cut and sealed over the open tops of standard glass permeability cups, each with a diameter of 2.0 cm, corresponding to an exposed area of 3.14 cm<sup>2</sup>. Inside each cup, 2.0–2.5 g of anhydrous calcium chloride was used as the desiccant to absorb incoming moisture. To ensure vapor-tight sealing and prevent edge leakage, silicone grease was applied along the cup rim, and O-rings were fitted tightly around the film edges. The mass gain of each cup was recorded periodically using a high-precision analytical balance (±0.001 mg resolution), with two measurements per day for a total of 3 consecutive days. The water vapor transmission rate (WVTR) was obtained from the slope of the linear region of the mass gain versus time curve and normalized over the exposed surface area to calculate the MVTR. Results were expressed in g/m<sup>2</sup>·day. Each formulation was tested in triplicate, and the mean values along with standard deviations were reported.

### **6.5.4 Coating and Drying Process**

The coating formulations were deposited onto the reverse side of the paper substrate using a semi-industrial rod coater (Endupap Universal Coating Machine, L&W BK, CTP, France), which integrates a standard coating rod system with an in-line infrared (IR) drying unit consisting of two lamps. A number 0.7 bar rod was employed under consistent pressure, and the coating bar was operated at a linear speed of 6.6 m/min. This setup reliably produced coatings with a dry thickness of approximately 15 µm.

The drying approach employed to evaluate its effect on coating structure and performance was infrared (IR) drying at 2500 W, using long-wave IR radiation. All samples underwent a double-coating process and were allowed to dry until touch-dry under the respective drying method.

### **6.5.5 Surface morphology**

The surface morphology of biobased coating films composed of TOCN-PPy-PVA and its glycerol-modified derivatives (Gly1, Gly2, Gly5) was characterized using a high-resolution 3D optical profilometer (Alicona InfiniteFocus G5), based on focus variation technology. This instrument enables precise, non-contact areal topography mapping at the microscale, suitable for capturing fine morphological variations in coating surfaces. Profilometric scans were acquired over 3 representative regions of each dried film. Surface leveling and background curvature removal were performed via best-fit plane correction using the Alicona analysis software. A comprehensive set of parameters was extracted to assess both amplitude and spatial features of surface texture: Sa: Arithmetic mean height Sq: Root mean square height Sp, Sv, Sz: Maximum peak, valley, and total surface height. This approach enables quantitative comparison of the microstructural evolution across film formulations as a function of glycerol content.

### **6.5.6 SEM spectroscopy**

Scanning electron microscopy (SEM) was employed to investigate the surface morphology of both uncoated UPM paper and coated samples prepared with TOCN-PPy-PVA-Gly formulations. The analyses were conducted using a QUANTA 200 at an accelerating voltage of 10 kV. Samples were mounted on aluminum stubs using conductive adhesive tape to ensure proper electrical contact. No additional conductive coating was applied, such as platinum or gold, since the samples exhibited sufficient surface conductivity for stable imaging. SEM was utilized to capture detailed micrographs of the surface features, allowing visualization of the coating's distribution, continuity, and interaction with the fibrous paper substrate. All observations were recorded under consistent imaging parameters to maintain comparability between the uncoated and coated specimens.

### 6.5.7 Integration of Life Cycle Assessment (LCA)

A preliminary life cycle assessment (LCA) was conducted in accordance with ISO 14040/44 standards using the SimaPro software platform with background data sourced from the Ecoinvent 3.10 database (Wernet et al., 2016). The functional unit was defined as one A4-sized coated UPM paper sheet (0.062 m<sup>2</sup>), based on laboratory experiments using a two-layer bar-coating process. The system boundaries included raw material acquisition (TOCN, pyrrole, FeCl<sub>3</sub>, PVA, and glycerol), in-situ synthesis and blending, paint formulation, coating deposition, washing procedures, and formulation. Each A4 sheet was coated using a total of approximately 10 mL of paint, applied in two successive layers via bar-coating (typically 5 mL + 5 mL). A single batch of paint formulation yielded about 60 mL of usable paint, allowing for six coated A4 sheets per batch (Malik et al., 2025). For one A4 sheet, the life cycle inventory included based of 10 mL from the recipe of approximately 100 mL of 0.45 wt% TOCN suspension, equivalent to ~0.45 g of dry TOCN. Other ingredients included 5 g of PVA, 5 mL of pyrrole, and 25 mL of 0.3 M FeCl<sub>3</sub>. Glycerol was used in varying amounts depending on the formulation: 1 mL (Gly1), 2 mL (Gly2), or 5 mL (Gly5). Figure 6.1 illustrates the system boundaries of the LCA.

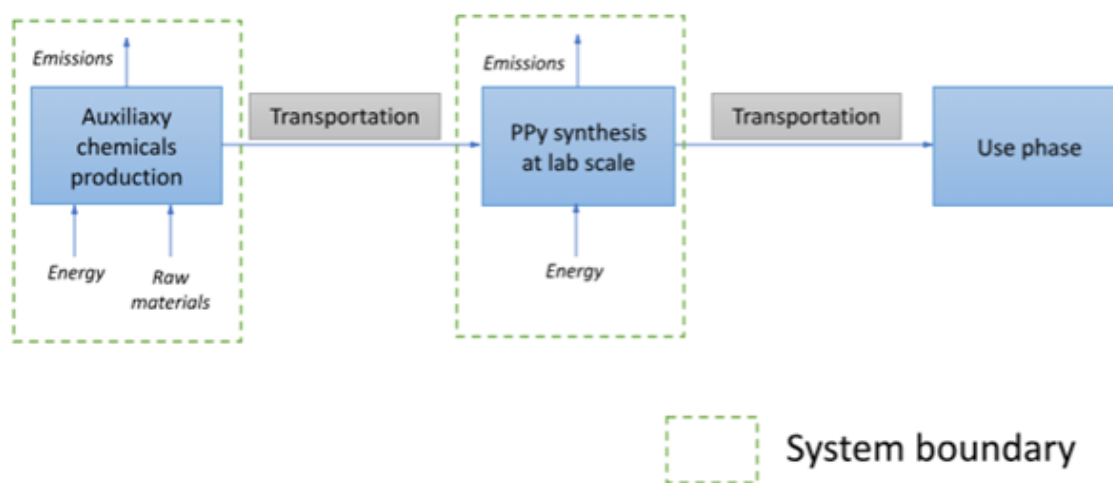


**Figure 6.1** System boundaries of the life cycle assessment (LCA) for TOCN-PPy-based paints, covering raw material acquisition, synthesis, coating deposition, washing, and projected end-of-life.

As shown in Figure 6.1, encompassing cradle-to-gate stages such as TOCN synthesis, in-situ oxidative polymerization of polypyrrole, formulation blending, coating application, and washing. The life cycle inventory for each A4-coated sample is summarized in Table 6.1. These values were used as the baseline for evaluating the environmental impacts of different formulations (Gly1, Gly2, and Gly5), enabling a comparison of plasticizer content on LCA results.

**Table 6.1** Composition of TOCN-PPy-based paint per A4 UPM paper sheet (0.062 m<sup>2</sup>), showing quantities of each raw material for scaling in LCA

Process Stage	Input Material/Energy	Quantity per 0.062 m <sup>2</sup>	Unit	Note
Raw Materials	TOCN suspension (0.45 wt%)	~100 mL	mL	TOCN content ~0.45 g; forms nanofiber matrix
	Pyrrole	5 mL	mL	Precursor for PPy formation
	FeCl <sub>3</sub> (0.3 M)	25 mL	mL	Oxidant for pyrrole polymerization
	Polyvinyl alcohol (PVA)	5 g	g	Binder for film formation
	Glycerol	1–5 mL	mL	Plasticizer; varies for Gly1, Gly2, Gly5

While PVA is typically derived from petrochemical sources, it can also be produced from renewable feedstocks such as biomass-based ethanol or natural polyols (Renewable Carbon, 2022). This aligns with the broader bio-based approach of the coating system, which also includes TOCN (derived from cellulose nanofibers; (Isogai et al., 2011) ), and glycerol (commonly sourced from biodiesel by-products or plant oils; (Valerio et al.,

2015). Replacing petro-based PVA with bio-based alternatives would further reduce the environmental footprint and support circular economy goals.

## 6.6 RESULTS AND DISCUSSION

### 6.6.1 Mechanical Performance of films

Table 6.2 shows the tensile properties of TOCN–PPy–PVA-based films were significantly influenced by the incorporation of glycerol, with clear evidence of plasticization as the glycerol content increased. The unplasticized TOCN–PPy–PVA film exhibited the highest tensile strength ( $35.30 \pm 3.51$  MPa) and stiffness (Young's modulus:  $704.65 \pm 98.50$  GPa), While the calculated Young's modulus of  $\sim 705$  GPa suggests exceptional material rigidity, this value likely reflects both the inherent stiffness of the TOCN–PPy matrix and the influence of experimental sensitivity or potential strain calculation artifacts.

The stress–deformation curves (Figure 6.2) does show a very steep increase for the material, indicative of a rigid and brittle matrix dominated by extensive hydrogen bonding and the presence of a densely packed TOCN–PPy–PVA network. Despite this rigidity, a moderate elongation at break ( $60.30 \pm 35.71\%$ ) was observed, which can be attributed to the presence of PVA as a flexible binder.

Upon the addition of 1 mL glycerol (Gly1), a substantial shift in mechanical behavior was observed. The material demonstrated a significant increase in elongation at break ( $394.24 \pm 71.63\%$ ), reflecting enhanced ductility and flexibility. This behavior coincided with a notable decrease in both tensile strength ( $16.36 \pm 2.87$  MPa) and Young's modulus ( $67.15 \pm 23.75$  GPa), confirming the plasticizing role of glycerol. The introduction of glycerol likely disrupted intermolecular hydrogen bonding and increased the free volume, thereby enhancing polymer chain mobility and reducing the resistance to deformation. Further glycerol addition (Gly2 and Gly5) exacerbated this softening trend. For Gly2, tensile strength dropped to  $11.56 \pm 3.83$  MPa, while the modulus decreased to  $34.46 \pm 6.15$  GPa.

Although the elongation remained high ( $387.60 \pm 156.52\%$ ), the mechanical integrity was further compromised. In the case of Gly5, the most plasticized formulation, the tensile

strength and modulus declined to  $7.63 \text{ MPa} \pm 1.32$  and  $17.78 \pm 3.34 \text{ GPa}$ , respectively. Interestingly, the elongation at break reached  $474.99 \pm 160.33\%$ , highlighting the highly elastic, yet structurally weakened nature of the film. This behavior is consistent with an over-plasticized system, wherein excessive glycerol content leads to phase separation, reduced interchain interactions, and lower load-bearing capacity. The stress–deformation curves (Figure 6.2) corroborate trends in glycerol addition. Glycerol-containing films displayed extended deformation plateaus and increased strain at break, confirming a transition from rigid to elastomeric behavior with increasing glycerol content.

**Table 6.2** Tensile properties of TOCN–PPy–PVA-based films

<b>Formulation</b>	<b>Breaking Force (N)</b>	<b>Width (mm)</b>	<b>Thickness (<math>\mu\text{m}</math>)</b>	<b>Cross-sectional Area (<math>\text{m}^2</math>)</b>	<b>Stress (MPa)</b>	<b>Young's Modulus (GPa)</b>	<b>Elongation at Break (%)</b>
<b>TOCN-PPy-PVA</b>	66.04 $\pm$ 5.95	15.00 $\pm$ 0.00	125.00 $\pm$ 8.37	1.88 $\times$ 10 <sup>-6</sup> $\pm$ 1.25 $\times$ 10 <sup>-7</sup>	35.30 $\pm$ 3.51	704.65 $\pm$ 98.50	60.31 $\pm$ 35.71
<b>TOCN-PPy-PVA-Gly1</b>	91.70 $\pm$ 18.15	15.00 $\pm$ 0.00	378.33 $\pm$ 76.53	5.68 $\times$ 10 <sup>-6</sup> $\pm$ 1.15 $\times$ 10 <sup>-6</sup>	16.36 $\pm$ 2.87	67.15 $\pm$ 23.75	394.24 $\pm$ 71.63
<b>TOCN-PPy-PVA-Gly2</b>	51.53 $\pm$ 16.17	15.00 $\pm$ 0.00	298.33 $\pm$ 9.83	4.48 $\times$ 10 <sup>-6</sup> $\pm$ 1.47 $\times$ 10 <sup>-7</sup>	11.57 $\pm$ 3.84	34.47 $\pm$ 6.15	387.61 $\pm$ 156.52
<b>TOCN-PPy-PVA-Gly5</b>	53.34 $\pm$ 8.80	15.00 $\pm$ 0.00	472.17 $\pm$ 81.17	7.08 $\times$ 10 <sup>-6</sup> $\pm$ 1.22 $\times$ 10 <sup>-6</sup>	7.63 $\pm$ 1.32	17.78 $\pm$ 3.34	474.99 $\pm$ 160,33

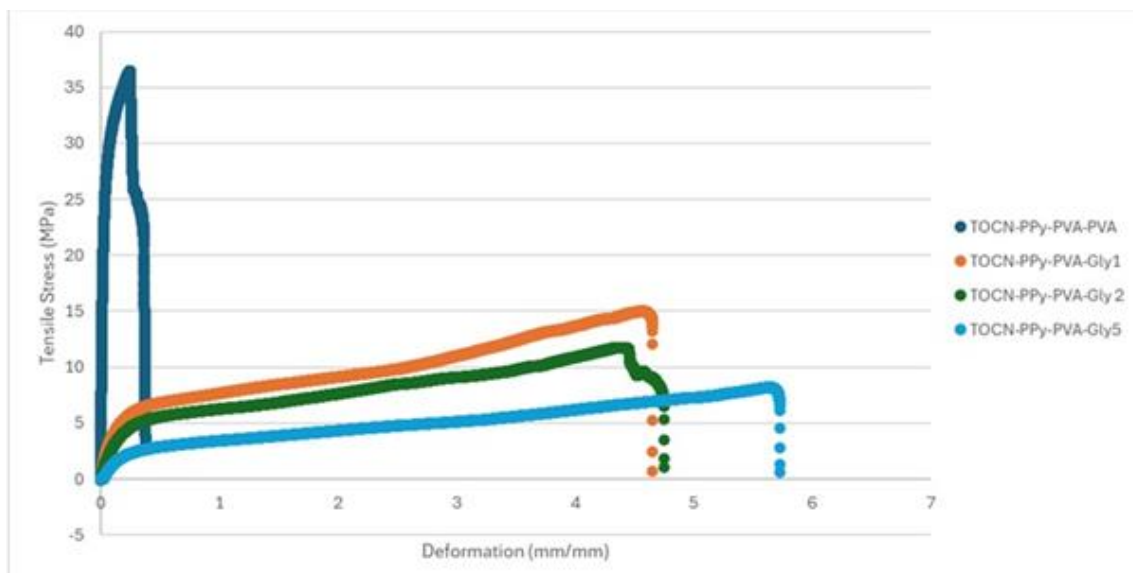


**Figure 6.2** Tensile Stress vs Deformation for TOCN-PPy-PVA-Glycerol base paint films

Overall, these findings demonstrate the tunability of mechanical properties via plasticizer concentration, enabling formulation of coatings with tailored performance. Films with low glycerol content offer improved strength and structural integrity, while those with higher glycerol concentrations are more suited for flexible packaging applications where elongation and conformability are prioritized.

## 6.6.2 Barrier Properties of films

### 6.6.2.1 OTR

All TOCN-PPy-PVA and TOCN-PPy-PVA-Gly films (Gly1, Gly2, Gly5) exhibited OTR values below the detection limit of the instrument under standard testing conditions (23 °C, 50% RH) as per Table 6.3. This consistently undetectable oxygen permeation suggests that the films possess an exceptionally dense polymeric network, likely attributed to the combined effects of hydrogen bonding among TOCN nanofibers, the presence of PVA as a cohesive binder, and polypyrrole's rigid, conjugated structure (Malik et al., 2025). The incorporation of glycerol, even at the highest loading (5 mL), did not significantly alter this behavior in terms of oxygen barrier performance. This indicates that while glycerol may increase chain mobility and affect moisture diffusion (as will be in next section of WVTR data), it does not substantially compromise the compact

morphology or reduce the tortuosity of oxygen diffusion pathways at the nanostructural level. These findings demonstrate the strong oxygen barrier potential of TOCN–PPy–PVA–Gly systems, positioning them as effective candidates for applications where oxygen-sensitive preservation is critical, such as in food or pharmaceutical packaging.

**Table 6.3** OTR data for the TOCN-PPy-PVA-Gly coating

Samples	Composition Description	OTR (cc/m <sup>2</sup> -day)
TOCN-PPy-PVA	0 ml Glycerol	Below detecting limit
TOCN-PPy-PVA-Gly1	1 ml Glycerol	Below detecting limit
TOCN-PPy-PVA-Gly2	2 ml Glycerol	Below detecting limit
TOCN-PPy-PVA-Gly5	5 ml Glycerol	Below detecting limit

#### 6.6.2.2 WVTR

The water vapor barrier performance of TOCN–PPy–PVA-based films was evaluated under two relative humidity conditions ( $50 \pm 2\%$  and  $70 \pm 2\%$ ) at  $23 \pm 0.5$  °C. As shown in Figure 6.3, the WVTR increased substantially with rising glycerol content in both conditions, indicating a deterioration in the moisture barrier properties. Under 50% RH conditions, the control sample (TOCN–PPy–PVA) exhibited excellent water vapor resistance with a WVTR of  $3 \pm 1$  g/m<sup>2</sup>·day. The addition of glycerol linearly increased the WVTR to  $66 \pm 10$ ,  $244 \pm 78$ , and  $500 \pm 20$  g/m<sup>2</sup>·day for Gly1, Gly2, and Gly5 formulations, respectively. At elevated humidity (70% RH), this linear effect was even more pronounced. The WVTR values escalated from  $37 \pm 5$  g/m<sup>2</sup> in the control to  $295 \pm 15$ ,  $500 \pm 20$ , and  $1424 \pm 51$  g/m<sup>2</sup> in the Gly1, Gly2, and Gly5 films, respectively. The drastic rise in water vapor permeability under higher humidity further confirms the moisture-sensitivity of the glycerol-containing films, likely due to glycerol's capacity to absorb atmospheric water and swell, thereby enhancing diffusion pathways.

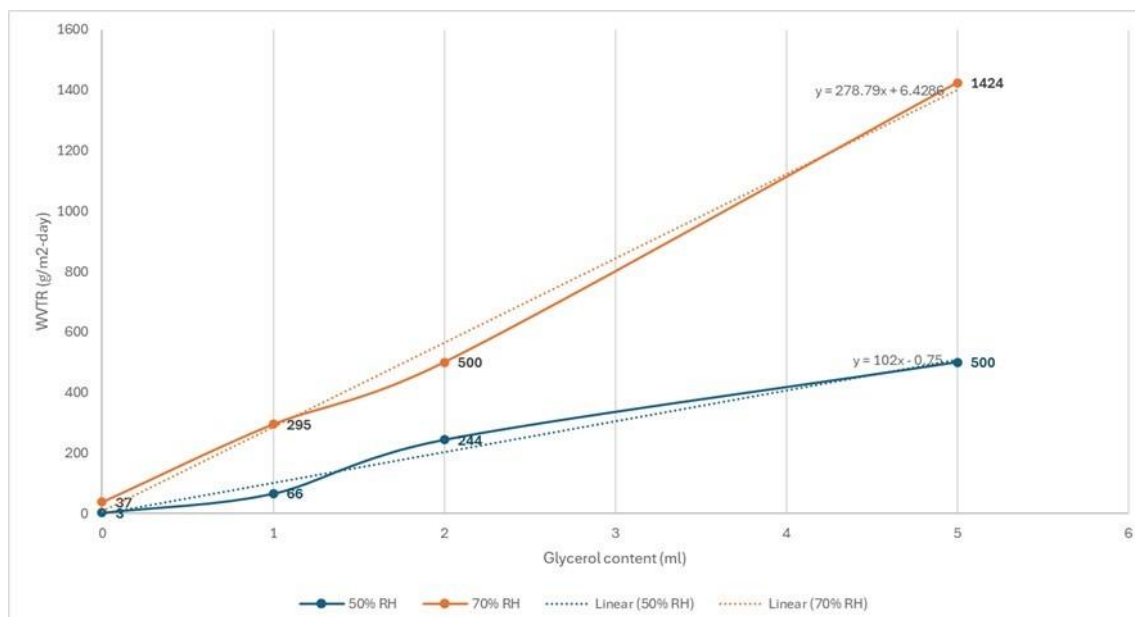


**Figure 6.3** Water Vapor Transmission Rate (WVTR) of TOCN-PPy-PVA-Glycerol Films at 50% and 70% Relative Humidity

These findings suggest that while glycerol imparts desirable flexibility and processability, its inclusion significantly compromises the water vapor barrier properties, especially under high humidity, limiting the use of such films in moisture-sensitive packaging applications unless additional hydrophobic barriers or lamination strategies are employed.

### 6.6.3 Surface morphology of coated paper surfaces

Surface roughness parameters obtained through Alicona profilometry reveal significant morphological differences between the uncoated UPM substrate and the TOCN-PPy-PVA-based coatings with varying glycerol concentrations (Table 6.4). The native UPM paper, known for its inherent heterogeneity due to its fibrous and porous cellulose structure, exhibited relatively low roughness values, with an average surface height ( $S_a$ ) of 1.55  $\mu\text{m}$  and a root mean square height ( $S_q$ ) of 2.03  $\mu\text{m}$ .

**Table 6.4** Quantitative Surface Topography Parameters of TOCN–PPy–PVA–Glycerol Coated and Uncoated UPM paper Analyzed by Alicona Profilometry

	Unit	Description	UPM	TOCN-PPy-PVA	TOCN-PPy-PVA-Gly1	TOCN-PPy-PVA-Gly2	TOCN-PPy-PVA-Gly5
Sa	μm	Average height of selected area	1.55 ± 0.18	3.70 ± 0.10	4.50 ± 0.36	3.68 ± 0.29	3.69 ± 0.18
Sq	μm	Root-Mean-Square height of selected area	2.03 ± 0.28	4.76 ± 0.12	5.80 ± 0.53	4.76 ± 0.21	4.83 ± 0.39
Sp	μm	Maximum peak height of selected area	10.54 ± 4.16	36.81 ± 7.15	30.93 ± 4.70	34.68 ± 18.68	29.69 ± 12.73
Sv	μm	Maximum valley depth of selected area	14.91 ± 1.92	42.23 ± 15.29	27.82 ± 6.00	29.11 ± 16.25	38.19 ± 11.90
Sz	μm	Maximum height of selected area	25.45 ± 2.97	79.03 ± 15.29	58.74 ± 7.41	63.79 ± 34.93	67.89 ± 20.29

Upon application of the TOCN–PPy–PVA-based coatings, a substantial increase in surface roughness was observed, confirming successful deposition and film formation. The addition of glycerol influenced the topographical features across the different formulations. The average surface height (Sa) increased notably to values between ~3.68 and 4.50 μm for the coated samples, with the Gly1 formulation exhibiting the highest peak-to-valley variations (Sz = 58.75 μm). The Gly2 and Gly5 coatings also demonstrated elevated Sz values (63.79 and 67.89 μm, respectively), indicating enhanced surface structuring likely due to differential drying dynamics and film contraction behavior.

Although all coated samples showed increased roughness, slight differences in their topography are attributable to the glycerol content, which modulates film flexibility and internal stress during drying. The skewness values shifted towards more positive values after coating, suggesting a dominance of peak structures rather than deep valleys, while kurtosis remained around 4 for all samples, indicating surfaces with pronounced asperities but not excessively spiked (Figure 6.4). However, due to the heterogeneous nature of the UPM substrate, some localized irregularities may persist even after coating, which could explain small fluctuations observed in peak ( $S_p$ ) and valley ( $S_v$ ) metrics across the formulations. These findings confirm that the application of TOCN-PPy-PVA and its glycerol-based variants significantly alters the surface morphology of UPM paper.

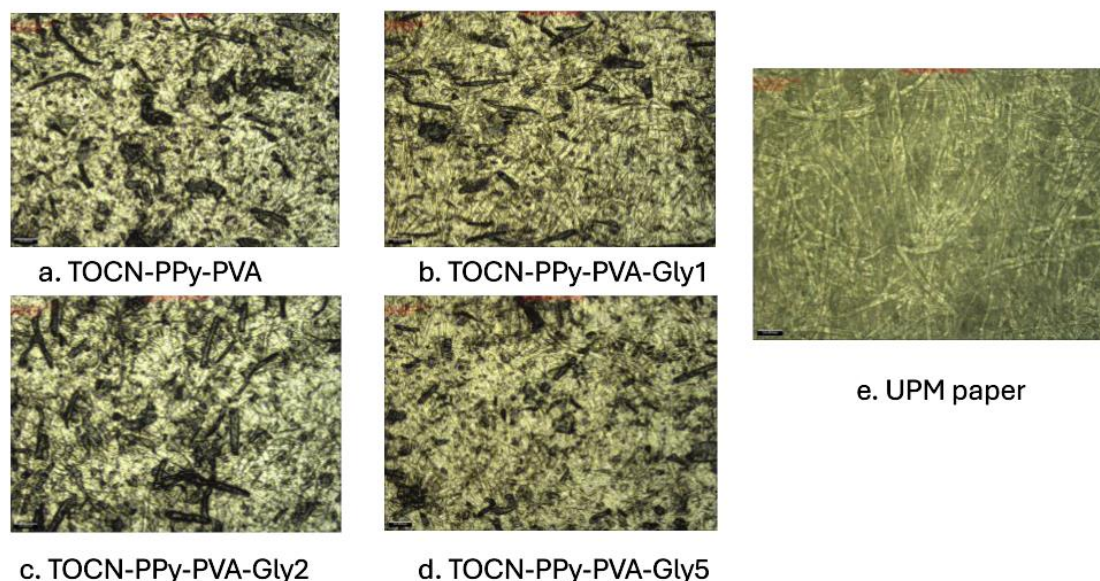


**Figure 6.4** 2D Alicona surface images showing morphological changes in coated and uncoated UPM paper

## 6.6.4 SEM spectroscopy

### 6.6.4.1 Paper uncoated and coated surface

The surface morphology of uncoated and coated UPM paper samples was investigated using SEM at 100 $\times$  magnification to assess the effect of TOCN-PPy-PVA-Glycerol coatings on film formation and surface uniformity. The uncoated UPM paper (Figure 6.5a)

exhibited a typical fibrous and porous structure, with loosely entangled cellulose fibers, open voids, and an overall heterogeneous texture characteristics that contribute to poor surface sealing and weak physical barriers. Upon application of the TOCN–PPy–PVA coating (Figure 6.5b), the surface became visibly more consolidated, with partial embedding of the fibrous network and an initial formation of a thin, continuous film across the substrate. The addition of 1 mL glycerol (Figure 6.5c) further improved the film homogeneity, leading to a denser and smoother coating layer with fewer apparent defects or voids. As explained numerous times, glycerol acts as a plasticizer, enhancing the mobility of polymer chains and promoting better interaction and conformal adhesion between TOCN, PVA, and polypyrrole within the coating matrix. With 2 mL glycerol (Figure 6.5d), the surface appeared even more uniformly covered, with minimal roughness and improved packing density, suggesting optimal plasticization that balances flexibility with structural integrity. However, at 5 mL glycerol (Figure 6.5e), subtle morphological irregularities re-emerged, possibly due to over-plasticization or partial phase separation, as evidenced by regions of uneven contrast and local surface defects. This behavior is likely linked to the saturation of hydrogen bonding sites and increased free volume, which can disrupt film cohesion during drying.

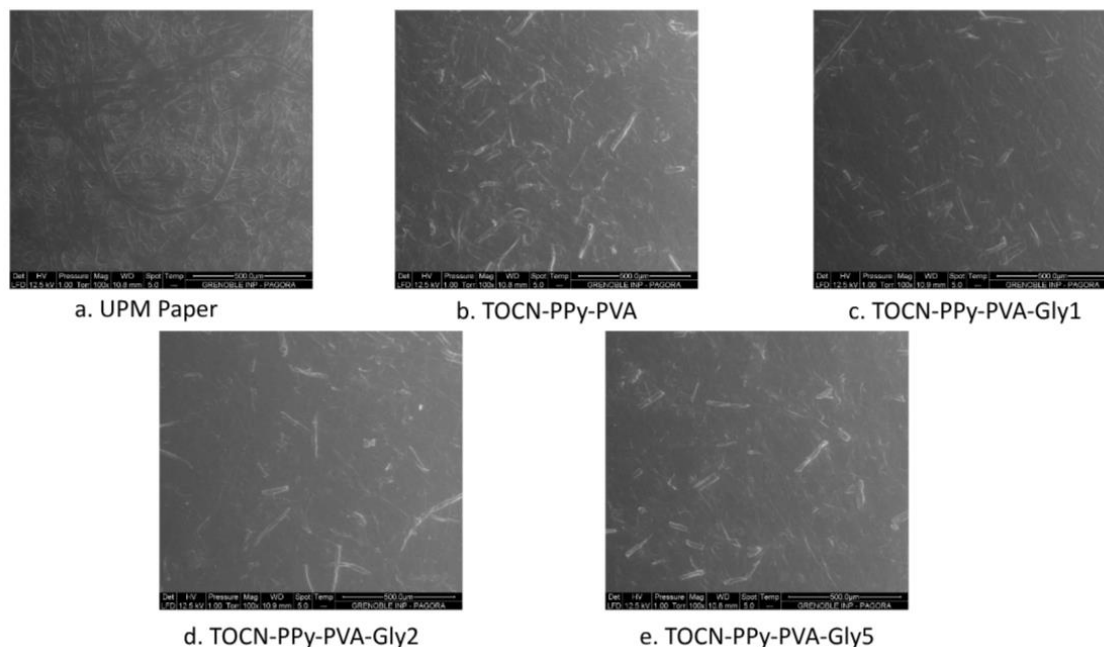


**Figure 6.5** SEM surface morphology of uncoated and TOCN–PPy–PVA–Gly-coated UPM paper at 100× magnification

Overall, the SEM analysis confirms that moderate glycerol incorporation significantly enhances surface smoothness and coating uniformity, while excessive plasticizer content may compromise film stability and microstructural consistency.

#### 6.6.4.2 Paper uncoated and coated cross-section surface

The cross-sectional SEM micrographs provide critical insights into the thickness, interfacial adhesion, and internal microstructure of the applied bio-based coatings on UPM paper substrates (Figure 6.6). The uncoated UPM paper (Figure 6.6a) reveals a multilayered fibrous network with pronounced porosity, irregular interfiber gaps, and an overall non-laminar structure. This morphology is typical of conventional paper substrates and is associated with poor barrier and mechanical performance due to high surface roughness and internal voids.

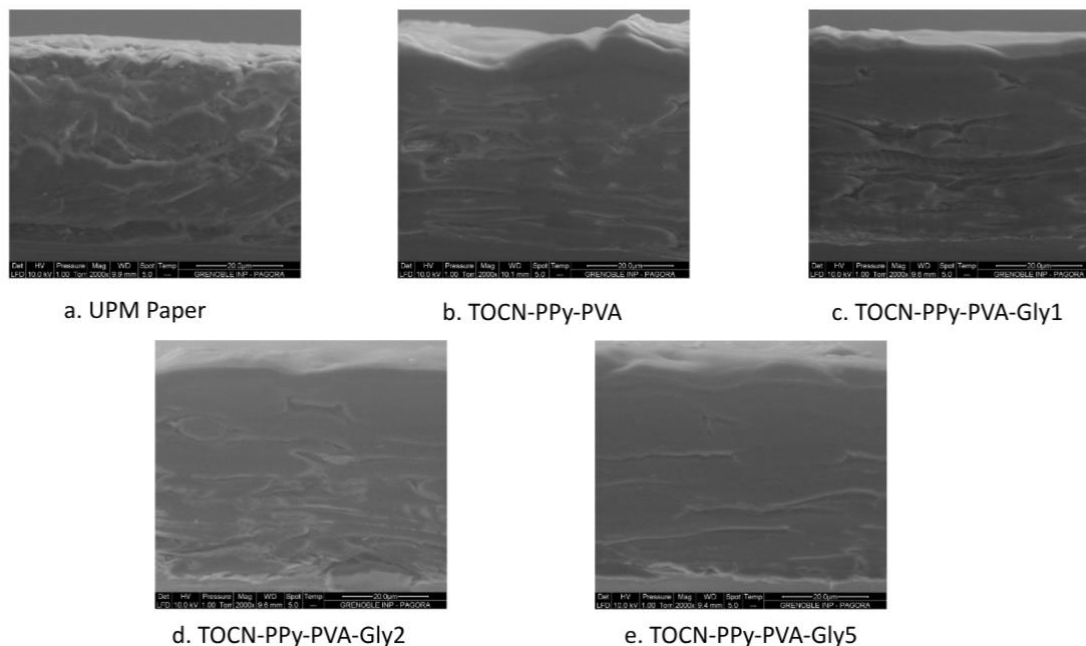


**Figure 6.6** Cross-sectional SEM images of uncoated and TOCN–PPy–PVA–Glycerol-coated UPM paper samples at 2000× magnification

In contrast, the sample coated with TOCN–PPy–PVA (Figure 6.6b) displays a distinct top layer over the fibrous base, indicating successful film deposition. The coating layer appears continuous and relatively well adhered to the paper substrate, although some surface undulations and minor interfacial voids are present, suggesting partial penetration into the porous structure. This partial infiltration likely enhances anchoring and mechanical integration, while the TOCN–PPy–PVA matrix contributes to improved surface sealing. Upon incorporation of 1 mL glycerol (Figure 6.6c), the coating layer becomes more defined and homogeneous, with fewer surface irregularities and better contact with the underlying paper fibers. The plasticizing effect of glycerol improves coating flow and flexibility during drying, allowing a more conformal and defect-free coverage. The film appears denser and more uniform, indicating enhanced polymeric chain mobility and packing. The sample with 2 mL glycerol (Figure 6.6d) exhibits an even smoother and more compact cross-section, with the coating layer showing a laminated, stratified structure that integrates more intimately with the paper matrix. This suggests an optimal level of plasticization that facilitates both surface leveling and internal cohesion. No delamination or cracks are visible, reflecting improved structural integrity and

interface bonding. However, at 5 mL glycerol (Figure 6.6e), the coating layer appears slightly thinner and more compressed, with signs of internal phase separation or microstructural softening.

### **6.6.5 Life Cycle Analysis**

While our analysis (from 6.5.1 to 6.5.3) are giving interesting results and promising applications for packaging, exploring the impact of the formulation over a Life Cycle Analysis seem logic at this stage of the development. Indeed, the glycerol content is having a great deal of impact on the properties, but it may also be of interest for the LCA of the final product. The LCA data reveal that pyrrole and PVA are the primary contributors to the environmental footprint of the coatings, reflecting their conventional fossil-based origins. However, it is important to note that PVA can also be synthesized from renewable sources such as biomass-derived ethanol or natural polyols (Renewable Carbon, 2022). In contrast, the coatings already incorporate biobased components, including TOCN derived from cellulose nanofibers and glycerol, which is commonly sourced from plant oils or biodiesel by-products. Together, the integration of renewable raw materials and the potential for substituting fossil-based PVA with biobased alternatives illustrate the coatings' promising sustainability profile.

The complete inventory of LCA inputs and associated background data is provided in

Table 6.5. Most data were sourced from the Ecoinvent 3.10 database; TOCN values were based on (Gallo Stampino et al., 2021), and pyrrole was modeled using aniline as a proxy compound. This inventory supports cradle-to-gate environmental modeling for the biobased coating system. The LCA results (Figure 6.7) reveal that the TOCN suspension (dry) is the largest contributor to the overall environmental impact, followed by pyrrole and polyvinyl alcohol (PVA). The high contribution from TOCN can be attributed to the intensive energy and chemical inputs required during TEMPO-mediated oxidation and ultrasonication, as previously reported by Gallo Stampino et al. (2021).

As demonstrated in Figure 6.8, formulations with higher glycerol content did not significantly increase environmental impact, indicating that biodegradability improvements can be achieved without major trade-offs in sustainability. This LCA analysis highlights the critical role of pyrrole in driving the overall environmental impact, suggesting that partial substitution with biobased alternatives could further enhance sustainability. Furthermore, the mild hydrothermal recyclability observed for these coatings can lower environmental burdens in circular scenarios. These findings support the potential of TOCN-PPy-PVA-Gly coatings as promising materials for safe, sustainable food packaging applications. Overall, the final properties of the composite should be targeted with no effect on the environmental impact of the final product.

In Ecoinvent/SimaPro datasets, the region codes denote the origin of the underlying process data. {CA-QC} denotes Canada, Quebec, indicating conditions particular to that province—particularly its low-carbon, hydroelectric-dominated energy composition. {RER} denotes Rest of Europe, signifying average conditions across European nations (EU + EFTA) lacking a specific dataset for individual countries. {RoW} denotes Rest of World, utilized when no regional dataset is available and signifies global-average circumstances, omitting regions with established datasets.

**Table 6.5** Input materials, energy flows, and emission factors used in the LCA model with corresponding data sources

<b>Inputs</b>	<b>Description</b>	<b>Source</b>
<b>Energy, for stirring CA</b>	Electricity, low voltage {CA-QC}   market for electricity, low voltage   Cut-off, U	Ecoinvent 3.10
<b>FeCl<sub>3</sub> 0.3M</b>	Iron(III) chloride, without water, in a 12% iron solution state {CA-QC}   iron(III) chloride production, without water, in 12% iron solution state   Cut-off, U	Ecoinvent 3.10
<b>Glycerol</b>	Glycerine {CA-QC}   treatment of used vegetable cooking oil, purified, esterification   Cut-off, U	Ecoinvent 3.10
<b>Energy, for heating CA</b>	Electricity, low voltage {CA-QC}   market for electricity, low voltage   Cut-off, U	Ecoinvent 3.10
<b>Polyvinyl alcohol (PVA)</b>	Emission Factor for bio-based PVOH according to Kuraray Poval LCA (2023)	(Kuraray Poval™, 2023)
<b>Pyrrole</b>	Proxy datum: Aniline {RER}   aniline production   Cut-off, U	Ecoinvent 3.10
<b>TOCN suspension, dry</b>	Emission Factor for TOSO-CNF. According to Stampino et al. (2021).	(Gallo Stampino et al., 2021) Table 1 TOSO. TEMPO-Oxidation and Ultrasonication (TOSO)
<b>Water DI</b>	Water, deionised {RoW}   water production, deionised   Cut-off, U	Ecoinvent 3.10

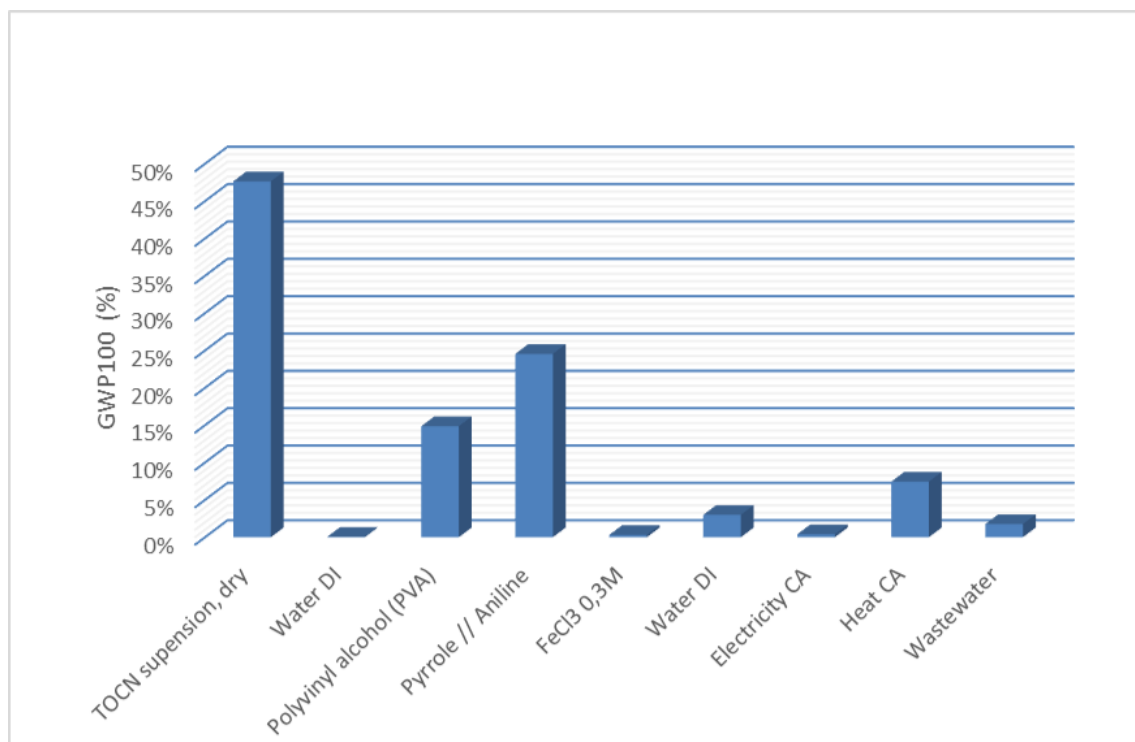


**Figure 6.7** LCA each component impact for TOCN-PPy-PVA

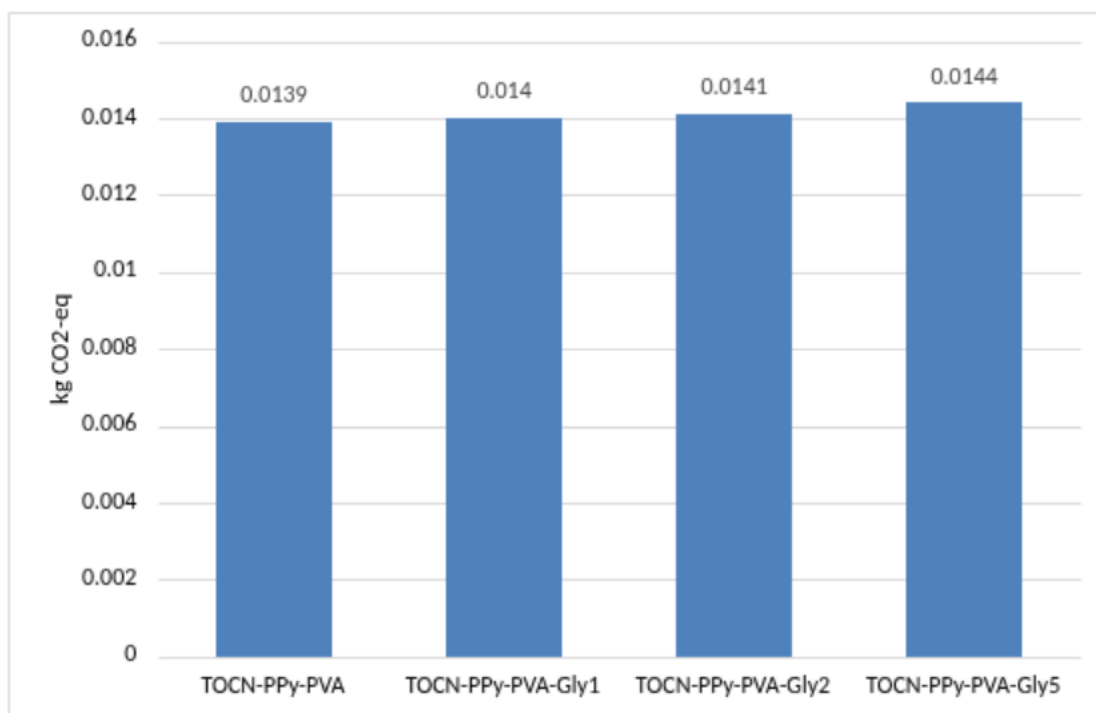


**Figure 6.8** Comparative life cycle impact of TOCN-PPy-based coatings formulated with varying glycerol content (Gly0, Gly1, Gly2, Gly5), indicating the influence of formulation on overall sustainability performance (According to IPCC 2021 GWP100 V1.03)

Compared to powder coatings, which generate approximately 0.0186 kg CO<sub>2</sub>-eq per A4-sized area (based on 0.3 kg CO<sub>2</sub>-eq/m<sup>2</sup>) (As per Covestro. (2021)), the biobased TOCN-PPy-PVA-Gly formulation exhibited a comparable or lower cradle-to-gate impact, supporting its suitability as a more environmentally responsible option for surface coating applications.

## 6.7 CONCLUSION

This study presents an investigation into the barrier, mechanical, and morphological behavior of TOCN-PPy-PVA-Glycerol films as potential bio-based coating systems for sustainable packaging.

Mechanical testing revealed a progressive decline in tensile strength and stiffness with higher glycerol loading, confirming its plasticizing effect and enabling tunability of film properties based on application-specific requirements. All formulations exhibited

exceptional oxygen barrier properties, with OTR values below the detection threshold, indicating dense polymer network structures capable of impeding gas diffusion. However, increasing glycerol content significantly elevated WVTR values, particularly under high relative humidity, attributable to enhanced polymer chain mobility and hygroscopic swelling, thereby demonstrating a well-defined trade-off between flexibility and moisture barrier performance.

Surface profilometry ( Alicona ) and SEM analyses of coated paper provided quantitative and visual evidence of increased surface roughness and morphological heterogeneity in glycerol-containing formulations. These findings offer a mechanistic understanding of how microstructural evolution during film drying influences coating behavior, particularly in relation to the 10 mL volume required for uniform application over A4-sized UPM paper substrates.

To investigate potential real-life application bottleneck, a preliminary life cycle assessment (LCA), based on this coating configuration, identified TOCN followed by pyrrole and fossil-derived PVA as the principal contributors to the environmental burden, while other components exhibited comparatively low impacts. These results emphasize the dual advantage of integrating biobased components for both functional performance and environmental sustainability.

Collectively, the data of this study support the advancement of TOCN–PPy–PVA–Gly systems as recyclable, tunable, and eco-efficient coatings for high-barrier packaging applications, with further optimization possible via incorporation of biobased PVA or crosslinking agents to enhance durability without compromising end-of-life compatibility.

## **6.8 CRediT (CONTRIBUTOR ROLES TAXONOMY)**

Aakash Malik was responsible for Conceptualization, Data Curation, Formal Analysis, Investigation, Methodology, Project Administration, Validation, Visualization, and Writing – Original Draft; Éric Loranger contributed to Funding Acquisition, Project Administration, Supervision, Validation, and Writing – Review & Editing; Simon

Barnabé contributed to Supervision and Writing – Review & Editing; Julien Bras contributed to Supervision, Project Administration, Writing – Review & Editing.

### **6.9 Declaration of generative AI and AI-assisted technologies in the writing process**

During the preparation of this work the author(s) did not use any generative or AI related tools.

### **6.10 ACKNOWLEDGEMENTS**

This research project is funded by the Natural Sciences and Engineering Research Council of Canada (Discovery grant RGPIN-2021-02861) and Municipal Research Chair for Sustainable Cities (UQTR – Victoriaville). Aakash Malik received an international mobility research grant under the Bioproductions (B-BEST) program, funded through the France 2030 initiative and managed by the Agence Nationale de la Recherche (ANR), reference ANR-22-PEBB-0001.

### **6.11 REFERENCES**

- Barbhuiya, S., Das, B. B., Kapoor, K., Das, A., & Katare, V. (2025). Mechanical performance of bio-based materials in structural applications: A comprehensive review. *Structures*, 75, 108726. <https://doi.org/10.1016/J.ISTRUC.2025.108726>
- Bideau, B., Bras, J., Adoui, N., Loranger, E., & Daneault, C. (2017). Polypyrrole/nanocellulose composite for food preservation: Barrier and antioxidant characterization. *Food Packaging and Shelf Life*, 12, 1–8. <https://doi.org/10.1016/j.fpsl.2017.01.007>
- Bideau, B., Cherpozat, L., Loranger, E., & Daneault, C. (2016). Conductive nanocomposites based on TEMPO-oxidized cellulose and poly(N-3-aminopropylpyrrole-co-pyrrole). *Industrial Crops and Products*, 93, 136–141. <https://doi.org/10.1016/j.indcrop.2016.06.003>

- Bideau, B., Loranger, E., & Daneault, C. (2016). Comparison of Three Polypyrrole-Cellulose Nanocomposites Synthesis. *Journal of Advances in Nanomaterials*, 1(2). <https://doi.org/10.22606/jan.2016.12007>
- Bideau, B., Loranger, E., & Daneault, C. (2018). Nanocellulose-polypyrrole-coated paperboard for food packaging application. *Progress in Organic Coatings*, 123, 128–133. <https://doi.org/10.1016/j.porgcoat.2018.07.003>
- Covestro, Carbon Footprint Study for Powder Coatings. [https://solutions.covestro.com/-/media/covestro/solution-center/story/brochures/rfm\\_carbon-footprint-study\\_brochure\\_en\\_digital.pdf](https://solutions.covestro.com/-/media/covestro/solution-center/story/brochures/rfm_carbon-footprint-study_brochure_en_digital.pdf), 2021 (accessed 23 July 2025).
- Dokl, M., Copot, A., Krajnc, D., Fan, Y. Van, Vujanović, A., Aviso, K. B., Tan, R. R., Kravanja, Z., & Čuček, L. (2024). Global projections of plastic use, end-of-life fate and potential changes in consumption, reduction, recycling and replacement with bioplastics to 2050. *Sustainable Production and Consumption*, 51, 498–518. <https://doi.org/10.1016/J.SPC.2024.09.025>
- Gallo Stampino, P., Riva, L., Punta, C., Elegir, G., Bussini, D., & Dotelli, G. (2021). Comparative life cycle assessment of cellulose nanofibres production routes from virgin and recycled raw materials. *Molecules*, 26(9). <https://doi.org/10.3390/molecules26092558>
- Isogai, A., Saito, T., & Fukuzumi, H. (2011). TEMPO-oxidized cellulose nanofibers. In *Nanoscale* (Vol. 3, Issue 1, pp. 71–85). <https://doi.org/10.1039/c0nr00583e>
- Liu, S., Low, Z. X., Xie, Z., & Wang, H. (2021). TEMPO-Oxidized Cellulose Nanofibers: A Renewable Nanomaterial for Environmental and Energy Applications. In *Advanced Materials Technologies* (Vol. 6, Issue 7). John Wiley and Sons Inc. <https://doi.org/10.1002/admt.202001180>
- Malik, A., Barnabe, S., & Loranger, E. (2025). Synthesis, formulation, and characterization of a bio-based paint derived from TOCN and polypyrrole. *Progress in Organic Coatings*, 208, 109511. <https://doi.org/10.1016/J.PORGCAT.2025.109511>

- Moshood, T. D., Nawanir, G., Mahmud, F., Mohamad, F., Ahmad, M. H., & AbdulGhani, A. (2022). Sustainability of biodegradable plastics: New problem or solution to solve the global plastic pollution? *Current Research in Green and Sustainable Chemistry*, 5, 100273. <https://doi.org/10.1016/J.CRGSC.2022.100273>
- Nguyen, T. H., Wang, X., Utomo, D., Gage, E., & Xu, B. (2025). Circular bioeconomy and sustainable food systems: What are the possible mechanisms? *Cleaner and Circular Bioeconomy*, 11, 100145. <https://doi.org/10.1016/J.CLCB.2025.100145>
- Prabhakaran, K., Jayasingh, E. M., Raghunath, S., Durgaprasad, C., & Sharma, S. C. (2009). Aqueous tape casting of PMN-PT powder prepared by the partial oxalate route. *Journal of Materials Processing Technology*, 209(8), 4217–4221. <https://doi.org/10.1016/J.JMATPROTEC.2008.11.009>
- Pratama, A. W., Piluharto, B., Mahardika, M., Widiastuti, N., Firmanda, A., & Norrrahim, M. N. F. (2024). Comparative study of oxidized cellulose nanofibrils properties from diverse sources via TEMPO-mediated oxidation. *Case Studies in Chemical and Environmental Engineering*, 10, 100823. <https://doi.org/10.1016/J.CSCEE.2024.100823>
- Renewable Carbon. (2022). Bioplastics International Creates World's First Sugar Cane Alcohol Water Soluble PVA to Replace Plastics. <https://Renewable-Carbon.Eu/News/Bioplastics-International-Creates-Worlds-First-Sugar-Cane-Alcohol-Water-Soluble-Pva-to-Replace-Plastics/>.
- Shimizu, M., Saito, T., & Isogai, A. (2016). Water-resistant and high oxygen-barrier nanocellulose films with interfibrillar cross-linkages formed through multivalent metal ions. *Journal of Membrane Science*, 500, 1–7. <https://doi.org/10.1016/J.MEMSCI.2015.11.002>
- Valerio, O., Horvath, T., Pond, C., Manjusri Misra, & Mohanty, A. (2015). Improved utilization of crude glycerol from biodiesel industries: Synthesis and characterization of sustainable biobased polyesters. *Industrial Crops and Products*, 78, 141–147. <https://doi.org/https://doi.org/10.1016/j.indcrop.2015.10.019>

- Wernet, G., Bauer, C., Steubing, B., Reinhard, J., Moreno-Ruiz, E., & Weidema, B. (2016). The ecoinvent database version 3 (part I): overview and methodology. *The International Journal of Life Cycle Assessment*, 21(9), 1218–1230. <https://doi.org/10.1007/s11367-016-1087-8>
- Wu, F., Misra, M., & Mohanty, A. K. (2021). Challenges and new opportunities on barrier performance of biodegradable polymers for sustainable packaging. *Progress in Polymer Science*, 117, 101395. <https://doi.org/10.1016/J.PROGPOLYMSCI.2021.101395>

## Chapter 7 - Supplementary Experimental Analyses and Methodological Constraints

While the principal scientific contributions of this dissertation are articulated through papers, the design and experimental advancement of the TOCN–PPy–PVA–glycerol coating system necessitated several supplementary studies that are not encompassed in the published pieces. The experiments, although not included in the formal article format, were essential for comprehending the practical behavior, processing restrictions, methodological hurdles, and functional limitations of the material system being examined.

This chapter consolidates supplemental efforts to deliver a full account of the research process, enhance the reproducibility of the study, and contextualize the experimental decisions that molded the optimum coating formulas. In the initial formulation phase, many empirical trials were conducted to investigate the interactions between TOCN–PPy dispersions, PVA as a structural polymer, and glycerol as a plasticizing agent. The initial studies demonstrated a significant sensitivity of the system to the relative ratios of PVA and glycerol, resulting in considerable variations in viscosity, film integrity, brittleness, and surface shape. These observations were crucial for establishing the viable composition range, informing the selection of ideal ratios employed in later studies. The failure to identify nitrogen, derived from the pyrrole polymerization catalyst, by EDS underscored the instrumental limitations related to low-concentration or embedded elements within nanocellulosic matrices.

Cataloging these restrictions is essential for evaluating the structural analyses discussed elsewhere in the thesis. Simultaneously, various antibacterial testing protocols were formulated and implemented to evaluate the potential intrinsic antimicrobial properties of the conductive TOCN–PPy coatings. Various methodological techniques, such as contact-based, diffusion-based, and washing-water assays, were assessed; however, none of the circumstances studied yielded significant inhibition of bacterial growth.

Despite the lack of positive antibacterial activity in these assays, they offer significant insight into the limitations of the material's functional performance and elucidate that antimicrobial properties cannot be merely deduced from the existence of conductive

polypyrrole. Furthermore, documenting these results enhances scientific transparency and mitigates the risk of overinterpretation of the system's multifunctionality.

This chapter collectively enhances the scientific narrative of the thesis by detailing formulation models, characterization issues, and experimental endeavors that guided the choice of final procedures and compositions.

## **7.1 Formulation Behavior and Initial Optimization**

The formulation of the TOCN–PPy–PVA–glycerol coating system necessitated a methodical investigation into the role of each constituent in influencing the rheology, film-forming capacity, mechanical strength, and surface characteristics of the resultant material. The primary focus of the thesis is on the optimized formulations; however, the process of attaining these compositions required comprehensive empirical evaluations to delineate the formulation window and comprehend the interactions among the nanocellulosic network, the conductive polymer, and the polymeric and molecular additives. This section outlines the initial optimization trials and the observed behaviors that informed the final formulation method.

### **7.1.1 Design of an Initial Formulation Model**

The formulation procedure commenced with the TOCN–PPy dispersion, which was generated via 4-acetamido-TEMPO oxidation and subsequent in situ oxidative polymerization of pyrrole. This base dispersion constituted the structural and functional foundation of the coating system but had considerable shortcomings when utilized independently, such as brittleness upon drying, inadequate flexibility, and the development of fragile films with weak cohesiveness. Consequently, the formulation model was augmented by using PVA as a structural polymer to aid film formation and glycerol as a plasticizer to increase flexibility. An empirical approach was employed to directly examine the link among PVA concentration, water content, and viscosity, facilitating the creation of a practical compositional map for the mixture. This mapping was essential for identifying formulations suitable for mixing and casting, while also preventing compositions that resulted in phase separation, insufficient consistency, or excessive solidification.

### 7.1.2 Influence of PVA Concentration on Viscosity and Film Integrity

PVA was included into the TOCN–PPy dispersion at various mass ratios compared to 100 mL of water to examine its effect on rheological properties and film formation. Tested concentrations comprised low amounts (1–2 g), a mid-range level (5 g), and a high concentration (10 g). These trials demonstrated clear changes in viscosity and mechanical coherence: Insufficient PVA content (1–2 g) led to excessively dilute, aqueous dispersions that exhibited inadequate polymeric entanglement, resulting in films with compromised structural integrity. The combination displayed negligible body and failed to create cohesive coatings, suggesting that the PVA concentration within this range was inadequate for network formation. A high PVA content (10 g) resulted in a significantly altered behavior, yielding an exceedingly thick, paste-like combination that functioned more as an adhesive than as a coating formulation. The elevated viscosity obstructed mixing, inhibited uniform distribution of PPy, and precluded consistent casting. The material aggregated during application, indicating that an excess of PVA interferes with the fluid dynamics necessary for film consistency. The intermediate PVA level (5 g) proved to be the ideal balance, producing a stable, moderately viscous dispersion that allowed for uniform application while retaining adequate cohesion for structural film production. This formulation yielded smooth, cohesive films devoid of phase separation or brittleness. The observations determined a baseline concentration of 5 g of PVA per 100 mL of total formulation for all subsequent trials, ensuring a dependable equilibrium between processability and mechanical performance.

### 7.1.3 The Function and Enhancement of Glycerol as a Plasticizer

Subsequent to PVA optimization, glycerol was used to mitigate the brittleness characteristic of TOCN–PPy–PVA films. Glycerol engages with hydroxyl-rich networks via hydrogen bonding, diminishing intermolecular stiffness and thus augmenting flexibility. The behavior of glycerol was significantly dependent on its concentration. The lack of glycerol produced films that were rigid and susceptible to squeezing during drying. The polymeric network exhibited inadequate mobility to alleviate stress, indicating that plasticization was crucial for functional flexibility. Excess glycerol (5 mL) caused undesired surface migration during the drying process. The films displayed glossy, sticky areas and

evident phase separation, suggesting that the glycerol content beyond the absorption capability of the TOCN–PVA matrix. This behavior undermines both mechanical integrity and barrier efficacy. The addition of moderate glycerol (e.g., 1–2 mL) enhanced flexibility without causing surface buildup. The conditions yielded films that were flexible, uniform, and mechanically robust, resulting in the choice of intermediate glycerol concentrations in the final formulations. Collectively, our findings indicate that glycerol requires meticulous regulation to prevent both excessive brittleness and unfavorable surface segregation. The formulation model established through these studies served as the foundation for later coating optimization and property assessment.

#### **7.1.4 Extra Validation and Optimization Data Acquired During Internship Work**

During a supervised research internship, a number of additional experimental activities were conducted in addition to the preliminary formulation investigations mentioned above (Noa Roger, IUT Rennes). The behaviors, trends, and material limits noted throughout this dissertation were valuably secondary validated by these tests, which were carried out independently yet inside the project's conceptual framework. They give the TOCN–PPy–PVA–glycerol coating system an extra degree of reproducibility, methodological transparency, and cross-verification.

The entire TOCN preparation procedure, including TEMPO-oxidation and in situ polymerization of pyrrole, PVA-glycerol film formulation, and final composite coatings, was replicated by the student. These experiments provide an objective validation of the formulation window and its mechanical and physicochemical constraints because they were carried out without access to the refined recipes developed later in the thesis work.

##### *Reproducibility of Carboxylate Content and TEMPO Oxidation*

With carboxylate concentrations ranging from about 1700 to approximately 1775 mmol·kg<sup>-1</sup>, several oxidation times (1–2.5 h) were examined. The plateau attained after 1–1.5 hours proves the stability of the chemical pathway utilized throughout the study and supports the oxidation time chosen in this thesis.

##### *Independent Verification of the Impact of PVA and Glycerol on Film Properties*

Tensile tests on PVA, PVA-glycerol, TOCN-PPy, and the finished paint films showed patterns similar to those found in the primary thesis work, brittle films with a modulus of about 364 MPa were produced using PVA alone. Strong plasticization (>300% elongation) was seen in PVA-glycerol. Films of TOCN-PPy stayed inflexible (56 MPa, <2% elongation). The final coating recipe showed great flexibility and an intermediate modulus. The empirical findings in Section 7.1 on the necessity of regulated glycerol addition are supported by these mechanical datasets.

#### *Verification of Surface Behavior and Hydrophilicity*

Measurements of the water contact angle (WCA  $\sim 88^\circ$  for the finished coating) support the TOCN-PPy-PVA-glycerol composite's improved hydrophobicity over TOCN alone. The wettability patterns reported in the publications are in line with these findings.

#### *Features of Optical Absorption*

The significant absorbance signature of PPy-rich coatings was replicated by reflectance studies (200–900 nm), demonstrating that even at low incorporation levels, the conductive polymer dominates optical activity.

#### *Conductivity in Relation to PPy Amount*

The expected improvement in conductivity was replicated in electrical resistance measurements (2 mL vs. 5 mL pyrrole additions), with resistance falling from  $\sim 14.6 \text{ k}\Omega \cdot \text{cm}$  to  $\sim 7.3 \text{ k}\Omega \cdot \text{cm}$ . This bolsters the links between structure and property that the thesis established.

Despite not being included in the dissertation's main dataset, these internship-derived results support the material's reproducibility and the strength of the formulation logic.

## 7.2 Early-Stage Antibacterial Observations

Using *Listeria monocytogenes* as the test organism, preliminary antibacterial experiments carried out early in the study and displayed in the 2023 poster assessed TOCN–PPy coatings. In disk-diffusion tests, TOCN–PPy films made without copolymer showed a discernible decrease in *Listeria* growth, as seen in the pretests results (Figure 7.1). However, the addition of PVA or the synthetic polyvinyl-acetate adhesive significantly reduced or eliminated the inhibitory effect. These patterns were initially thought to be proof of the TOCN–PPy matrix's innate antibacterial capability. The presence of residual Fe and Cl from incompletely removed  $\text{FeCl}_3$ , the oxidizing agent used during in situ pyrrole polymerization, was discovered during subsequent analytical characterization of early samples. The inhibitory halos seen in the Figure 7.1 assays are now attributed to  $\text{FeCl}_3$  leaching from inadequately purified early films rather than intrinsic activity of polypyrrole, since  $\text{FeCl}_3$  is known to have strong antibacterial effects through oxidative stress induction, membrane destabilization, and localized acidification.

Together, the poster results show that the apparent antibacterial effect linked to TOCN–PPy was an artifact of catalytic residue contamination rather than a fundamental characteristic of the biohybrid coating system, marking a significant methodological turning point in the project. Using *Listeria* spp. as the test organism, preliminary antibacterial experiments carried out early in the study and displayed in the initial tests assessed TOCN–PPy coatings. In disk-diffusion tests, TOCN–PPy films made without copolymer showed a discernible decrease in *Listeria* growth, as seen in the poster results (Figure 7.1). However, the addition of the synthetic polyvinyl-acetate adhesive significantly reduced or eliminated the inhibitory effect. These patterns were initially thought to be proof of the TOCN–PPy matrix's innate antibacterial capability but compared to TOCN there is still inhibition zone is still visible but less than TOCN-PPy.

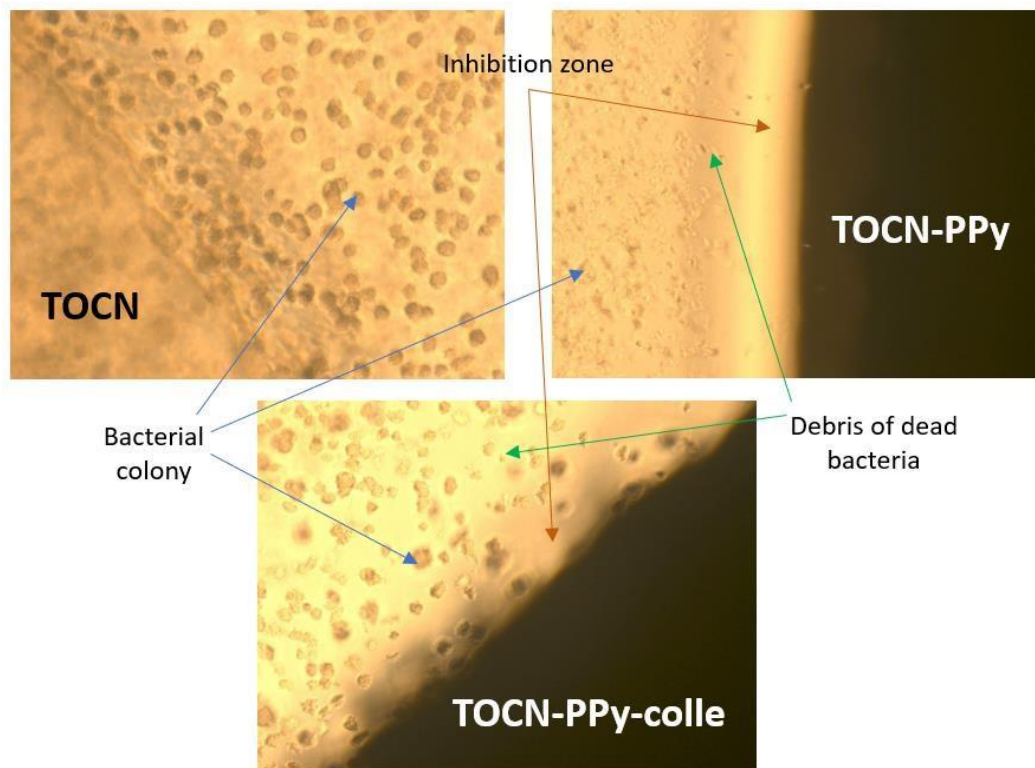


**Figure 7.1** *Listeria monocytogenes* impact on TOCN, TOCN-PPy, TOCN-PPy-Synthetic glue

### 7.3 Constraints of Characterization

While not entirely conclusive, an Energy Dispersive X-ray (EDS) analysis system (Oxford instrument X Max 20 mm<sup>2</sup>) was also used while acquiring the SEM photographs. Therefore, EDS analysis was conducted under the same conditions as SEM to determine the elemental composition of the samples as per Figure 7.2. This analysis was thought that it could provide insight into the elemental composition of TOCN-PPy-based composites and highlights the effects of PVA and glycerol incorporation on the material's structure.

In the TOCN-PPy sample (Figure 7.2a), the high carbon content (65.6 at%) originates from the polypyrrole (PPy) backbone and TOCN, while the oxygen content (25.8 at%) reflects the presence of hydroxyl and carboxyl functional groups on the TOCN. The detection of nitrogen (7.3 at%) confirms the presence of polypyrrole, as nitrogen is a key

element in its pyrrole rings. Additionally, a small amount of chlorine (1.3 at%) is observed, likely due to residual  $\text{FeCl}_3$  used in the oxidative polymerization process. With the incorporation of PVA in TOCN-PPy-PVA (Figure 7.2b), the carbon content increases to 69.1 at%, while oxygen content rises to 30.4 at%, reflecting the oxygen-rich nature of PVA. However, nitrogen is no longer detected. Additionally, a small amount of sodium (0.3 at%) is now observed, possibly from residual processing reagents. Further modification with glycerol in TOCN-PPy-PVA-Gly2 (c) results in a slight reduction in carbon content (66.4 at%) while increasing oxygen content (33.3 at%), consistent with the incorporation of oxygen-rich glycerol molecules. As with Figure 7.2, nitrogen remains undetected with trace amounts of sodium (0.2 at%) and chlorine (0.1 at%). The absence of nitrogen, which does not necessarily indicate its absence from the composite (PPy was indeed incorporated in the recipe), highlights a limitation of SEM-EDS in detecting light elements such as nitrogen. Nitrogen's  $K\alpha$  line (0.392 keV) is close to the detection limit of conventional EDS detectors, making it sometimes difficult to resolve due to signal absorption and low signal-to-noise ratio [103]. Nitrogen's low atomic number ( $Z = 7$ ) results in weak X-ray emissions that are easily absorbed or scattered, making it difficult to detect. Additionally, nitrogen peaks often overlap with signals from oxygen and carbon, further complicating its resolution in organic materials. The bulk distribution of nitrogen within the polymer network may also contribute to the detection challenge, as EDS primarily analyzes the sample's surface composition.

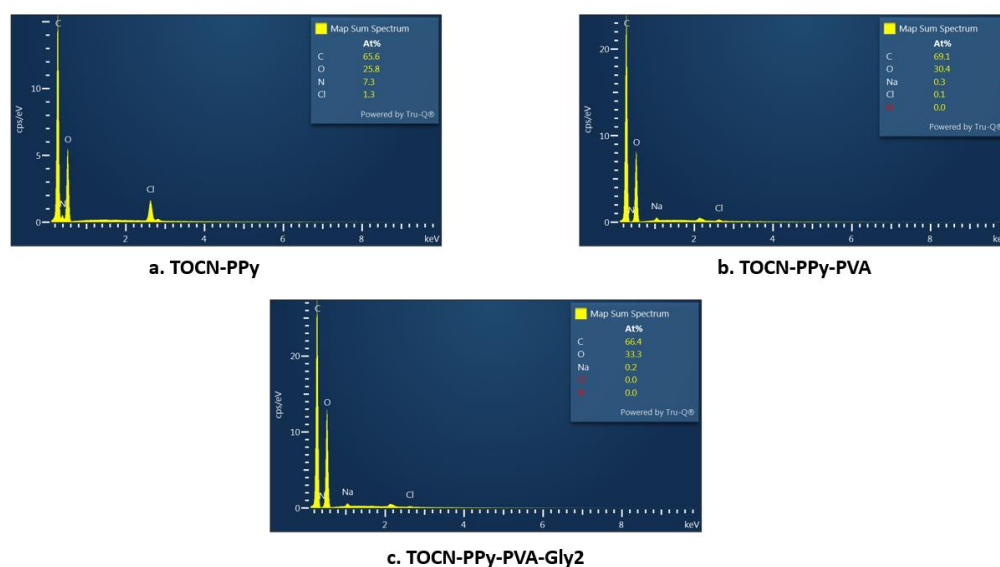


**Figure 7.2** EDS of TOCN-PPy, TOCN-PPy-PVA and TOCN-PPy-PVA-Gly2

Overall, the EDS results confirm the successful incorporation of PVA and glycerol into the TOCN-PPy matrix while demonstrating variations in elemental composition consistent with the expected chemical structures of each component. Despite the absence of nitrogen detection, its presence within the polypyrrole framework remains valid based on synthesis conditions and prior characterization. In the absence of direct nitrogen detection and to further validate the incorporation of polypyrrole, we have employed Raman spectroscopy. As a reminder, the antibacterial and electricity conductive properties are from the PPy and its presence must be clearly assessed.

#### 7.4 Antibacterial Testing Initiatives

A variety of antibacterial experiments were performed to determine if the TOCN-PPy-PVA-glycerol coatings possessed inherent antibacterial capabilities, especially for food packaging or surface protection applications. While polypyrrole has been shown in the literature to demonstrate some antibacterial properties under specific conditions, the behavior of PPy when integrated into a nanocellulosic and polymeric matrix remains inadequately characterized. Consequently, many experimental techniques were devised and evaluated. This section encapsulates these endeavors, delineates the methodological

frameworks employed, and evaluates the results that uniformly exhibited no discernible antibacterial activity under all examined situations.

#### **7.4.1 Justification for Antibacterial Assessment**

The incorporation of polypyrrole (PPy) into a nanocellulosic matrix prompts an inquiry into the potential antibacterial or bacteriostatic characteristics of the conductive polymer. Prior research has linked PPy to antimicrobial activity via mechanisms including membrane rupture, generation of oxidative stress, or interactions with negatively charged bacterial surfaces [81]. Nonetheless, these effects are significantly influenced by polymer shape, doping state, conductivity, and microbe accessibility. Considering the anticipated environmental applications of the coatings—specifically in packaging, surface protection, or barrier films—assessing antibacterial efficacy was scientifically warranted. Furthermore, due to the numerous chemical and physical alterations in the formulations of this thesis (including the incorporation of PVA, the introduction of glycerol, variations in viscosity and dispersion quality, and sequences of water washing), it was essential to ascertain whether any of these modifications affected microbial interactions. Consequently, the antibacterial testing initiative aimed to (i) characterize a novel attribute of the material and (ii) assess the safety and inertness of the coatings concerning microbial communities.

#### **7.4.2 Formulation of Antibacterial Testing Protocols**

Numerous antibacterial procedures were developed and enhanced over time to target three synergistic mechanisms of possible antimicrobial action:

Contact-based inhibition, for assessing if bacterial proliferation is inhibited directly beneath or in the vicinity of the coated film surface. Diffusion-based inhibition, for evaluating the antibacterial properties of water-soluble components derived from washing water. Combined interaction testing, for merging solid-film contact and leachate diffusion within a single Petri dish to identify synergistic or compound effects.

These methodologies culminated in the creation of several experimental documents, including the Plan for Antibacterial Testing of 2×2 cm Material Sample with Liquid Exposure, Effect of Washing Antibacterial Testing, Antimicrobial Test on Washing Liquid, and

the Detailed Protocol: Combined Testing of TOCN-PPy Solid and Washing Water in One Petri Dish, which informed the design and reproducibility of the assays.

### **7.4.3 Bacterial Strains and Their Preparation**

Two representative bacterial species were utilized, *Escherichia coli* (Gram-negative) to evaluate susceptibility to charged surfaces and oxidative conditions and *Bacillus subtilis* (Gram-positive, spore-forming) to assess resilience against surface-active polymers and hydrophilic matrices.

In the Cultural Norms and Standardization, cultures were cultivated overnight in nutrient-dense medium at 37 °C. Optical density measurements ( $OD_{600} \approx 0.2-0.3$ ) were employed to normalize bacterial concentrations to approximately  $10^6$  CFU/mL. Bacteria were evenly distributed to establish a confluent lawn during plate inoculation.

Significance of Strain Selection: The amalgamation of Gram-negative and Gram-positive species guaranteed comprehensive coverage of diverse cell-wall structures and susceptibility patterns.

### **7.4.4 Comprehensive Examination of Antibacterial Testing Methodologies and Outcomes**

A thorough series of antibacterial assessments were performed to determine if the TOCN-PPy-PVA-glycerol composite coatings demonstrated inhibitory effects against representative Gram-negative (*E. coli*) and Gram-positive (*Bacillus subtilis*) bacterial strains, utilizing direct-contact assays, diffusion-based testing of washing water, and integrated solid-liquid interaction methods. In the direct-contact configuration, 2×2 cm coated films with varying PVA content (ranging from 1 g to 10 g) and glycerol levels (0–5 mL) were positioned on inoculated agar surfaces and incubated for 24 hours to ascertain the occurrence of surface-associated inhibition or suppression of colony formation beneath the material. Simultaneously, disk-diffusion experiments were conducted utilizing washing water acquired from immersing the coatings in deionized water, facilitating the identification of any bactericidal or bacteriostatic substances leached from the film. Hybrid tests were conducted wherein a solid film and its equivalent washing-water disk were placed on the

same Petri dish, facilitating the simultaneous assessment of both contact- and diffusion-mediated antimicrobial processes.

No inhibition zones, reduced bacterial lawn density, or growth suppression beneath the films were observed across all protocols, irrespective of PVA loading, glycerol concentration, film viscosity, washing cycles, or bacterial species, with the behavior of both the coated samples and washing-water disks consistently aligning with that of negative controls. The consistent negative outcomes affirm that the formulations developed in this study lack inherent antibacterial activity under passive settings. Multiple mechanistic factors may elucidate this outcome. Initially, polypyrrole within the nanocellulose–PVA matrix is predominantly immobilized, restricting its accessibility for microbial membrane contact and diminishing its capacity to produce charge-driven antibacterial effects commonly observed in more exposed or doped PPy systems. The concentration of PPy integrated into the films may be insufficient to elicit bacteriostatic or bactericidal effects. Third, specific antibacterial properties of conductive polymers necessitate electrical activation or redox cycling, both of which were absent in the passive agar-based experiments performed in this study. The hydrophilic characteristics conferred by PVA and glycerol may improve moisture retention, perhaps fostering conditions that promote bacterial adhesion and proliferation. Finally, analytical evaluations (ICP-OES, HPLC-MS/MS) verified negligible leaching of inorganic or organic species, signifying the lack of diffusible hazardous elements capable of producing antibacterial zones via migration. The results collectively indicate that the TOCN–PPy–PVA–glycerol coatings are microbiologically inert under the tested conditions, a scientifically significant finding that delineates the functional boundaries of the material system and guides future efforts to incorporate or engineer antimicrobial properties as needed.

## Chapter 8 - Conclusion

The worldwide shift towards a circular and sustainable bioeconomy increasingly prioritizes materials that provide superior technical performance while reducing environmental impacts over their life cycle. In this changing environment, bio-based coatings present a significant opportunity, as they immediately engage with high-volume industrial sectors including packaging, electronics, and functional surfaces. This thesis advances the broader initiative by formulating, characterizing, and assessing a multifunctional water-based coating system including TEMPO-oxidized cellulose nanofibers (TOCN), polypyrrole (PPy), polyvinyl alcohol (PVA), and glycerol. The primary objective was to develop a scalable formulation that integrates barrier qualities, mechanical adaptability, and electrical functionality into a single, environmentally sustainable system.

The initial aspect of this research concentrated on the methodical design and synthesis of TOCN–PPy composites using 4-acetamido-TEMPO-mediated oxidation, succeeded by in situ oxidative polymerization of pyrrole in the presence of  $\text{FeCl}_3$ . This method facilitated the regulated incorporation of conductive PPy into the nanocellulosic framework, resulting in a resilient hybrid system. Nevertheless, initial formulations demonstrated brittleness, inadequate film integrity, and restricted adherence to substrates—challenges frequently observed in nanocellulosic and conductive polymer materials. To address these limitations, PVA and glycerol were methodically integrated, facilitating the precise adjustment of mechanical flexibility and moisture sensitivity. Subsequently, four formulations with rising glycerol concentration were produced and examined. Thorough rheological, microscale (SEM, Raman), and thermal investigations revealed that the incorporation of PVA markedly improved polymer network stability, whilst glycerol functioned as a plasticizer that adjusted chain mobility and film flexibility. The structural and physicochemical insights established a basis for comprehending the macroscopic performance of the coatings.

The subsequent second primary research focus was on assessing the environmental efficacy and circularity potential of the coating systems. A comprehensive assessment strategy was utilized, including aqueous leaching testing, chemical release profile by pH, ICP-

OES and HPLC-MS/MS, soil biodegradation analysis, and an innovative hydrothermal solubilization method for recovery and reuse. The coatings exhibited significant environmental compatibility, with limited pyrrole emission and zero iron leaching. Glycerol was identified solely in high-glycerol formulations, aligning with its hydrophilic characteristics and mobility. Soil burial investigations validated partial biodegradation, especially for formulations with elevated glycerol concentrations, consistent with predictions for hydrophilic bio-based constituents. The hydrothermal solubilization process facilitated the total dispersion and recovery of the coating components without structural degradation, presenting an unforeseen yet advantageous potential for recycling and circular material flow. This characteristic situates the formulated products within the nascent category of reversible and reprocessable bio-based materials.

The third and final axis of this research involves comprehensive characterization demonstrated that all formulations films displayed superior oxygen barrier qualities ( $\text{OTR} < 0.05 \text{ cc/m}^2 \cdot \text{day}$ ), achieving performance levels comparable to or surpassing most commercial bio-based coatings. In contrast, water vapor transmission increased increasing glycerol content, highlighting the trade-off between mechanical flexibility and barrier resistance. Tensile tests demonstrated that glycerol improved ductility and elongation while decreasing stiffness, enabling the formulation to be customized for certain performance objectives. Furthermore, the coatings to UPM paper substrates to evaluate LCA and surface characterisation using Alicona 3D profilometry and SEM revealed heightened roughness and microstructural variability with increased glycerol concentrations, potentially affecting printability and adhesion in practical applications. The results collectively indicate that the mechanical, barrier, and surface properties of the coatings can be precisely adjusted through formulation design, facilitating diverse applications in sustainable packaging and functional surface coatings.

A preliminary attributional life cycle assessment (LCA) offered a comprehensive environmental overview and quantitatively determined the primary contributors to environmental damage. Although TOCN, PPy and fossil-derived PVA mostly contributed to global warming potential due to their synthesis methods, the inclusion of renewable TOCN and glycerol slightly alleviated these effects. The research clearly indicates a path

for future enhancement: substituting PVA with entirely bio-based or biodegradable alternatives and refining PPy synthesis or incorporating bio-derived conducting systems. The correlation between experimental results and LCA outputs illustrates the significance of integrating materials development with sustainability measures to influence environmentally conscious design.

### **Overall Conclusions**

The findings of this thesis demonstrate that bio-based multifunctional coatings can be engineered to achieve enhanced performance in mechanical, barrier, electrical, and environmental domains. The formulations developed here offer a flexible design framework, enabling independent adjustments of stiffness, flexibility, moisture responsiveness, and conductivity through regulated alterations in the polymer–nanocellulose–plasticizer ratio. The shown recyclability through hydrothermal recovery and partial biodegradability categorize these materials within a growing sector of circular and sustainable coating technologies. This thesis combines thorough materials characterization with environmental assessment to establish a comprehensive and scientifically grounded framework for improving sustainable coating systems.

### **Future Perspectives**

Several viable routes for improving the coating technologies established in this thesis are anticipated. A primary objective is to substitute fossil-derived PVA with entirely bio-based or biodegradable polymers—such as modified polysaccharides, hemicellulose derivatives, or bio-sourced PVA—to improve the renewability and environmental efficacy of the formulations. Simultaneously, incorporating active or intelligent features via natural antimicrobial agents could expand the utility of these coatings in food packaging, medical surfaces, and advanced sensing technologies. Future research should examine how the integration of different copolymers, such as PVA and glycerol, may affect or possibly reduce the antibacterial properties. Attaining industrial significance necessitates the shift from laboratory-scale casting to continuous large-scale deposition techniques, such as roll-to-roll, slot-die, curtain, or spray coating, thus facilitating performance validation in authentic manufacturing environments. Future research should integrate

dynamic life-cycle assessment methodologies, current inventory databases, and thorough techno-economic assessments to enhance comprehension of cost-performance trade-offs and facilitate informed industrial decision-making from a sustainability perspective. Ultimately, investigating alternate conductive systems—spanning bio-derived carbonaceous materials to doped biopolymer-based conductive phases—provides a means to diminish dependence on polypyrrole while enhancing the adjustable electrical functions accessible for next-generation bio-based coatings.

## References

- [1] M. De Schoenmakere, Y. Hoogeveen, J. Gillabel, and S. Manshoven, “The circular economy and the bioeconomy - Partners in sustainability,” *European Environment Agency*, 2018, Accessed: May 14, 2025. [Online]. Available: [https://circulareconomy.europa.eu/platform/sites/default/files/the\\_circular\\_economy\\_and\\_the\\_bioeconomy\\_-\\_partners\\_in\\_sustainabilitythal18009enn.pdf](https://circulareconomy.europa.eu/platform/sites/default/files/the_circular_economy_and_the_bioeconomy_-_partners_in_sustainabilitythal18009enn.pdf)
- [2] A. N. Matheri, Z. B. Sithole, and B. Mohamed, “Data-Driven Circular Economy of Biowaste to Bioenergy with Conventional Prediction Modelling and Machine Learning,” *Circular Economy and Sustainability*, vol. 4, no. 2, pp. 929–950, Jun. 2024, doi: 10.1007/s43615-023-00329-3.
- [3] N. S. Caetano, S. Xu, J. R. Banu, R. K. Sani, and O. P. Karthikeyan, “Editorial: Biomass, Bioenergy and Biofuels for Circular Bioeconomy,” Feb. 14, 2022, *Frontiers Media S.A.* doi: 10.3389/fenrg.2022.851047.
- [4] L. Piergiovanni, F. Li, and S. Farris, “Coatings of Bio-based Materials on Flexible Food Packaging: Opportunities for Problem Solving and Innovations,” 2014. [Online]. Available: <https://www.researchgate.net/publication/267334442>
- [5] M. N. Tamburri *et al.*, “Understanding the potential release of microplastics from coatings used on commercial ships,” *Front Mar Sci*, vol. 9, Nov. 2022, doi: 10.3389/fmars.2022.1074654.
- [6] R. Mori, “Replacing all petroleum-based chemical products with natural biomass-based chemical products: a tutorial review,” Jan. 03, 2023, *Royal Society of Chemistry*. doi: 10.1039/d2su00014h.
- [7] Z. Mo, S. Lu, and M. Shao, “Volatile organic compound (VOC) emissions and health risk assessment in paint and coatings industry in the Yangtze River Delta, China,” *Environmental Pollution*, vol. 269, p. 115740, Jan. 2021, doi: 10.1016/J.ENVPOL.2020.115740.

- [8] X. Zhao *et al.*, “Sustainable bioplastics derived from renewable natural resources for food packaging,” Jan. 04, 2023, *Cell Press*. doi: 10.1016/j.matt.2022.11.006.
- [9] W. Yang *et al.*, “Biomass-derived nanostructured coatings based on cellulose nanofibers-melanin hybrids toward solar-enabled multifunctional energy management,” *Nano Energy*, vol. 97, p. 107180, Jun. 2022, doi: 10.1016/J.NANOEN.2022.107180.
- [10] V. K. Rastogi and P. Samyn, “Bio-based coatings for paper applications,” Dec. 01, 2015, *MDPI AG*. doi: 10.3390/coatings5040887.
- [11] S. Barbhuiya, B. B. Das, K. Kapoor, A. Das, and V. Katare, “Mechanical performance of bio-based materials in structural applications: A comprehensive review,” *Structures*, vol. 75, p. 108726, May 2025, doi: 10.1016/J.ISTRUC.2025.108726.
- [12] K. Benhamou, A. Dufresne, A. Magnin, G. Mortha, and H. Kaddami, “Control of size and viscoelastic properties of nanofibrillated cellulose from palm tree by varying the TEMPO-mediated oxidation time,” *Carbohydr Polym*, vol. 99, pp. 74–83, 2014, doi: 10.1016/j.carbpol.2013.08.032.
- [13] I. Besbes, S. Alila, and S. Boufi, “Nanofibrillated cellulose from TEMPO-oxidized eucalyptus fibres: Effect of the carboxyl content,” *Carbohydr Polym*, vol. 84, no. 3, pp. 975–983, Mar. 2011, doi: 10.1016/j.carbpol.2010.12.052.
- [14] A. Isogai, T. Saito, and H. Fukuzumi, “TEMPO-oxidized cellulose nanofibers,” Jan. 2011. doi: 10.1039/c0nr00583e.
- [15] R. Aaen Sébastien Simon Fredrik Wernersson Brodin Kristin Syverud, F. Wernersson Brodin, and K. Syverud, “The potential of TEMPO-oxidized cellulose nanofibrils as rheology modifiers in food systems,” *Cellulose*, vol. 26, pp. 5483–5496, 2019, doi: 10.1007/s10570.
- [16] B. Bideau, L. Cherpozat, E. Loranger, and C. Daneault, “Conductive nanocomposites based on TEMPO-oxidized cellulose and poly(N-3-aminopropylpyrrole-co-

- pyrrole),” *Ind Crops Prod*, vol. 93, pp. 136–141, Dec. 2016, doi: 10.1016/j.indcrop.2016.06.003.
- [17] B. Bideau, J. Bras, N. Adoui, E. Loranger, and C. Daneault, “Polypyrrole/nanocellulose composite for food preservation: Barrier and antioxidant characterization,” *Food Packag Shelf Life*, vol. 12, pp. 1–8, Mar. 2017, doi: 10.1016/j.fpsl.2017.01.007.
- [18] S. Shrestha, X. Fonoll, S. K. Khanal, and L. Raskin, “Biological strategies for enhanced hydrolysis of lignocellulosic biomass during anaerobic digestion: Current status and future perspectives,” *Bioresour Technol*, vol. 245, pp. 1245–1257, Dec. 2017, doi: 10.1016/J.BIORTECH.2017.08.089.
- [19] P. Fratzl and R. Weinkamer, “Nature’s hierarchical materials,” *Prog Mater Sci*, vol. 52, no. 8, pp. 1263–1334, Nov. 2007, doi: 10.1016/J.PMATSCI.2007.06.001.
- [20] I. Bukhari, F. Haq, M. Kiran, T. Aziz, S. Mehmood, and M. Haroon, “Lignocellulosic biomass as a renewable resource: Driving second-generation biofuel innovation from agricultural waste,” *Biomass Bioenergy*, vol. 201, p. 108133, Oct. 2025, doi: 10.1016/J.BIOMBIOE.2025.108133.
- [21] J. J. Andrew and H. N. Dhakal, “Sustainable biobased composites for advanced applications: recent trends and future opportunities – A critical review,” *Composites Part C: Open Access*, vol. 7, p. 100220, Mar. 2022, doi: 10.1016/J.JCOMC.2021.100220.
- [22] H. A. Ruiz *et al.*, “Advances in process design, techno-economic assessment and environmental aspects for hydrothermal pretreatment in the fractionation of biomass under biorefinery concept,” *Bioresour Technol*, vol. 369, p. 128469, Feb. 2023, doi: 10.1016/J.BIORTECH.2022.128469.
- [23] C. Huang, C. Xu, X. Meng, L. Wang, and X. Zhou, “Editorial: Isolation, Modification, and Characterization of the Constituents (Cellulose, Hemicellulose, Lignin, et

- al.) in Biomass and Their Bio-Based Applications,” May 13, 2022, *Frontiers Media S.A.* doi: 10.3389/fbioe.2022.866531.
- [24] Z. Zhou, D. Ouyang, D. Liu, and X. Zhao, “Oxidative pretreatment of lignocellulosic biomass for enzymatic hydrolysis: Progress and challenges,” *Bioresour Technol*, vol. 367, p. 128208, Jan. 2023, doi: 10.1016/J.BIORTECH.2022.128208.
- [25] J. V. Madeira *et al.*, “Agro-Industrial Residues and Microbial Enzymes: An Overview on the Eco-Friendly Bioconversion into High Value-Added Products,” *Biotechnology of Microbial Enzymes: Production, Biocatalysis and Industrial Applications*, pp. 475–511, Jan. 2017, doi: 10.1016/B978-0-12-803725-6.00018-2.
- [26] S. Sun, S. Sun, X. Cao, and R. Sun, “The role of pretreatment in improving the enzymatic hydrolysis of lignocellulosic materials,” Jan. 01, 2016, *Elsevier Ltd.* doi: 10.1016/j.biortech.2015.08.061.
- [27] R. Ahonen, “Functionalized nanocelluloses and their use in barrier and membrane thin films,” 2015, doi: 10.13140/RG.2.1.4859.9769.
- [28] X. Liu, C. M. G. C. Renard, S. Bureau, and C. Le Bourvellec, “Interactions between heterogeneous cell walls and two procyanidins: Insights from the effects of chemical composition and physical structure,” *Food Hydrocoll*, vol. 121, p. 107018, Dec. 2021, doi: 10.1016/J.FOODHYD.2021.107018.
- [29] Y. Musa and I. B. Bwatanglang, “Current role and future developments of biopolymers in green and sustainable chemistry and catalysis,” in *Sustainable Nanocellulose and Nanohydrogels from Natural Sources*, Elsevier, 2020, pp. 131–154. doi: 10.1016/B978-0-12-816789-2.00006-7.
- [30] R. A. Zabel and J. J. Morrell, “Chemical changes in wood caused by decay fungi,” *Wood Microbiology*, pp. 215–244, Jan. 2020, doi: 10.1016/B978-0-12-819465-2.00008-5.
- [31] M. M. Alam, A. Greco, Z. Rajabimashhadi, and C. Esposito Corcione, “Efficient and environmentally friendly techniques for extracting lignin from lignocellulose

- biomass and subsequent uses: A review,” *Cleaner Materials*, vol. 13, p. 100253, Sep. 2024, doi: 10.1016/J.CLEMA.2024.100253.
- [32] M. S. Karunaratna and R. C. Smith, “Valorization of lignin as a sustainable component of structural materials and composites: Advances from 2011 to 2019,” Jan. 01, 2020, *MDPI*. doi: 10.3390/su12020734.
- [33] O. M. Terrett and P. Dupree, “Covalent interactions between lignin and hemicelluloses in plant secondary cell walls,” *Curr Opin Biotechnol*, vol. 56, pp. 97–104, Apr. 2019, doi: 10.1016/J.COPBIO.2018.10.010.
- [34] X. Zhang, W. Yang, and W. Blasiak, “Modeling study of woody biomass: Interactions of cellulose, hemicellulose, and lignin,” *Energy and Fuels*, vol. 25, no. 10, pp. 4786–4795, Oct. 2011, doi: 10.1021/ef201097d.
- [35] A. Sharma, M. Thakur, M. Bhattacharya, T. Mandal, and S. Goswami, “Commercial application of cellulose nano-composites – A review,” *Biotechnology Reports*, vol. 21, p. e00316, Mar. 2019, doi: 10.1016/J.BTRE.2019.E00316.
- [36] A. Dufresne, “Nanocellulose: a new ageless bionanomaterial,” *Materials Today*, vol. 16, no. 6, pp. 220–227, Jun. 2013, doi: 10.1016/J.MATTOD.2013.06.004.
- [37] S. Li, H. Chen, X. Liu, P. Li, and W. Wu, “Nanocellulose as a promising substrate for advanced sensors and their applications,” *Int J Biol Macromol*, vol. 218, pp. 473–487, Oct. 2022, doi: 10.1016/J.IJBIOMAC.2022.07.124.
- [38] B. E. Channab, A. El Idrissi, Y. Essamlali, and M. Zahouily, “Nanocellulose: Structure, modification, biodegradation and applications in agriculture as slow/controlled release fertilizer, superabsorbent, and crop protection: A review,” *J Environ Manage*, vol. 352, p. 119928, Feb. 2024, doi: 10.1016/J.JENVMAN.2023.119928.
- [39] F. Fneich, J. Ville, B. Seantier, and T. Aubry, “Structure and rheology of aqueous suspensions and hydrogels of cellulose nanofibrils: Effect of volume fraction and ionic strength,” *Carbohydr Polym*, vol. 211, pp. 315–321, May 2019, doi: 10.1016/J.CARBPOL.2019.01.099.

- [40] K. M. Guevara, G. Martínez-Valenzuela, V. Sánchez-Vásquez, K. Guerrero-Ruiz, and M. Fiallos-Cárdenas, “Trends and perspectives on bacterial nanocellulose: A comprehensive analysis from the three helixes of innovation,” *Materials Today Sustainability*, vol. 30, p. 101090, Jun. 2025, doi: 10.1016/J.MTSUST.2025.101090.
- [41] C. Amara, A. El Mahdi, R. Medimagh, and K. Khwaldia, “Nanocellulose-based composites for packaging applications,” *Curr Opin Green Sustain Chem*, vol. 31, p. 100512, Oct. 2021, doi: 10.1016/J.COGSC.2021.100512.
- [42] B. Adak, S. Baidya, and Y. Teramoto, “Biopolymers and their nanocomposites coated paper-based high barrier and sustainable food packaging materials,” *Carbohydr Polym*, vol. 367, p. 123966, Nov. 2025, doi: 10.1016/J.CAR-BPOL.2025.123966.
- [43] M. Y. Leong, Y. L. Kong, M. Y. Harun, C. Y. Looi, and W. F. Wong, “Current advances of nanocellulose application in biomedical field,” *Carbohydr Res*, vol. 532, p. 108899, Oct. 2023, doi: 10.1016/J.CARRES.2023.108899.
- [44] H. Kargarzadeh *et al.*, “Recent developments on nanocellulose reinforced polymer nanocomposites: A review,” *Polymer (Guildf)*, vol. 132, pp. 368–393, Dec. 2017, doi: 10.1016/J.POLYMER.2017.09.043.
- [45] G. A. Tafete, M. K. Abera, and G. Thothadri, “Review on nanocellulose-based materials for supercapacitors applications,” *J Energy Storage*, vol. 48, p. 103938, Apr. 2022, doi: 10.1016/J.EST.2021.103938.
- [46] R. T. Varghese *et al.*, “A review on the best bioadsorbent membrane- nanocellulose for effective removal of pollutants from aqueous solutions,” *Carbohydrate Polymer Technologies and Applications*, vol. 3, p. 100209, Jun. 2022, doi: 10.1016/J.CARPTA.2022.100209.

- [47] B. Thomas *et al.*, “Nanocellulose, a Versatile Green Platform: From Biosources to Materials and Their Applications,” Dec. 26, 2018, *American Chemical Society*. doi: 10.1021/acs.chemrev.7b00627.
- [48] C. Ventura, F. Pinto, A. F. Lourenço, P. J. T. Ferreira, H. Louro, and M. J. Silva, “On the toxicity of cellulose nanocrystals and nanofibrils in animal and cellular models,” Jul. 01, 2020, *Springer*. doi: 10.1007/s10570-020-03176-9.
- [49] M. Ghanadpour, F. Carosio, P. T. Larsson, and L. Wågberg, “Phosphorylated Cellulose Nanofibrils: A Renewable Nanomaterial for the Preparation of Intrinsically Flame-Retardant Materials,” *Biomacromolecules*, vol. 16, no. 10, pp. 3399–3410, Oct. 2015, doi: 10.1021/acs.biomac.5b01117.
- [50] L. Wågberg, G. Decher, M. Norgren, T. Lindström, M. Ankerfors, and K. Axnäs, “The build-up of polyelectrolyte multilayers of microfibrillated cellulose and cationic polyelectrolytes,” *Langmuir*, vol. 24, no. 3, pp. 784–795, Mar. 2008, doi: 10.1021/la702481v.
- [51] L. Wågberg, G. Decher, M. Norgren, T. Lindström, M. Ankerfors, and K. Axnäs, “The build-up of polyelectrolyte multilayers of microfibrillated cellulose and cationic polyelectrolytes,” *Langmuir*, vol. 24, no. 3, pp. 784–795, Feb. 2008, doi: 10.1021/la702481v.
- [52] B. G. Bengt Ranby, “Lehrbuch der Kolloidchemie (Spamer, Leipzig, 8 Hengstenberg and Mark, 2. Krzst,” *Polynzeve Kohlenhydrate (Akad. Verlagsges*, 1913.
- [53] A. Isogai, T. Hänninen, S. Fujisawa, and T. Saito, “Review: Catalytic oxidation of cellulose with nitroxyl radicals under aqueous conditions,” Nov. 01, 2018, *Elsevier Ltd*. doi: 10.1016/j.progpolymsci.2018.07.007.
- [54] B. Bideau, E. Loranger, and C. Daneault, “Nanocellulose-polypyrrole-coated paperboard for food packaging application,” *Prog Org Coat*, vol. 123, pp. 128–133, Oct. 2018, doi: 10.1016/j.porgcoat.2018.07.003.

- [55] B. Bideau, J. Bras, N. Adoui, E. Loranger, and C. Daneault, “Polypyrrole/nanocellulose composite for food preservation: Barrier and antioxidant characterization,” *Food Packag Shelf Life*, vol. 12, pp. 1–8, Jun. 2017, doi: 10.1016/j.fpsl.2017.01.007.
- [56] B. Bideau, J. Bras, S. Saini, C. Daneault, and E. Loranger, “Mechanical and antibacterial properties of a nanocellulose-polypyrrole multilayer composite,” *Materials Science and Engineering C*, vol. 69, pp. 977–984, Dec. 2016, doi: 10.1016/j.msec.2016.08.005.
- [57] E. Kaffashsaie *et al.*, “Direct conversion of raw wood to TEMPO-oxidized cellulose nanofibers,” *Carbohydr Polym*, vol. 262, Jun. 2021, doi: 10.1016/j.carbpol.2021.117938.
- [58] “montanari2006”.
- [59] I. Patel *et al.*, “Side reactions of 4-acetamidotemponium as the catalyst in cellulose oxidation systems,” *Holzforschung*, vol. 64, no. 5, pp. 549–554, Mar. 2010, doi: 10.1515/HF.2010.072.
- [60] “4-Acetamido-TEMPO.” [Online]. Available: <http://www.chemspider.com/Chemical-Structure.452722.html>
- [61] D. D. Ateh, H. A. Navsaria, and P. Vadgama, “Polypyrrole-based conducting polymers and interactions with biological tissues,” Dec. 22, 2006, *Royal Society*. doi: 10.1098/rsif.2006.0141.
- [62] K. Arshak, V. Velusamy, O. Korostynska, K. Oliwa-Stasiak, and C. Adley, “Conducting polymers and their applications to biosensors: Emphasizing on foodborne pathogen detection,” *IEEE Sens J*, vol. 9, no. 12, pp. 1942–1951, 2009, doi: 10.1109/JSEN.2009.2032052.

- [63] J. Robertson, M. Gizdavic-Nikolaidis, M. K. Nieuwoudt, and S. Swift, “The anti-microbial action of polyaniline involves production of oxidative stress while functionalisation of polyaniline introduces additional mechanisms,” *PeerJ*, vol. 2018, no. 6, 2018, doi: 10.7717/peerj.5135.
- [64] Z. Zhou, X. Xiao, W. Wang, S. Wei, and Y. Wang, “Enhanced hydrophobicity and barrier property of anticorrosive coatings with silicified polyaniline filler,” *Colloids Surf A Physicochem Eng Asp*, vol. 645, Mar. 2022, doi: 10.1016/j.colsurfa.2022.128848.
- [65] M. Beygisangchin, S. A. Rashid, S. Shafie, A. R. Sadrolhosseini, and H. N. Lim, “Preparations, properties, and applications of polyaniline and polyaniline thin films—a review,” *Polymers (Basel)*, vol. 13, no. 12, Jun. 2021, doi: 10.3390/polym13122003.
- [66] L. Liu, J. Chen, and S. Wang, “Flexible Antibacterial Film Deposited with Polythiophene-Porphyrin Composite,” *Adv Healthc Mater*, vol. 2, no. 12, pp. 1582–1585, 2013, doi: 10.1002/adhm.201300106.
- [67] N. A. Abdelwahab, D. E. El-Nashar, and M. A. A. El-Ghaffar, “Polyfuran, polythiophene and their blend as novel antioxidants for styrene- butadiene rubber vulcanizates,” *Mater Des*, vol. 32, no. 1, pp. 238–245, Mar. 2011, doi: 10.1016/j.matdes.2010.06.003.
- [68] H. Liu, J. Ge, E. Ma, and L. Yang, “Advanced biomaterials for biosensor and theranostics,” Mar. 2018, *Elsevier*. doi: 10.1016/B978-0-12-813477-1.00010-4.
- [69] A. Malik, S. Barnabe, and E. Loranger, “Synthesis, formulation, and characterization of a bio-based paint derived from TOCN and polypyrrole,” *Prog Org Coat*, vol. 208, p. 109511, Nov. 2025, doi: 10.1016/J.PORGCOAT.2025.109511.

- [70] Shaily, A. Shahzaib, F. Zafar, and N. Nishat, “Biobased advanced coating materials,” *Advanced Applications of Biobased Materials: Food, Biomedical, and Environmental Applications*, pp. 673–697, Jan. 2023, doi: 10.1016/B978-0-323-91677-6.00032-5.
- [71] Y. Tian *et al.*, “Corrosion resistant nanoscale polymer-based coatings,” *Polymer-Based Nanoscale Materials for Surface Coatings*, pp. 547–584, Jan. 2023, doi: 10.1016/B978-0-32-390778-1.00031-1.
- [72] A. A. Firoozi, A. A. Firoozi, D. O. Oyejobi, S. Avudaiappan, and E. S. Flores, “Enhanced durability and environmental sustainability in marine infrastructure: Innovations in anti-corrosive coating technologies,” *Results in Engineering*, vol. 26, p. 105144, Jun. 2025, doi: 10.1016/J.RINENG.2025.105144.
- [73] M. Stoica *et al.*, “Review of Bio-Based Biodegradable Polymers: Smart Solutions for Sustainable Food Packaging,” Oct. 01, 2024, *Multidisciplinary Digital Publishing Institute (MDPI)*. doi: 10.3390/foods13193027.
- [74] M. Mujtaba, J. Lipponen, M. Ojanen, S. Puttonen, and H. Vaittinen, “Trends and challenges in the development of bio-based barrier coating materials for paper/cardboard food packaging; a review,” *Science of The Total Environment*, vol. 851, p. 158328, Dec. 2022, doi: 10.1016/J.SCITOTENV.2022.158328.
- [75] J. Yusuf *et al.*, “Exploring nanocellulose frontiers: A comprehensive review of its extraction, properties, and pioneering applications in the automotive and biomedical industries,” *Int J Biol Macromol*, vol. 255, p. 128121, Jan. 2024, doi: 10.1016/J.IJBIOMAC.2023.128121.
- [76] M. R. Yazdani McCord, A. Seppälä, M. Pourakbari-Kasmaei, J. B. Zimmerman, and O. J. Rojas, “From low conductivity to high energy efficiency: The role of conductive polymers in phase change materials,” *Chemical Engineering Journal*, vol. 508, p. 160804, Mar. 2025, doi: 10.1016/J.CEJ.2025.160804.

- [77] G. Roselló-Márquez, D. M. García-García, M. Cifre-Herrando, and J. García-Antón, “Electropolymerization of PPy, PEDOT, and PANi on WO<sub>3</sub> nanostructures for high-performance anodes in Li-ion batteries,” *Heliyon*, vol. 10, no. 24, p. e41075, Dec. 2024, doi: 10.1016/J.HELIYON.2024.E41075.
- [78] B. Bideau, E. Loranger, and C. Daneault, “Comparison of Three Polypyrrole-Celulose Nanocomposites Synthesis,” *Journal of Advances in Nanomaterials*, vol. 1, no. 2, Mar. 2016, doi: 10.22606/jan.2016.12007.
- [79] B. Bideau, L. Cherpozat, E. Loranger, and C. Daneault, “Conductive nanocomposites based on TEMPO-oxidized cellulose and poly(N-3-aminopropylpyrrole-copolyrrole),” *Ind Crops Prod*, vol. 93, pp. 136–141, Dec. 2016, doi: 10.1016/j.indcrop.2016.06.003.
- [80] B. Bideau, E. Loranger, and C. Daneault, “Nanocellulose-polypyrrole-coated paperboard for food packaging application,” *Prog Org Coat*, vol. 123, pp. 128–133, Oct. 2018, doi: 10.1016/j.porgcoat.2018.07.003.
- [81] B. Bideau, J. Bras, S. Saini, C. Daneault, and E. Loranger, “Mechanical and antibacterial properties of a nanocellulose-polypyrrole multilayer composite,” *Materials Science and Engineering C*, vol. 69, pp. 977–984, Dec. 2016, doi: 10.1016/j.msec.2016.08.005.
- [82] J. O. Adeyemi and O. A. Fawole, “Metal-Based Nanoparticles in Food Packaging and Coating Technologies: A Review,” Jul. 01, 2023, *Multidisciplinary Digital Publishing Institute (MDPI)*. doi: 10.3390/biom13071092.
- [83] M. Vargas-Ramella, N. Echegaray, P. C. B. Campagnol, and J. M. Lorenzo, “Natural Polymer-Based Coatings for Animal-Derived Products: A Review of Applications, Functionality, Characterization, and Challenges,” Jul. 01, 2025, *Multidisciplinary Digital Publishing Institute (MDPI)*. doi: 10.3390/foods14132255.

- [84] M. M. Sreejaya *et al.*, “Lignin-based organic coatings and their applications: A review,” *Mater Today Proc*, vol. 60, pp. 494–501, Jan. 2022, doi: 10.1016/J.MATPR.2022.01.325.
- [85] I. Zvonkina and M. Soucek, “Inorganic–organic hybrid coatings: common and new approaches,” *Curr Opin Chem Eng*, vol. 11, pp. 123–127, Feb. 2016, doi: 10.1016/J.COCHE.2016.01.008.
- [86] S. Barbhuiya, B. B. Das, K. Kapoor, A. Das, and V. Katare, “Mechanical performance of bio-based materials in structural applications: A comprehensive review,” *Structures*, vol. 75, p. 108726, May 2025, doi: 10.1016/J.ISTRUC.2025.108726.
- [87] R. Ahonen, “Functionalized nanocelluloses and their use in barrier and membrane thin films,” 2015, doi: 10.13140/RG.2.1.4859.9769.
- [88] A. Srisa *et al.*, “Antibacterial, Antifungal and Antiviral Polymeric Food Packaging in Post-COVID-19 Era,” Mar. 2022, *MDPI*. doi: 10.3390/polym14194042.
- [89] M. Ghosh, A. Roy, A. Ghosh, H. Kumar, and G. Saha, “Antibacterial and antimicrobial coatings on metal substrates by cold spray technique: Present and future perspectives,” Mar. 2020, *Elsevier*. doi: 10.1016/B978-0-12-817592-7.00002-2.
- [90] E. Dube and G. E. Okuthe, “Silver Nanoparticle-Based Antimicrobial Coatings: Sustainable Strategies for Microbial Contamination Control,” Jun. 01, 2025, *Multidisciplinary Digital Publishing Institute (MDPI)*. doi: 10.3390/microbiolres16060110.
- [91] O. Vasilev, A. Hayles, D. Campbell, R. Jaarsma, L. Johnson, and K. Vasilev, “Nanoscale antibacterial coatings incorporating silver nanoparticles derived by plasma techniques – A state-of-the-art perspective,” *Mater Today Chem*, vol. 41, p. 102341, Oct. 2024, doi: 10.1016/J.MTCHEM.2024.102341.
- [92] S. Kumar, A. Mukherjee, and J. Dutta, “Chitosan based nanocomposite films and coatings: Emerging antimicrobial food packaging alternatives,” *Trends Food Sci Technol*, vol. 97, pp. 196–209, Mar. 2020, doi: 10.1016/J.TIFS.2020.01.002.

- [93] M. Barik, G. V. S. BhagyaRaj, K. K. Dash, and R. Shams, “A thorough evaluation of chitosan-based packaging film and coating for food product shelf-life extension,” *J Agric Food Res*, vol. 16, p. 101164, Jun. 2024, doi: 10.1016/J.JAFR.2024.101164.
- [94] R. Teixeira-Santos, M. Lima, L. C. Gomes, and F. J. Mergulhão, “Antimicrobial coatings based on chitosan to prevent implant-associated infections: A systematic review,” *iScience*, vol. 24, no. 12, p. 103480, Dec. 2021, doi: 10.1016/J.ISCI.2021.103480.
- [95] J. Ruwoldt, F. H. Blindheim, and G. Chinga-Carrasco, “Functional surfaces, films, and coatings with lignin - a critical review,” Apr. 24, 2023, *Royal Society of Chemistry*. doi: 10.1039/d2ra08179b.
- [96] L. L. Yuan, H. M. Wang, Y. C. Wu, Q. X. Hou, and R. C. Sun, “The booming lignin-derived functional composites/nanocomposites,” *Compos B Eng*, vol. 287, p. 111869, Dec. 2024, doi: 10.1016/J.COMPOSITESB.2024.111869.
- [97] R. Liu, S. Willför, and C. Xu, “New insights into the effects of structural and constituent heterogeneities in lignin on the formation of nanoparticles,” *Ind Crops Prod*, vol. 220, p. 119149, Nov. 2024, doi: 10.1016/J.INDCROP.2024.119149.
- [98] A. S. Gnedenkov *et al.*, “Efficient and smart hybrid coatings for active corrosion protection of magnesium alloys,” *Journal of Magnesium and Alloys*, vol. 13, no. 9, pp. 4475–4499, Sep. 2025, doi: 10.1016/J.JMA.2025.07.017.
- [99] P. Irizar *et al.*, “Bio-based hybrid nanocomposites as multifunctional sustainable materials for stone conservation,” *Prog Org Coat*, vol. 185, p. 107899, Dec. 2023, doi: 10.1016/J.PORGOAT.2023.107899.
- [100] A. Isogai, T. Saito, and H. Fukuzumi, “TEMPO-oxidized cellulose nanofibers,” Jan. 2011. doi: 10.1039/c0nr00583e.

- [101] A. Rattaz, S. P. Mishra, B. Chabot, and C. Daneault, “Cellulose nanofibres by sonocatalysed-TEMPO-oxidation,” *Cellulose*, vol. 18, no. 3, pp. 585–593, Jun. 2011, doi: 10.1007/s10570-011-9529-8.
- [102] E. Loranger, A. O. Piché, and C. Daneault, “Influence of high shear dispersion on the production of cellulose nanofibers by ultrasound-assisted tempo-oxidation of kraft pulp,” *Nanomaterials*, vol. 2, no. 3, pp. 286–297, Sep. 2012, doi: 10.3390/nano2030286.
- [103] W. O. Nachlas, S. Bushmaker, and E. Sasson, “X-ray Spectroscopy of Nitrogen in Jarosite, Ammoniojarosite, and other NH<sub>4</sub>-Bearing Sulfate Minerals,” *Microsc Microanal*, vol. 29, no. 1, pp. 862–864, Jul. 2023, doi: 10.1093/micmic/ozad067.427.